MODEL SEGMENTATION AND SIMPLIFICATION FOR ELECTRIC POWER DISTRIBUTION SYSTEMS

by

Andrew Paul Reiman

B.S.E., University of Michigan College of Engineering, 2009

M.S., University of Pittsburgh, 2015

Submitted to the Graduate Faculty of

the Swanson School of Engineering in partial fulfillment

of the requirements for the degree of

Doctor of Philosophy

University of Pittsburgh

2017

UNIVERSITY OF PITTSBURGH

SWANSON SCHOOL OF ENGINEERING

This dissertation was presented

by

Andrew P. Reiman

It was defended on

March 15, 2017

and approved by

Murat Akcakaya, PhD, Assistant Professor,
Department of Electrical and Computer Engineering

Alexis Kwasinski, PhD, Associate Professor,
Department of Electrical and Computer Engineering

William E. Stanchina, PhD, Professor,
Department of Electrical and Computer Engineering

Bo Zeng, PhD, Assistant Professor,
Department of Industrial Engineering

Dissertation Co-Advisor: Thomas E. McDermott, PhD, Assistant Professor,
Department of Electrical and Computer Engineering

Dissertation Co-Advisor: Gregory F. Reed, PhD, Professor,
Department of Electrical and Computer Engineering

MODEL SEGMENTATION AND SIMPLIFICATION FOR ELECTRIC POWER DISTRIBUTION SYSTEMS

Andrew P. Reiman, PhD

University of Pittsburgh, 2017

Quasi-static time-series (QSTS) simulation is used to simulate the behavior of electric power distribution systems over long periods of time (typically hours to years). The technique involves repeatedly solving the load-flow problem for a distribution system model. This is useful in accounting for solar power variations in distributed energy resource (DER) planning. When a QSTS simulation has a small enough time step and a long enough duration, the computational burden of the simulation can be prohibitive. One way to relieve the computational burden is to simplify the model of the distribution system.

This dissertation includes an overview of existing methods of distribution system simplification and also introduces a new method, segment substitution, which addresses many of the limitations of the existing methods. The segment substitution method offers dramatic (i.e. more than 98%) model order reduction with a simplification error that is expected to be acceptable for many applications. In contrast to existing methods of distribution system model simplification, which rely on topological inspection and linearization, the segment substitution method can be used to produce a simplified model using black-box segment data and an assumed simplified topology. It also produces a more realistic simplified approximation of constant-power load models than existing methods.

Simplification using segment substitution is demonstrated using two full-scale distribution system models to achieve simulation performance gains of over 90% while introducing a state error less than 0.2%.

TABLE OF CONTENTS

LIST OF TABLES

LIST OF FIGURES

ACRONYMS AND DEFINITIONS

AAC: All Aluminum Conductor

ACSR: Aluminum Conductor, Steel Reinforced

AMI: Advanced Metering Infrastructure

DER: Distributed Energy Resource

KCL: Kirchhoff's Current Law

KVL: Kirchhoff's Voltage Law

PMF: Probability Mass Function

PV: Photovoltaic (system or panel)

QSTS: Quasi-Static Time-Series

Customer: An individual metered load on a distribution system; often the paying customer of a utility that owns the distribution system.

Distribution Primary: The medium-voltage portion of a distribution system between the substation and the distribution transformers. Some distribution systems have more than one primary voltage level.

High-Voltage: Transmission or subtransmission system voltage; greater than 35 kilovolts.

Lateral: A branch off of the trunk or a larger lateral in a distribution system, usually with lower impedance than the upstream lateral or trunk.

Low-Voltage: Distribution secondary voltage; less than 1000 volts.

Medium-Voltage: Distribution primary voltage; between 1 and 35 kilovolts.

Radial System: A network in which each bus has exactly one pathway to an origin bus.

Trunk (Line): The largest or lowest-impedance line in a distribution system.

ZIP (load): A load model consisting of any or all of a constant-impedance (Z) component, a constant-current (I) component, and a constant-power (P) component.

1.0 INTRODUCTION

This dissertation introduces a new method of electric power distribution system model simplification called segment substitution that can be used to reduce the complexity of models. Segment substitution uses the process of induction to map system measurements onto a greatly simplified topology. This is in contrast with traditional methods, which rely on topological inspection and parameter knowledge. Simplified distribution system models enable faster load-flow simulation to support complex studies including high-temporal-resolution QSTS analysis for distributed energy resource deployment and real-time distribution state estimation.

Section 1 of this dissertation includes an overview of the research as well as background information on power systems and distribution system modeling. Section 2 provides an overview of methods of characterizing distribution systems and distribution system models. In section 3, new induction methods and existing inspection methods for distribution system model simplification are described and demonstrated using a simple circuit. In section 4, the performance of the methods is compared using the demonstration circuit from the previous section. In section 5, a case study is performed using a more realistic (but simple) circuit derived from an example in a common text. In section 6, segment substitution is extended to full-scale distribution system models. Section 7 details two examples of full-scale distribution system models simplified by segment substitution. Section 8 contains summary of the research performed for this work.

1.1 RESEARCH OVERVIEW

Electric power system modeling and static or steady-state simulation is used by electric utilities to inform both system operations [1] and planning [2]. The unique large scale of power systems means that even for models composed of the most basic component representations, simulation of a full system model consisting of many independent components becomes complex [3]. At any scale, the balance between model detail and computational complexity should be considered.

Distribution system models for static simulation are composed of buses, which can have a shunt load, interconnected by branches [4]. Buses, loads, and branches can consist of one or more phases. For distribution systems, model complexity arises from factors such as the imbalance of phases, the number of individually modeled buses, and the behavior of loads and generators [5]. To reduce simulation run time and the time required for system studies, methods have been developed that exploit the radial or weakly-meshed structure common among distribution systems [6-9]. These methods reduce the computational burden of the power flow computation algorithmically.

The recent and anticipated introduction of DER, including photovoltaic (PV) systems [10-12], electric vehicles (EV) [13], and distributed energy storage (DES) [14], to distribution systems demands more complex modeling and analysis [15]. In the utility industry, these trends affect both distribution operations and planning. In operations, distribution state estimation algorithms [16-19] can be used to compute the probable bus voltages and branch currents throughout the system based on real system measurements. In planning, the impacts of proposed PV systems can be analyzed by comparing the model with and without PV using a series of power flow solutions at different possible levels of PV and load [20]. When a series of power flow computations is performed with inputs corresponding to consecutive points in time, the

simulation is called QSTS [21, 22]. QSTS simulations with high temporal resolution and long duration require an especially large number of power flow computations, ideally in a short period of execution time.

Today, powerful software tools exist for distribution system simulation, including QSTS simulation, such as OpenDSS [23, 24], GridLAB-D [25, 26], and commercial tools [27-29]. These simulation tools offer highly-developed and/or user selectable power flow solution algorithms. As an alternative to the algorithmic simplification used in [6-9], the system topology itself can be simplified. If loads are assumed to be constant-impedance, the model is a linear system and its topology can be simplified accordingly [30]. If loads are assumed to be constant-current, buses can be eliminated by combining branches and loads [31]. However, experimentation has shown that loads are better represented by nonlinear ZIP models [32-35]. Topological simplification methods compatible with loads that have a constant-power component have not been developed in the literature; the segment substitution method, introduced in this dissertation, addresses this gap.

Distribution parameter estimation [36, 37], a reformulation of the state estimation problem, attempts to identify parameters such as line impedance using system state information. Segment substitution, a distribution system model simplification method introduced in this dissertation, uses concepts similar to parameter estimation to construct a simplified segment, which approximates the full segment, while eliminating internal buses.

1.1.1 Problem

QSTS simulations can capture the variability of loads and DER. Distribution system QSTS simulation involves repetitive solving of non-linear time-varying distribution system models.

This requires multiple iterative steps at each point in time. This introduces a computational burden for high-resolution simulations with long duration. For example, a QSTS simulation with a period of one year at one-second resolution can take several hours to perform, exceeding the practical limits of a routine study for system planners.

1.1.2 Assessment of Gaps

There are two notable gaps in the body of previous work:

Simplification of Distribution Systems with Constant-Power or ZIP Loads

Linear systems including power systems with constant-impedance loads are very well understood [38-40] and methods for simplifying power systems with constant-current loads have been developed [31, 41]. However, no such methods have been developed for power systems with constant-power or ZIP loads.

In some cases, it may be acceptable to model distribution system loads as constant-current loads [31]. However, the best-fit ZIP coefficients for individual customer loads on a distribution depend heavily on the compressors, appliances, electronics, and other loads operating at a given point in time [32]. As more detail is introduced into distribution system modeling, it becomes more important for modeling tools to be able to handle diverse load behavior. When computational constraints demand a simplified model, it is desirable to use a model that preserves the original load behavior as much as possible.

This dissertation introduces methods developed specifically to simplify power distribution system segments with realistic constant-power and ZIP loads.

Model Identification from Segment Input-Output Measurements

Existing methods of distribution system model simplification require full topological and parameter knowledge of the system. Individual mathematical computations are performed for each bus elimination and each branch combination. The segment substitution method, introduced in this dissertation, uses an approach similar to parameter estimation to create a segment model between two points from simulated or monitored data.

1.1.3 Approach

Segment substitution has three advantages over existing simplification methods: (1) unlike methods described in [6-9], segment substitution is agnostic to the power flow algorithm and is compatible with advanced distribution simulation tools, (2) segment substitution does not require simplifying assumptions about load behavior; unlike methods described in [30, 31], it can be used with constant-power and, in general, ZIP loads, and (3) it can be used to create a simplified model directly from field-measured data without requiring a full system model as a starting point. In addition, unlike parameter estimation methods, which attempt to identify physical model parameters and are not concerned with reducing simulation time, segment substitution can be used to create streamlined nonlinear segment realizations which greatly reduce simulation time compared to a full detailed model.

1.2 POWER SYSTEMS OVERVIEW

This section is intended to provide high-level background about power systems which may be helpful for understanding the rest of this dissertation. For additional detail, please consult a power systems text such as [42] or [43]. It is important to note that power system infrastructure can vary widely throughout the United States; this section is included to give the reader some context for distribution system modeling and simulation.

In the United States, most of the power system infrastructure was originally designed to deliver power from large power plants to load centers. Power produced at power plants is interconnected by the transmission system to local distribution systems, where power is delivered to loads.

Figure 1 shows a high-level diagram of a traditional power system.

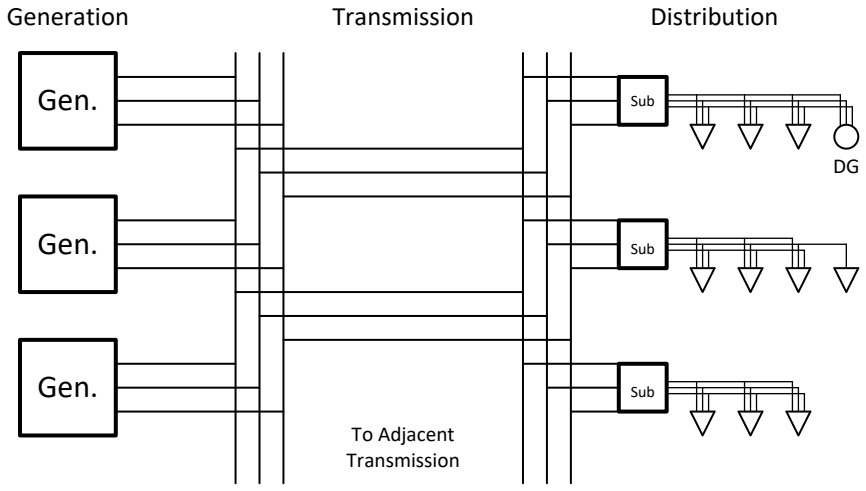

Figure 1. Power System Overview

1.2.1 Mathematical Concepts

This section is included to provide a high-level introduction to some mathematical concepts and conventions that are used in throughout this document. For a full treatment of these concepts, consult a power systems text such as [42] or [43].

1.2.1.1 Phasors for Power Systems

A sinusoidal signal can be characterized by its amplitude A and its phase θ as shown in Equation 1.

$$V(t) = A * \cos(\omega t + \theta) \quad \textbf{(1)}$$

These parameters can be mapped to the complex plane. In power system circuit analysis, the root mean squared (RMS) magnitude of the signal, which is useful in many calculations, is used as the magnitude in the complex plane; the phase of the sinusoid with respect to the zero-reference is the angle in the complex plane. Equation 2 shows the voltage signal from equation 1 expressed as a phasor.

$$V = \frac{A}{\sqrt{2}} \angle \theta = V(t) \quad \textbf{(2)}$$

Throughout this dissertation, AC voltage, current, and apparent power values are expressed as phasors.

1.2.1.2 Real, Reactive, and Complex Power

Complex power is a phasor value obtained from the product of the voltage phasor and the complex conjugate of the current phasor as shown in Equation 3

$$S = VI^* \tag{3}$$

The real power is the real component of the complex power (Equation 4) and the reactive power is the imaginary component of the complex power (Equation 5).

$$P = Re\{S\} \tag{4}$$

$$Q = Im\{S\} \tag{5}$$

Intuitively, the magnitude of the complex power (also called the apparent power) is equal to the product of the magnitudes of the voltage and the current: the power that would be obtained if the voltage and current were in phase.

1.2.1.3 Per-Unit System

A quantity can be expressed as a unitless ratio of its value to its nominal or base value as shown in Equation 6.

$$A\,[per\ unit] = \frac{A\,[units]}{A_{base}\,[units]} \tag{6}$$

The base values can be chosen arbitrarily to simplify mathematical computations. This is particularly useful in power system circuit analysis when transformers are present as the base values can be selected such that voltages, currents, and impedances do not need to be referred to one side or the other. The normal range of voltages throughout the system is usually 0.95 to 1.05 per-unit. The abbreviation for per-unit is p.u. or pu.

1.2.2 Bulk Generation

Traditionally and in general, it is logistically and/or thermodynamically more efficient to generate power at large power plants than to generate power at individual load sites. To leverage economies of scale, some nuclear plants exceed one gigawatt in capacity; individual coal and natural gas plants have a capacity on the order of hundreds of megawatts. Distributed PV systems, as a point of comparison, have capacities on the order of ten kilowatts for a large residential system or hundreds of kilowatts for a typical commercial system. In order to maintain stable frequency and voltage, power generation minus loss must match load at all times.

1.2.3 Transmission

The transmission system interconnects bulk generation and load centers at high voltage (at least 69 kV) and serves power to very large industrial customers (e.g. manufacturing plants). Transmission systems have a meshed topology. Design priorities for the transmission system include reliability and low power loss.

1.2.3.1 Reliability

Transmission system operators in the United States are responsible for ensuring reliable system operation such that the system will continue to operate through any event that causes the loss of any three-phase transmission line or bulk generator.

1.2.3.2 Loss

The complex power loss of a single conductor is proportional to the square of the current through the line as shown in equation 7.

$$S_{loss} = |I|^2 Z \tag{7}$$

A power transformer increases voltage and decreases current proportionately to a winding ratio (n), holding the apparent power constant (minus losses). Equations 8, 9, and 10 describe an ideal transformer connecting input (in) and output (out) terminals.

$$S_{out} = S_{in} \tag{8}$$

$$V_{out} = n * V_{in} \tag{9}$$

$$I_{out} = \frac{I_{in}}{n} \tag{10}$$

In order to reduce line losses, the transmission voltage is increased as high as practical, reducing conductor currents.

1.2.3.3 Subtransmission

In some cases, a subtransmission system, operating at an intermediate medium-voltage or high-voltage level connects several medium-voltage distribution systems to an even higher transmission system voltage at one or more points.

1.2.4 Distribution

At distribution substations, one or more transformers reduce the voltage to a medium-voltage level (1 kV to 35 kV) and supply one or more feeders. Most North American distribution systems are topologically radial with notable exceptions in many urban areas, which can have lightly-meshed or tightly-meshed distribution systems.

1.2.4.1 Feeders

A feeder is a radial or lightly-meshed section of a distribution system that connects customer loads to a substation. A typical feeder size is on the order of 5-10 MW, serving some combination of several hundred residential customers, larger commercial customers and/or a few industrial customers.

Voltage is regulated using a combination of substation load tap changers and voltage regulators (both discrete variable ratio transformers) and medium voltage capacitors, which may have automatically controlled switching.

For residential and commercial customers, a distribution transformer is used to reduce the voltage to a low-voltage level: typically 480 V three-phase, 208 V three-phase, or 240 V split-phase. Low-voltage connections between a distribution transformer and its associated customers are referred to as a distribution secondary.

1.2.4.2 Distributed Generation

Distributed generation, including residential and commercial PV, is connected directly to the distribution system. This configuration can incrementally decrease loss when power is consumed at the site of generation; however, several changes and complications are introduced including:

- Local voltage increase due to decreased positive (or net negative) current.
- Reverse current flow, which could exceed line ratings.
- Local fault current supply, which can complicate protection system design.
- Increased controller actuation corresponding to resource variability.
- Variability in aggregate net substation load complicates bulk generation dispatch.

These issues can have a profound impact on distribution system planning when high levels of distributed generation, especially from variable solar and wind resources, are planned or deployed. Accurate modeling can allow system planners and operators to account for these issues without using overly conservative measures, ultimately increasing the amount of allowable distributed generation without requiring system upgrades. Guidelines for high penetration of PV on single-phase laterals and secondaries of distribution systems are developed in [12]. Efficient simulation techniques can reduce the burden of studying the impact of proposed distributed generation.

1.3 DISTRIBUTION SYSTEM MODELING

Distribution system substations often have monitoring equipment used to support system operations and transmission system simulations. Monitoring equipment is not common outside of

substations. Models can be used to understand distribution system behavior in parts of the system without monitoring. They can also be used to study transients or other system changes. Examples include:

- Proposed infrastructure upgrades.
- Residential solar applications.
- Temporary reconfigurations for maintenance.
- Switching transients.
- Lightning transients.

Distribution system simulations can be classified as either transient simulations or load-flow simulations. Transient simulations are performed in the time domain and are used to study events on the order of micro-seconds to seconds in duration. Load-flow calculations are performed in the phasor domain and are used to study behavior at a point in time. Load-flow calculations can be used to study the steady-state behavior of a system (for state estimation or planning) or system stability. Harmonics can be studied by performing steady-state load-flow calculations over a range of system frequencies. System behavior in response to slower changes (such as load and distributed generation variability) that don't exceed the normal operating conditions can be studied using a series of steady-state load-flow simulations; this kind of simulation is called quasi-static time-series simulation. This dissertation is primarily concerned with static and quasi-static simulation; this is reflected in the discussion of modeling in this section.

1.3.1 Components

Distribution systems are generally modeled as nodal networks with current flowing between nodes and voltages measured between a (sometimes implicit) reference or ground node and each other node. Nodes can be connected to or coupled to other nodes by an impedance or an admittance. In addition, voltage sources, current sources, and/or ZIP loads can be connected between the reference node and any other node. In this document, consistent with OpenDSS nomenclature, a bus refers to a group of one or more single-phase nodes at the same physical location.

1.3.1.1 Substation

Distribution substations are the interface between a transmission (or subtransmission) system and one or more distribution system feeders. Substations include high-voltage-to-medium-voltage transformers that supply feeders. A substation is a load on the transmission system and the power source of a distribution system. A Substation can be modeled as a stiff voltage source behind a Thevenin equivalent source impedance supplying the distribution system. The impedance of the substation transformer can be included within the source impedance or modeled separately.

1.3.1.2 Conductors

Conductors connect nodes or complete buses to each other. Conductors that physically connect nodes are modeled as a finite impedance between the two nodes. In addition, conductors introduce an admittance to the reference node. For multi-phase systems, electromagnetic coupling between phase conductors is also modeled.

1.3.1.3 Transformers

Transformers also connect buses to each other. Step-down and step-up transformers connect distribution system segments with different operating voltages. Distribution transformers connect the distribution primary to a distribution secondary, where it is connected to residential and commercial customers. Magnetically coupled transformer windings are modeled by a series impedance between the two buses representing load loss plus leakage flux as well as a shunt admittance representing no-load loss plus magnetizing flux. The changes in voltage and current from the input of a transformer to the output can be expressed in physical units or in per-unit; often the voltage bases for a model will be selected to match transformer ratings, causing the nominal voltage on either side of the transformer to be 1 p.u.

1.3.1.4 Loads

Distribution system loads represent one or more customers. The instantaneous demand for a customer depends on the sum of appliances, electronics, climate control, lighting, and other powered devices operating on the premises in a given moment. The behavior of an individual customer load is nonlinear and highly variable. In many cases, individual customer loads are modeled in aggregate to create a more stable and predictable load than that of a single customer. Customer loads can be modeled as constant-impedance, constant-current, or constant-power or as a combination of the three called a ZIP model [32, 33].

1.3.1.5 Load Shapes

Loads that vary over time follow a load shape. The load shape is a time-array of scalar load multipliers (often between 0 and 1). The nominal value of a load multiplied by an instantaneous load multiplier determines the value of the load at that point in time.

1.3.1.6 Other Components

Other components including voltage regulators, capacitors, fuses, sectionalizers, reclosers, switches, and circuit breakers, switch between discrete system states in various ways but in steady-state operation, the components can be modeled either as a short-circuit or as one of the components mentioned above (i.e. regulators can be modeled as transformers and capacitors can be modeled as constant-impedance loads).

1.3.2 Non-Linearities and Time-Variance

In addition to the AC nature of distribution systems, which can be handled in a linear way using phasors, there are several other non-linear and time-variant aspects of distribution systems.

1.3.2.1 Linear Time-Varying Components

Distribution systems can include components such as load tap changers, voltage regulators, switched capacitors, fuses, sectionalizers, reclosers, switches, and circuit breakers that switch between discrete system states of configuration. For a given state of configuration, these components do not introduce any non-linearity into the system; however, the state of all of these linear time-varying components must be known or determined in order to perform a simulation. Some of these components maintain a single mode of operation during normal conditions; others, specifically load tap changers, voltage regulators, and certain kinds of switched capacitors change state based on system parameters such as a measured node voltage or line current.

1.3.2.2 Constant-Power and Constant-Current Loads

The voltage and current phasors of constant-power, constant-current, and ZIP loads cannot be determined directly from system inputs and outputs (constant-current loads have a constant-current magnitude but the angle is a degree of freedom). The equations, derived from KVL and KCL, which describe systems with these kinds of loads are non-linear. It is necessary to use iterative numerical methods to solve these circuit equations. In a distribution system model, any node with a constant-power load cannot be eliminated without loss of model accuracy.

1.3.2.3 Transformers

The coupled windings of transformers are subject to the non-linear electromagnetic physics equations; however, transformers are designed to operate in a linear region during normal operation. Nonlinear modeling of transformers is generally not necessary except during transient simulation. Transformer modeling for transient simulation is discussed in [44].

1.3.2.4 Surge Arresters

Surge arresters have a highly nonlinear I-V characteristic: they conduct minimal current under normal voltage conditions but sink a very high amount of current when subjected to an overvoltage condition. This behavior helps to protect other system components from transient overvoltage. It is generally not necessary to model the nonlinear characteristics of surge arrestors except during transient simulation. Surge Arrester modeling for transient simulation is discussed in [45].

1.3.3 Load-Flow Simulation

Load-flow simulations are used to determine the node voltages and line currents of a system given the source voltage and load magnitudes. For AC distribution systems, load-flow simulations are performed in the steady-state phasor domain. Load-flow algorithms can solve systems with constant-power, constant-current, and ZIP loads. Additional simulation of control logic can be used to determine the state of linear time-varying components whose states depend on node voltages and/or line currents. Several industrial and open source tools exist to perform load-flow simulations for distribution systems including CYMDIST [27], Synergi [28], WindMil [29], OpenDSS [24], and GridLAB-D [26].

1.3.3.1 Forward-Backward Sweep Algorithm

The forward-backward sweep algorithm can be used to solve the load-flow problem for systems with radial topology. The algorithm is developed for distribution systems in detail in [4]. The algorithm is summarized as follows:

Forward Sweep

Beginning with the nodes at the source voltage and progressing downstream, the voltage of each adjacent downstream node is calculated using Ohm's law, the interconnecting line impedance, and the previously estimated (or zero-initialized) line current.

Backward Sweep

Beginning with each end-of-line nodes and progressing upstream, the current flowing into the node from the upstream line is calculated using KCL, the downstream line current, any

adjacent branch currents, and the shunt current obtained using the previously estimated node voltage.

Iteration and Convergence

The forward sweep and backward sweep are alternated iteratively until a set of convergence criteria are met.

1.3.3.2 System Equation Algorithms

Distribution system models can be expressed as a system of non-linear equations. Algorithms such as the Newton-Raphson method can be used to solve systems of non-linear equations and applied to solve the load-flow problem as discussed in [42] and in other power systems texts. The net power flow into a node must equal zero according to KCL. A system of non-linear equations can be developed to express the net power flow into each node in terms of the admittance to adjacent nodes, the node voltages, and the shunt load (constant-power or otherwise). The Jacobian of this system of equations can be obtained and used to solve for the unknown system voltages in terms of the other known quantities. The sparseness of the matrix of admittances between nodes in large systems can be leveraged to improve the efficiency of the algorithm. Other methods of solving the load-flow problem using systems of equations include current injection methods [46] and fixed-point iteration methods [23].

1.3.3.3 Simulation of Control Logic

In physical distribution systems, load tap changers, line regulators, and some switched capacitors change state based on measured voltages or currents. In order to simulate this behavior, an initial load-flow solution is performed; the appropriate voltages and currents for

each controlled component are checked and, if necessary, the appropriate component states are changed and the load-flow problem is resolved. This introduces an additional iterative control loop external to the iterative load-flow algorithms. Device time coordination can also be simulated by prioritizing components by lowest delay time: component states are changed in order, as required until a satisfactory solution is found. When devices are poorly coordinated, this algorithm is not guaranteed to converge. In the physical world, this non-convergence manifests as hunting behavior.

1.3.3.4 Quasi-Static Time-Series Simulation

Slow changes (e.g. on the order of seconds, minutes, or hours) can be simulated using a series of load-flow solutions. At each time step, a load-flow solution with control logic simulation is obtained using the inputs (source voltage and load levels) for that time step and an initial set of component states from the control logic simulation from the previous state. This method can be used to simulate load and distributed generation variability on a distribution system over a period of time. A QSTS simulation introduces a third temporal loop outside of the base load-flow algorithm control logic loop. Quasi-static time-series simulation was initially developed on the open source platforms OpenDSS and GridLAB-D; industry need has led to implementation in CYMDIST.

2.0 MODEL CHARACTERIZATION

Linear time-invariant (LTI) system characterization is well understood [38, 39]; however, power systems models contain both time-varying and non-linear components. Non-LTI components can be put into two categories: (1) time-varying controlled elements such as switches and voltage regulators, and (2) nonlinear ZIP loads. Each of these types of components must be considered in power system model characterization.

2.1 PHASOR-DOMAIN CHARACTERISTIC EQUATIONS

In QSTS analysis, node voltages and branch currents are expressed as steady-state phasors. For some circuit segments, it is possible to uniquely determine the change in voltage across the segment (using KVL) and the change in current from input to output (using KCL) or change in power in terms of the input and output voltages and currents. In this dissertation, a distribution system phasor-domain characteristic equation is defined as an expression steady-state input and output voltages and currents as well as topological parameters (e.g. impedance between two buses or power of a shunt load). Equation 11 shows a general characteristic equation of a distribution system segment.

$$\begin{bmatrix}0\\0\end{bmatrix} = \begin{bmatrix}f(V_{in}, I_{in}, V_{out}, I_{out})\\g(V_{in}, I_{in}, V_{out}, I_{out})\end{bmatrix} \quad \textbf{(11)}$$

In some cases it is possible to rearrange the characteristic equations to express the steady-state output voltage and current each in terms of the input voltages and currents. In this dissertation, such a relationship is defined as a transfer equation. Equation 12 shows a general matrix formulation of the voltage and current transfer functions for a distribution system segment.

$$\begin{bmatrix}V_{out}\\I_{out}\end{bmatrix} = \begin{bmatrix}f(V_{in}, I_{in})\\g(V_{in}, I_{in})\end{bmatrix} \quad \textbf{(12)}$$

The orientation of voltages and currents that will be used in this dissertation are shown in Figure 2. This convention is intuitive when considering load flow in power systems, but is not universal in electrical engineering.

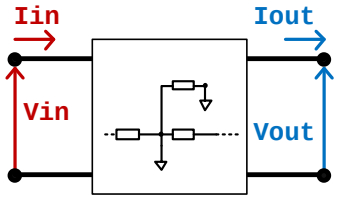

Figure 2. Segment Represented as a Non-Linear Two-Port Network

Note that not all segments have characteristic equations and not all segments that have characteristic equations have transfer equations as defined in this dissertation. The realization of a phasor domain transfer function can be substituted into a distribution system model to

approximate the behavior of that segment. When a complex system segment is represented by a simpler transfer function, quasi-static time-series analysis computation effort is reduced. In section 5 of this dissertation, a case study is performed in which a six-bus segment is reduced to a two-bus segment. It is anticipated that it will be possible to achieve even more reduction for larger systems.

2.2 DISTRIBUTION MODEL SEGMENTATION AND REDUCTION

A full distribution system model can be simplified by isolating buses of interest to a particular study. The full detail of the model between buses of interest can be replaced with simplified segments. The result of this process is a simplified, segmented model.

Branches and loads can be combined according to various sets of simplifying assumptions [31, 40]. In this dissertation, methods of deriving segments by combining branches and loads will be called inspection methods.

An alternative method for distribution system segment simplification can be achieved using the characteristic transfer equations of a particular segment topology. Known data from the terminals of a distribution system segment are applied to the transfer functions of an assumed simplified topology, solving for the parameters of the simplified topology. In this dissertation, a simplification method that involves simplifying individual segments of a model individually, called segment substitution, is introduced.

2.2.1 Inspection Methods

Distribution system segments can be simplified by inspection. This type of model order reduction requires a system model with segments of higher complexity and a set of simplifying assumptions about load behavior. The performance of the equivalent segment will depend on how close the original load behavior is to the simplified load behavior.

Step 1: Eliminate Trivial Nodes

Distribution system models can include nodes of physical significance but trivial electrical significance. For example, a section of ACSR overhead conductor spliced during a repair between pre-existing AAC overhead conductors might be modeled as separate conductors. The nodes in between may not directly serve any load. In this dissertation, a trivial node is defined as a node with linear or nonexistent load between two linear branches. The adjacent linear branches can be simplified into an equivalent linear branch without loss of model fidelity.

Step 2: Adopt a Simplified Load Type

Nodes containing constant-power loads or ZIP loads cannot be combined without loss of model fidelity. However, constant-impedance loads and constant-current loads can be combined. Assuming that the load behaves similarly to a constant-impedance or constant-power load allows the branches to be combined and nodes to be eliminated.

Step 3: Combine Branches and Eliminated Nodes

Using KVL and KCL, nodes with constant-impedance or constant-current load can be eliminated or combined and adjacent branches can be combined to create an equivalent segment.

2.2.2 Induction Methods and Segment Substitution

Distribution system segments can be simplified by induction using a process called segment substitution. This type of model order reduction requires system data at the input and output of full segments. The data can be obtained from sensors or by simulation of the full system model. The simplified segment will match the behavior of the original system for operating conditions similar to those that produced the input and output data. More complex topologies model segment behavior for a wider range of conditions but: (1) require more input and output data, (2) have transfer functions that are more difficult to obtain and more difficult to solve, and (3) ultimately reduce the order of the distribution system model to a lesser degree.

Step 1: Assume a Simplified Segment Topology

A general topology appropriate for distribution systems may be used or, if any physical topological information is available, a more targeted topology for a particular segment may be selected (e.g. if it is known that there are no step-down transformers in a distribution system, simplified segments do not need to contain a transformer).

Step 2: Determine the Transfer Equations for the Assumed Topology

The transfer functions are obtained using KVL and KCL. The transfer functions may be nonlinear.

Step 3: Solve for the Parameters of the Topology Using Input and Output Data

Voltage and current data under different operating conditions are substituted into one or more instances of the transfer functions and used to solve for the topological parameters.

3.0 SEGMENT SIMPLIFICATION

Once nodes of interest have been identified, the interconnecting segments can be simplified. In this section, various methods of constructing a low-order approximation of a distribution system segment by inspection and by induction are presented.

A simple demonstration circuit is shown in Figure 3. The boxed portion represents the segment to be simplified.

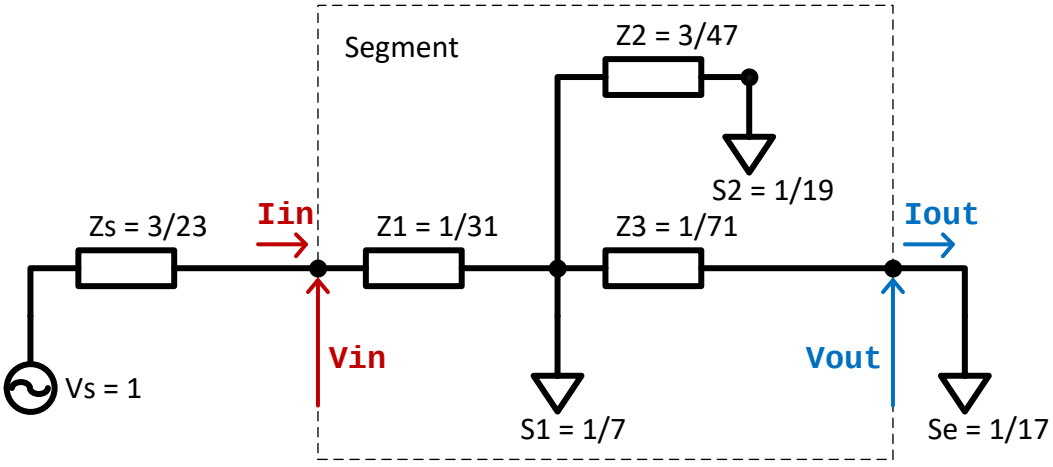

Figure 3. Demonstration Circuit

The schematic includes a rudimentary representation of distribution system lines and loads. All component values are in per-unit.

3.1 CONSTANT-IMPEDANCE SEGMENTS

For many distribution system segments, the only nonlinear components are the loads. If the loads can be considered to have constant-impedance behavior, the segment can be treated as a linear system.

3.1.1 Simplification by Inspection

A constant-impedance simplified segment can be obtained by combining impedances and eliminating internal nodes.

Step 1: Eliminate Trivial Nodes

There are no trivial nodes in the demonstration circuit.

Step 2: Adopt a Simplified Load Type

Figure 4 shows the demonstration circuit with loads modeled as constant impedances.

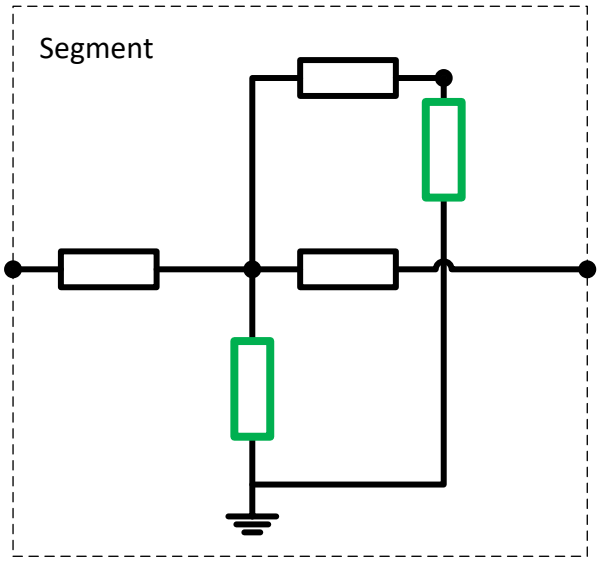

Figure 4. Demonstration Circuit with Constant-Impedance Load Approximation

Load impedance is determined according to Equation 13.

$$Z_{load} = \left(\frac{|V_{base}|^2}{S_{load}}\right)^* \quad \textbf{(13)}$$

The system base voltage is used as the base voltage at the load. Note that the model could be improved by using node voltages obtained from a load-flow solution at typical conditions.

Computed load impedances are listed in Table 1.

Table 1. Effective Load Impedances For Demonstration Circuit

Load	Size (pu)	Base Voltage (pu)	Impedance (pu)
S1	1/7	1	7
S2	1/13	1	13

Step 3: Combine Branches and Eliminate Nodes

The resulting impedance network can be simplified using KVL and KCL:

1. Series combination of Z2 and Z_load2
2. Parallel combination of (1) and Z_load1
3. Wye-delta transformation to eliminate the internal node
4. Invert shunt resistances to express as admittances

The resulting PI segment is shown in Figure 5 with impedance and admittance values in per-unit rounded to six digits.

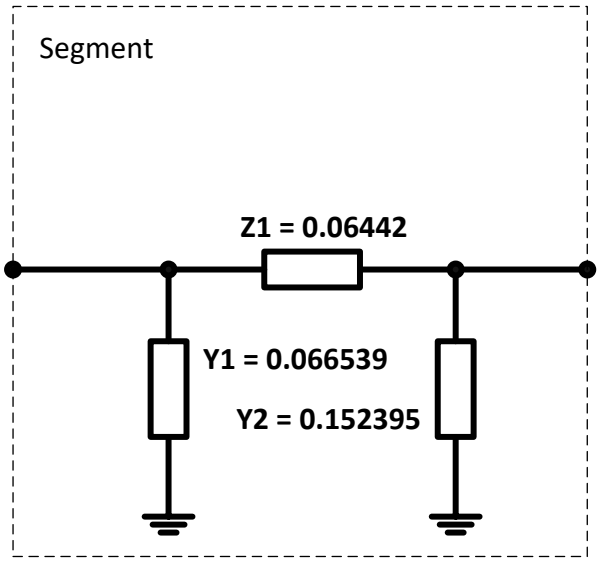

Figure 5. Demonstration Circuit Simplified with Constant-Impedance Approximation

3.1.2 Simplification by Induction

The demonstration circuit segment can be mapped onto a number of different constant-impedance topologies using induction. In this section, a balanced PI segment will be used.

Step 1: Assume a Simplified System Topology

A balanced PI section is shown in Figure 6.

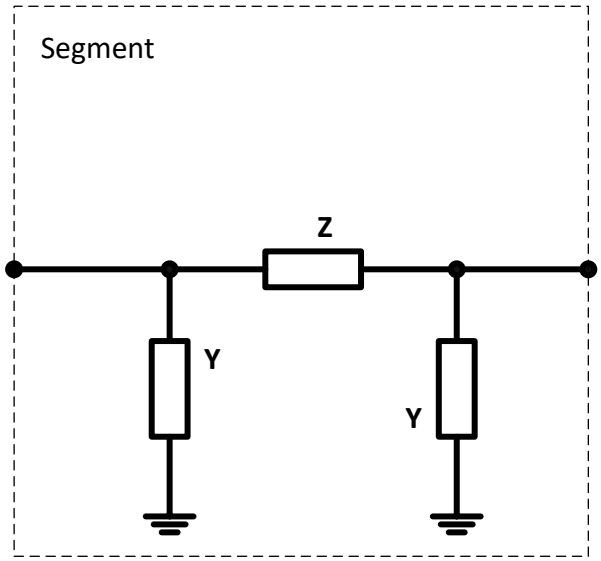

Figure 6. Constant-Impedance PI Section Topology for Simplification by Induction

Step 2: Determine the Transfer Equations for the Assumed Topology

The transfer equations are obtained using KVL and KCL and shown in Equations 14 and 15.

$$V_{out} = V_{in} * (1 + YZ) + I_{in} * (-Z) \quad \textbf{(14)}$$

$$I_{out} = V_{in} * (-2Y - Y^2Z) + I_{in} * (1 + YZ) \quad \textbf{(15)}$$

Step 3: Solve for the Parameters of the Topology Using Input and Output Data

The balanced PI section has one series parameter corresponding to the change in voltage from input to output and one shunt parameter corresponding to the change in current from input to output; therefore, this is a one-measurement segment.

Data for the demonstration circuit is shown in Table 2.

Table 2. Demonstration Circuit One-Measurement Load-Flow Data

#	Vsrc	Vin	Vout	Iin	Iout
1	1.05	1.013779	1.003996	0.277691	0.058589

The Vsrc parameter represents the voltage at the substation and does not change when the load level changes. The other parameters correspond to load-dependent values for a segment out on the feeder. One Vsrc value may lead to many sets of segment measurements, corresponding to different load levels.

The parameter values obtained from the solving the transfer functions for Y and Z using the data from Table 2 are shown in Table 3.

Table 3. Topological Parameters for Balanced PI Section Simplified Segment

Parameter	Value
Z	0.058368
Y	0.108586

The simplified segment is shown in Figure 7.

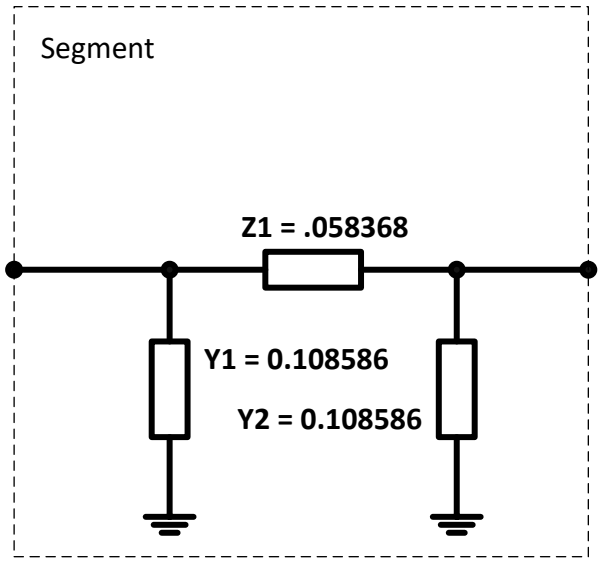

Figure 7. Demonstration Circuit Simplified with PI Section Topology

The shunt impedance values obtained using this induction method are different from the shunt impedance values obtained using the inspection method because the simplifying constraints were different: the induction method requires that the input and output measurements of the simplified model match the full model while requiring both shunt elements of the PI section to be equal; the inspection method preserves the linear network created by the simplifying constant-impedance load assumption.

3.2 CONSTANT-CURRENT APPROXIMATIONS

The load-flow problem with constant-current loads is non-linear because the current angle will vary in an absolute sense (although it is fixed relative to the local voltage angle). However,

constant-current loads at different nodes can be combined without losing accuracy because the load current magnitude does not depend on the node voltage.

3.2.1 Simplification by Inspection

Reduction of power circuits with constant-current loads are discussed in [30]. Distribution system reduction is discussed in detail in [31]. The methods described in [31] are summarized below and applied to the demonstration circuit.

Step 1: Eliminate Trivial Nodes

There are no trivial nodes in the demonstration circuit.

Step 2: Adopt a Simplified Load Type

Figure 8 shows the demonstration circuit with constant-current loads.

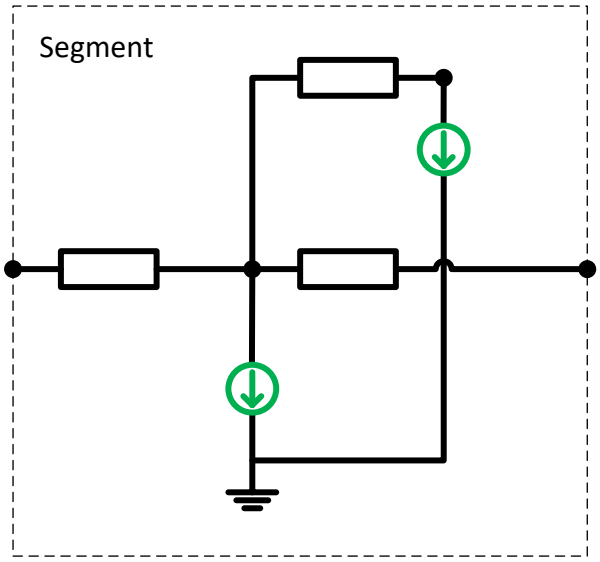

Figure 8. Demonstration Circuit with Constant-Current Load Approximation

Load current is determined according to Equation 16.

$$|I_{load}| = \left|\frac{S_{load}}{V_{base}}\right| \quad \textbf{(16)}$$

The system base voltage is used as the base voltage at the load. Note that the model could be improved by using node voltages obtained from a load-flow solution at typical conditions. Computed load currents are listed in Table 4.

Table 4. Effective Load Currents for Demonstration Circuit

Load	Size (pu)	Base Voltage (pu)	Current (pu)
S1	1/7	1	1/7
S2	1/13	1	1/13

Step 3: Combine Branches and Eliminated Nodes

The resulting impedance network can be simplified using KVL and KCL:

1. Elimination of Z2
2. Summation of I_load1 and I_load2
3. Redistribution to eliminate the internal node
4. Summation of Z1 and Z3

The resulting segment is shown in Figure 9 with impedance and current values in per-unit rounded to six digits.

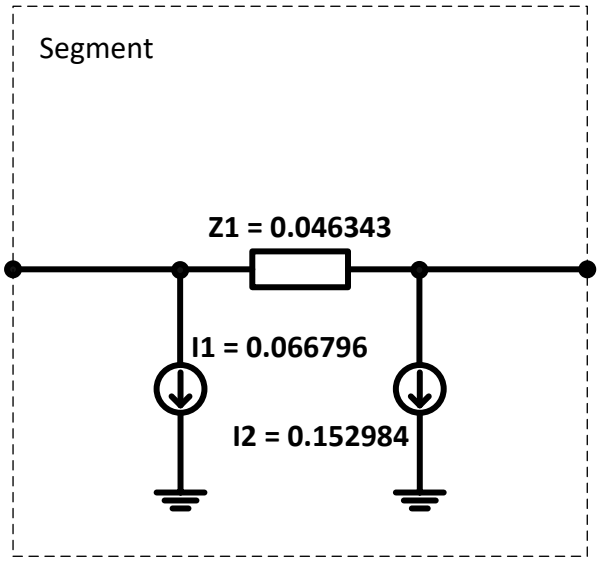

Figure 9. Demonstration Circuit Simplified with Constant-Current Approximation

3.2.2 Simplification by Induction

Using a constant-current assumption and one set of input-output voltage and current measurements, a segment can be mapped to a shunt constant-current load and a series impedance. In this simple topology, change in current is mapped to the constant-current load and voltage drop is caused by the internal load and external load, proportionate to their current drawn.

Step 1: Assume a Simplified System Topology

A one-measurement constant-current topology is shown in Figure 10.

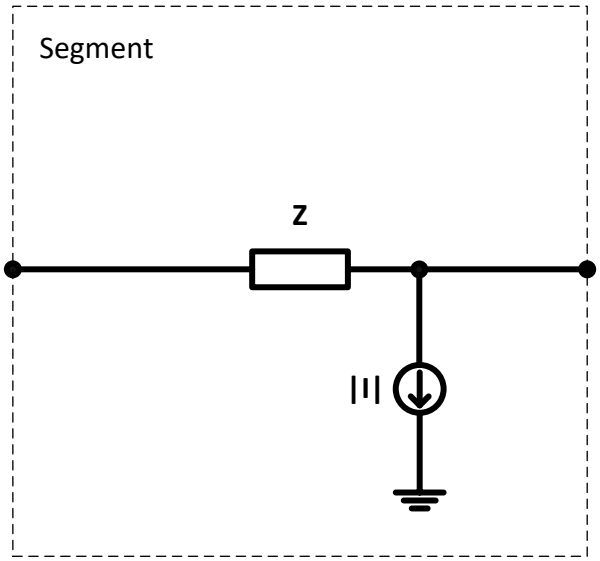

Figure 10. Constant-Current One-Load Topology for Simplification by Induction

Step 2: Determine the Transfer Equations for the Assumed Topology

The transfer equations are obtained using KVL and KCL and shown in Equations 17 and 18.

$$V_{out} = V_{in} - I_{in} * Z \quad \textbf{(17)}$$

$$I_{out} = I_{in} - I \quad \textbf{(18)}$$

Note that the load in this topology is constant current magnitude; for complex systems, I may be complex and |I| is a characteristic parameter of this topology.

Step 3: Solve for the Parameters of the Topology Using Input and Output Data

This segment has one series parameter and one shunt parameter and is therefore a one-measurement segment. Data for the demonstration circuit was shown in Table 2. The parameter values obtained from the transfer functions using the data are shown in Table 5.

Table 5. Topological Parameters for Constant-Current One-Load Simplified Segment

Parameter	Value
Z	0.035230
|I|	0.219102

The simplified segment is shown in Figure 11.

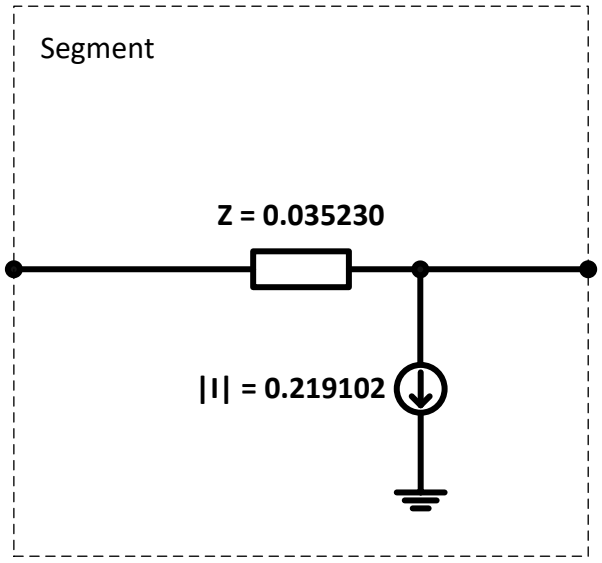

Figure 11. Demonstration Circuit Simplified with Constant-Current Topology

3.3 LINEAR TWO-PORT NETWORK APPROXIMATIONS

When the transfer functions for a distribution system segment express the output voltage and current as a linear combination of the input voltage and current, the segment constitutes a linear two-port network [38, 40]. Analytical advantages of linear two-port networks include (1) matrix multiplication to obtain transfer functions of a cascaded system, solution of a linear system of equations to obtain the characteristic parameters, and (3) immediate compatibility with load-flow solution algorithms (e.g. the forward-backward sweep) without requiring a topological realization. In Equation 19, constants a, b, c, and d referred to as inverse transmission line parameters; one set of characteristic parameters of a two-port network [40].

$$\begin{bmatrix} V_{out} \\ I_{out} \end{bmatrix} = \begin{bmatrix} f(V_{in}, I_{in}) \\ g(V_{in}, I_{in}) \end{bmatrix} = \begin{bmatrix} a & b \\ c & d \end{bmatrix} \begin{bmatrix} V_{in} \\ I_{in} \end{bmatrix} \quad \textbf{(19)}$$

Linear two-port networks can model passive components and dependent sources but not independent sources. This means that linear two-port network models may be reasonable when the internal segment load is either passive or follows a global system load shape (i.e. the internal load depends on the input current or output current). An induction method can be used to obtain a linear two-port network approximation of a system. Impedance networks including the simplified segment in section 3.1.1 can be obtained by inspection using simplifying assumptions; however, this section is concerned with obtaining linear two-port networks with four independent parameters by induction.

3.3.1 Solving for Characteristic Parameters by Induction

A linear two-port network can be characterized by parameters a, b, c, and d instead of topological parameters like Z, Y, or I. The parameters can be obtained by induction with two sets of input-output measurements. Using these measurements, the transfer matrix can be expanded to obtain a linear algebraic expression that can be solved for the characteristic parameters as shown in Equation 20.

$$\begin{bmatrix} V'_{out} \\ V''_{out} \\ I'_{out} \\ I''_{out} \end{bmatrix} = \begin{bmatrix} V'_{in} & I'_{in} & 0 & 0 \\ V''_{in} & I''_{in} & 0 & 0 \\ 0 & 0 & V'_{in} & I'_{in} \\ 0 & 0 & V''_{in} & I''_{in} \end{bmatrix} * \begin{bmatrix} a \\ b \\ c \\ d \end{bmatrix} \quad \textbf{(20)}$$

Data for the demonstration circuit is shown in Table 6. Row 1 is the same as in Table 2; row 2 is obtained from a second load flow.

Table 6. Demonstration Circuit Two-Measurement Load-Flow Data

#	Vsrc	Vin	Vout	Iin	Iout
1	1.05	1.013779	1.003996	0.277691	0.058589
2	1.04	1.003397	0.993510	0.280626	0.059208

The parameter values obtained from solving equation 20 for a, b, c, and d are shown in Table 7.

Table 7. Inverse Transmission Line Parameters for Two-Port Network Simplified Segment

Parameter	Value
a	0.999999
b	-0.035228
c	0.000043
d	0.210832

3.3.2 Stability of Characteristic Parameters in Distribution System Circuits

The suitability of a simplified segment depends on the resemblance of the full circuit to the assumed topology. Because the two-port network does not require a topological mapping, it is not immediately obvious that the framework is suitable to represent distribution system segments. Preliminary testing suggests that a two-port network can adequately represent a distribution system segment for QSTS when the system loads follow a global load shape but not when the internal segment load follows a different load shape than the external downstream load. When the external load multiplier is larger than the internal load multiplier, the two-port network approximation tends to underestimate the output current and when the external load multiplier is smaller than the internal load multiplier, the two-port network approximation tends to overestimate the output current.

A per-phase circuit based on problem 3.3 in [4] shown in Figure 12 was simulated to obtain two-port network parameters under a variety of conditions.

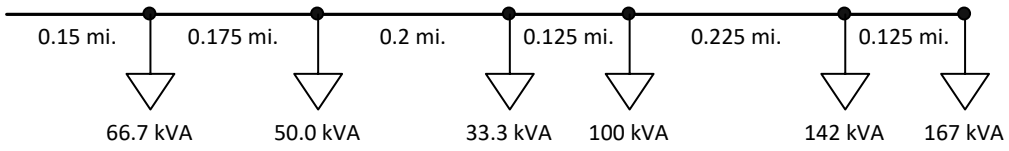

Figure 12. Per-Phase Version of Problem 3.3 in [4]

Global Load Shape

Two-port parameters were obtained for load-flow solution pairs symmetric about the nominal operating point (source voltage 1.04 p.u. and load multiplier 1). Solution pairs were rejected when the source voltage and global load multiplier produced an end-of-line voltage below 0.95 p.u. or above 1.05 p.u. Figure 13 shows the operating point pairs that were used to compute a, b, c, and d.

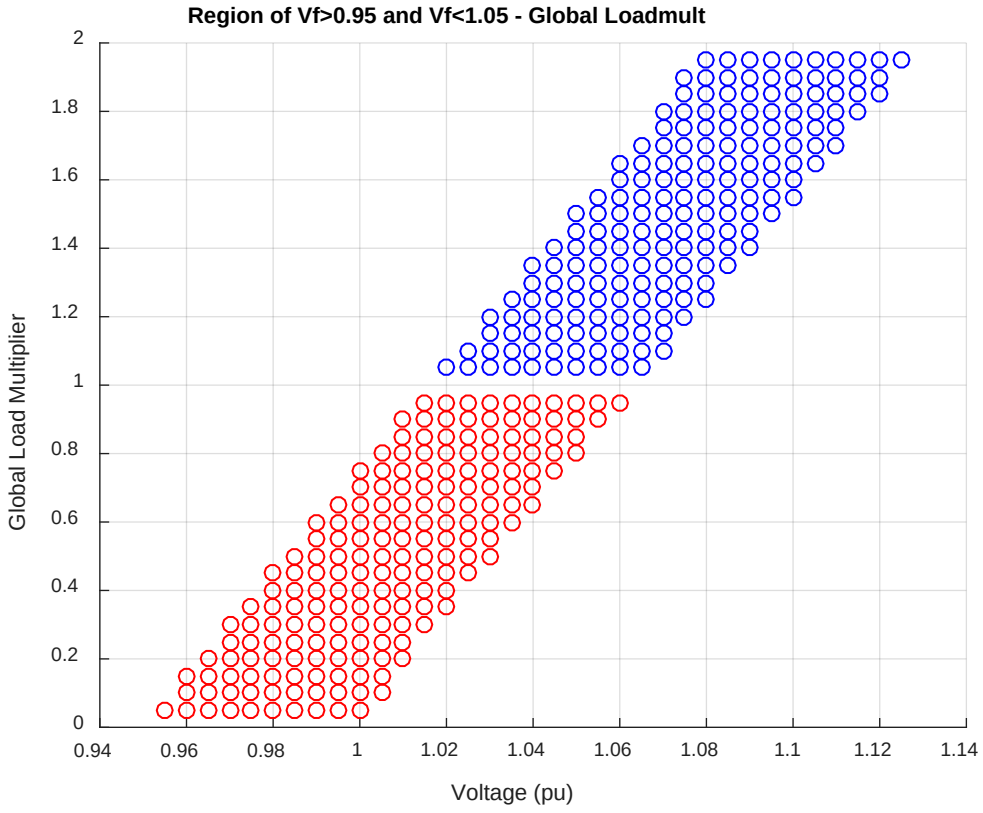

Figure 13. Operating Condition Pairs with Global Load Multiplier

The scatter plot of inverse transmission line parameters shown in Figure 14 qualitatively show that the parameters are similar for a range of source voltages and load multipliers. This suggests that the linear two-port network approximation is reasonable for a range of conditions.

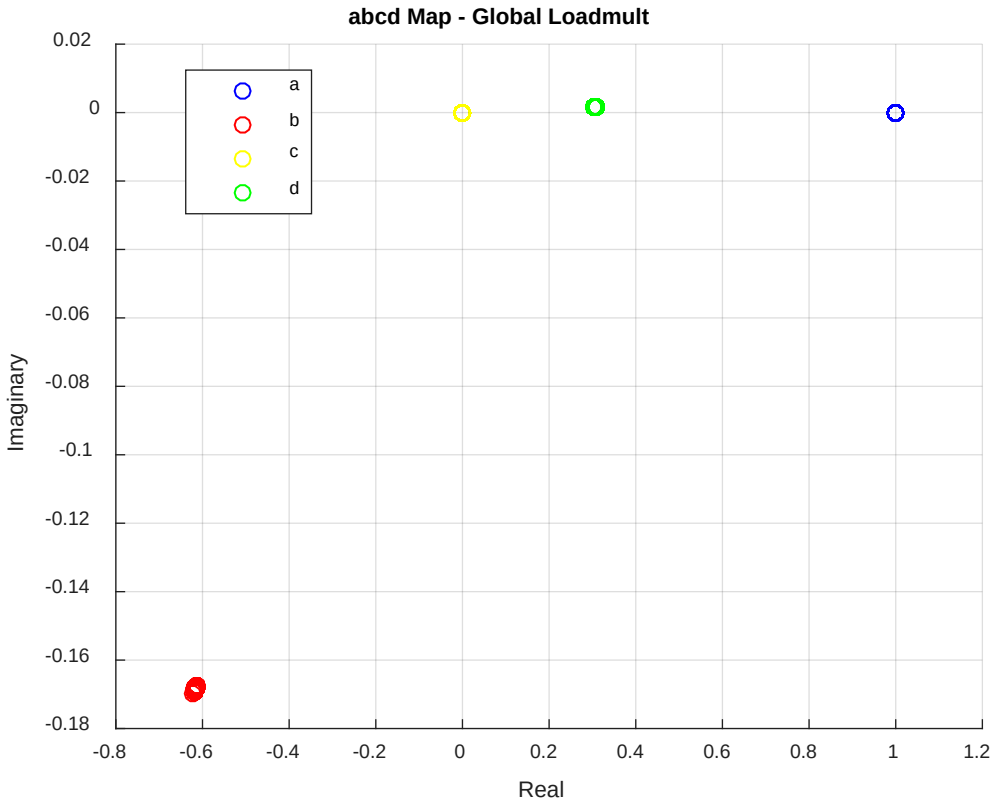

Figure 14. Discovered Parameters with Global Load Multiplier

Independent External Load Shape

Two-port parameters were obtained for load-flow solution pairs symmetric about the nominal operating point (source voltage 1.04 p.u. and load multiplier 1). Solution pairs were rejected when the source voltage and external load multiplier produced an end-of-line voltage was below 0.95 p.u. or above 1.05 p.u.

Figure 15 shows the operating point pairs that were used to compute a, b, c, and d.

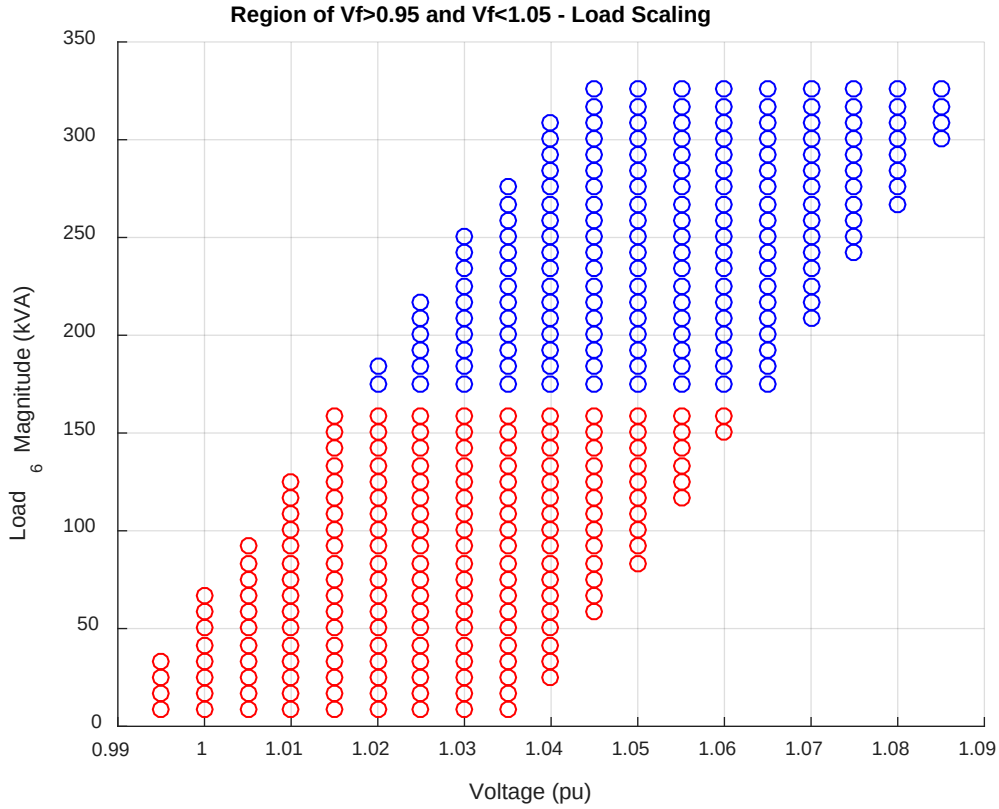

Figure 15. Operating Condition Pairs with Separate Load Multipliers

The scatter plot of inverse transmission line parameters shown in Figure 16 qualitatively shows that the parameters move significantly with source voltage and/or external load magnitude. This parameter movement suggests that the linear two-port network approximation is not reasonable when the internal and external load multipliers vary independently.

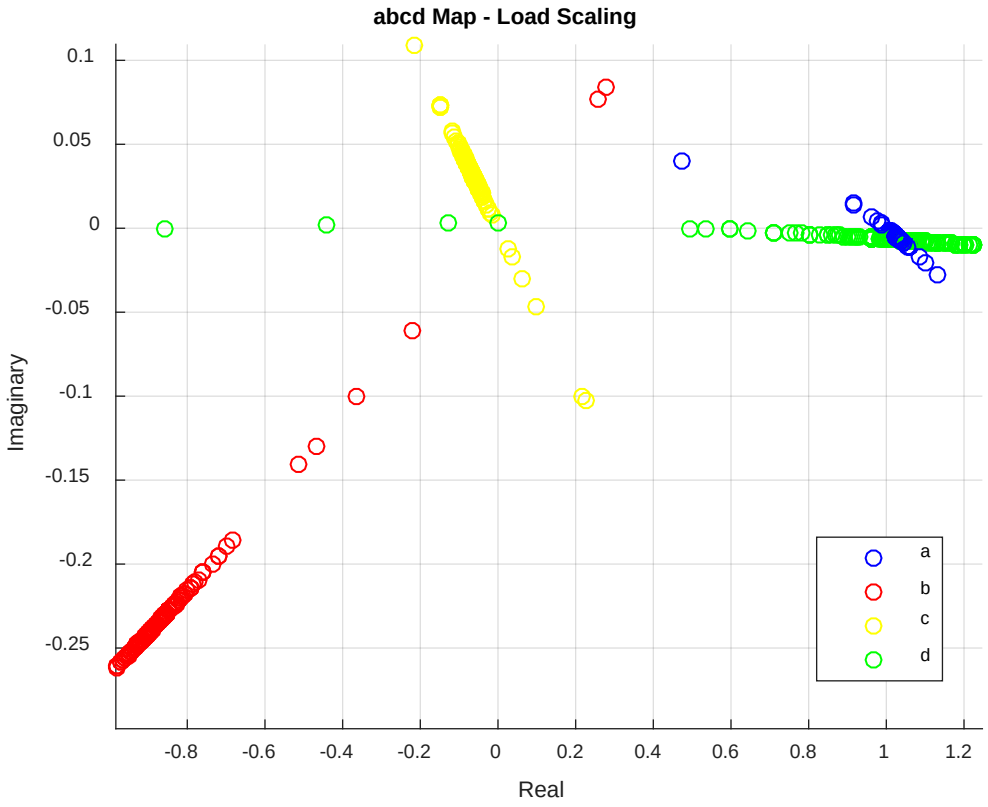

Figure 16. Discovered Parameters with Separate Load Multipliers

3.3.3 Forward-Backward Sweep for Two-Port Segments

The linear two-port network transfer equations can be used directly in the forward-backward sweep algorithm [4].

Forward Sweep

During the forward sweep, the output voltage is estimated according to the voltage transfer function (Equation 21) using the voltage estimate from the upstream segment and the current estimated in the previous backward sweep.

$$V_{out} = a * V_{in} + b * I_{in} \tag{21}$$

Backward Sweep

During the backward sweep, the input current is estimated according to the reformulated current transfer function (Equation 22) using the current estimate from the downstream segment and the voltage estimate from the previous forward sweep.

$$I_{in} = \frac{I_{out} - c * V_{in}}{d} \tag{22}$$

3.3.4 Realization of the General Linear Two-Port Network

While a topological realization is not required for the linear two-port network, it is possible to develop a realization. For a general realization, expressions for a, b, c, and d must be linearly independent such a set of arbitrary inverse transmission line parameters be mapped. More than one realization of the general linear two-port network is possible; however, not all segment topologies that are linear two-port networks can realize the general linear two-port network.

The topology shown in Figure 17 satisfies the requirements for general linear two-port network realization and provides some intuition into linear two-port network segment behavior in distribution systems. This topology includes a shunt admittance Y, a series impedance Z, a current-dependent current source output equal to h times the input current, and a transformer with turns ratio N:1. These parameters loosely correspond to components that occur in a distribution system including series impedances, shunt admittances, internal loads, and step-down transformers; however, it is important to note that the component parameter values represent mathematical degrees of freedom constrained by input and output measurements.

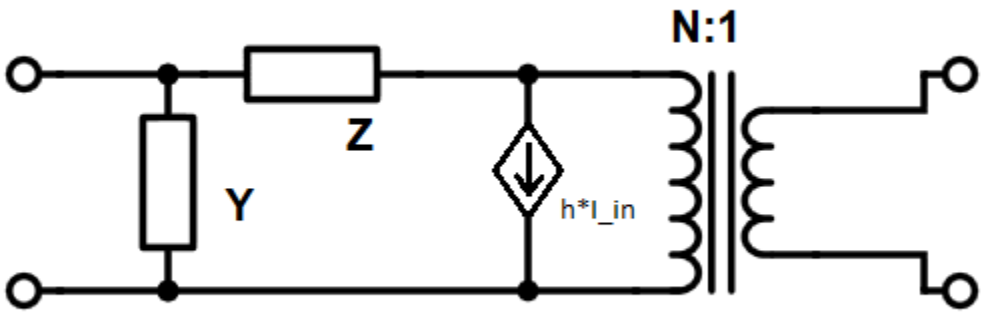

Figure 17. Topological Realization of Linear Two-Port Network

The transfer equations can be obtained using KVL and KCL and are shown in Equations 23 and 24.

$$V_{out} = V_{in} * \left(\frac{1+YZ}{N}\right) + I_{in} * \left(\frac{-Z}{N}\right) \quad \textbf{(23)}$$

$$I_{out} = V_{in} * (-NY) + I_{in} * (N - Nh) \quad \textbf{(24)}$$

The expressions used to map inverse transmission line parameters are shown in Equations 25, 26, 27, and 28 and are linearly independent.

$$a = \frac{1 + YZ}{N} \quad \textbf{(25)}$$

$$b = \frac{-Z}{N} \quad \textbf{(26)}$$

$$c = -NY \quad \textbf{(27)}$$

$$d = N - Nh \quad \textbf{(28)}$$

These expressions only apply to the realization of the linear two-port network shown in Figure 17.

3.4 CONSTANT-POWER AND ZIP LOADS

Loads with a constant power component cannot be combined without loss of accuracy. Inspection methods require some assumption about load behavior in order to combine loads in a mathematically rigorous way; they are not directly compatible with ZIP loads and are not applicable to this section. Inductive methods can be used to map system measurements onto a simplified topology containing constant-power or ZIP loads.

The methods discussed in this section can be used to fit measurement data from a system onto any assumed topology of arbitrary complexity. Each set of input and output current and

voltage measurements yields two independent equations up to the number of characteristic parameters for an assumed topology.

3.4.1 Constant-Power Load Approximations

The inductive method can be used to map the demonstration circuit segment onto a constant-power load topology.

Step 1: Assume a Simplified System Topology

A simple constant-power load topology is shown in Figure 18 .

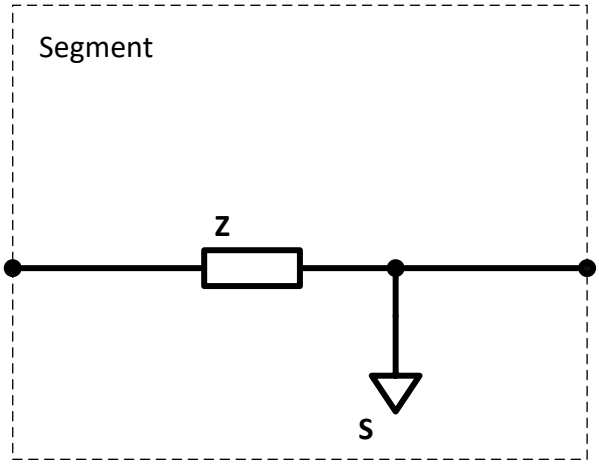

Figure 18. Constant-Power One-Load Topology for Simplification by Induction

Step 2: Determine the Transfer Equations for the Assumed Topology

The transfer equations are obtained using KVL and KCL and are shown in Equations 29 and 30.

$$V_{out} = V_{in} - I_{in} * Z \quad \textbf{(29)}$$

$$I_{out} = I_{in} - \left(\frac{S}{V_{in} - I_{in} * Z}\right)^{*} \quad \textbf{(30)}$$

Step 3: Solve for the Parameters of the Topology Using Input and Output Data

This topology has one series parameter and one shunt parameter and is therefore a one-measurement segment. Data for the demonstration circuit was shown in Table 2. The parameter values obtained from the transfer functions using the data are shown in Table 8.

Table 8. Topological Parameters for One-Measurement Constant-Power Simplified Segment

Parameter	Value
Z	0.035230
S	0.219977

The simplified segment is shown in Figure 19.

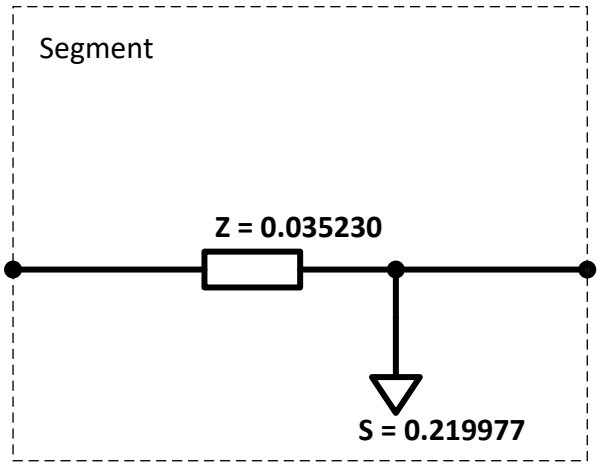

Figure 19. Demonstration Circuit Simplified with Constant-Power Topology

3.4.2 A Two-Measurement Segment Topology

In this section, a topology based on the realization of the two-port network discussed in section 3.3.4 is analyzed. This topology includes the following components:

- Z: series impedance to capture load losses
- Y: shunt admittance to capture no-load losses
- S: constant-power load
- N: transformer

The topology captures a range of possible distribution system behavior and is referred to as the Z-Y-S-N topology.

Step 1: Assume a Simplified System Topology

The Z-Y-S-N topology is shown in Figure 20.

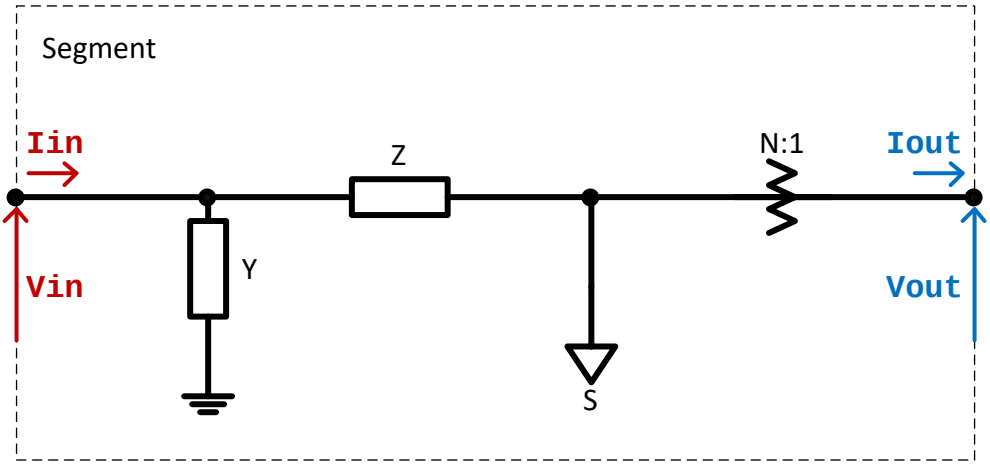

Figure 20. Z-Y-S-N Topology for Simplification by Induction

Step 2: Determine the Transfer Equations for the Assumed Topology

The transfer equations are obtained using KVL and KCL and are shown in Equations 31 and 32.

$$V_{out} = V_{in} * \left(\frac{1+YZ}{N}\right) + I_{in} * \left(\frac{-Z}{N}\right) \quad \textbf{(31)}$$

$$I_{out} = V_{in} * (-NY) + I_{in} * (N) - N * \left(\frac{S}{V_{in} * (1+YZ) - I_{in} * (Z)}\right)^{*} \quad \textbf{(32)}$$

Step 3: Solve for the Parameters of the Topology Using Input and Output Data

This topology has two series parameters and two shunt parameters and is therefore a two-measurement segment.

Data for the demonstration circuit was shown in Table 6. The parameter values obtained from the transfer functions using the data are shown in Table 9.

Table 9. Topological Parameters for Z-Y-S-N Simplified Segment

Parameter	Value
N	0.999993
S	0.220182
Y	-0.000203
Z	0.035227

The simplified segment is shown in Figure 21.

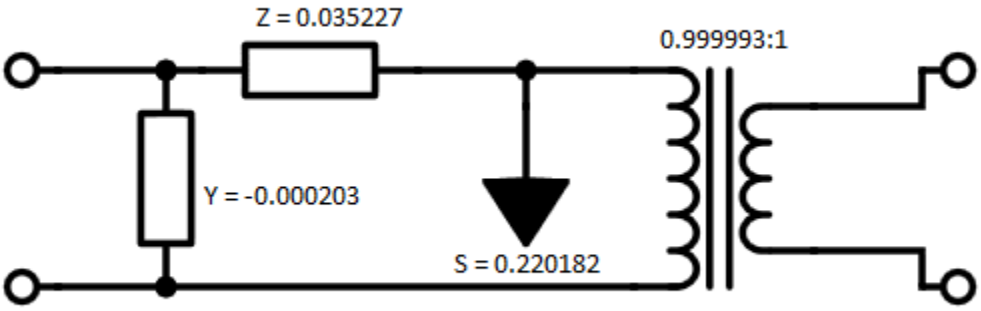

Figure 21. Demonstration Circuit Simplified by Induction with Z-Y-S-N Topology

3.4.3 Special Case – Parameter Recovery from Full Topology

A special case of the inductive method arises when the full system topology is known. The topological parameters can be fully recovered using input and output data. This process will be applied to the demonstration circuit.

Step 1: Assume a Simplified System Topology

The topology is shown with parameters masked in Figure 22.

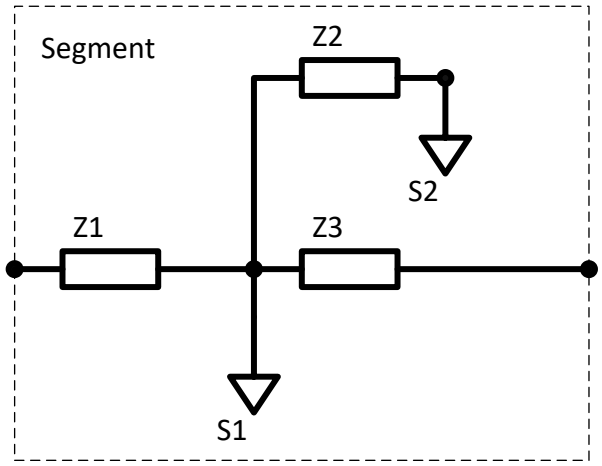

Figure 22. Known Segment Topology for Parameter Identification

Step 2: Determine the Transfer Equations for the Assumed Topology

The characteristic equations are obtained using KVL and balance of power and are shown in Equations 33 and 34. Note that it is not possible to solve for transfer functions in terms of the input parameters. These expressions can still be solved numerically.

$$V_{out} = V_{in} - I_{in}Z_1 - I_{out}Z_3 \tag{33}$$

$$S_1 + S_2 + \left| I_{in} - I_{out} - \left(\frac{S_1}{V_{in} - I_{in}Z1}\right)^* \right|^2 * Z_2 = (V_{in} - I_{in}Z_1) * (I_{in} - I_{out})^* \tag{34}$$

Step 3: Solve for the Parameters of the Topology Using Input and Output Data

This topology has five unknown parameters: two series parameters and three shunt parameters. Therefore, Equation 33 will be used with two measurements and Equation 34 will be used with three measurements. Data from three measurements is shown in Table 10. Data in the first two rows is the same as in Table 6.

Table 10. Demonstration Circuit Load-Flow Data for Parameter Recovery

#	Vsrc	Vin	Vout	Iin	Iout
1	1.05	1.013779	1.003996	0.277691	0.058589
2	1.04	1.003397	0.993510	0.280626	0.059208
3	1.02	0.982605	0.972505	0.286697	0.060487

The parameter values recovered from the numerical solution of transfer functions using the data are shown in Table 11.

Table 11. Topological Parameters Recovered by Induction

Parameter	Value
S1	0.142857
S2	0.076923
Z1	0.032258
Z2	0.063830
Z3	0.014085

3.4.4 ZIP Load Topologies

This section has demonstrated segment simplification for induction using topologies with constant-impedance, constant-current, and constant-power loads. The inductive process can be used for topologies with combined ZIP loads in two ways: (1) the ZIP coefficients are known as part of the topology and the total load is determined as a single parameter inductively, or (2) the ZIP coefficients are unknown and determined inductively alongside the total load using additional system measurements.

3.4.5 Observations

This section discussed various methods of simplifying a segment of the demonstration circuit shown in Figure 3. The effectiveness of each of these methods is compared in Section 4. The inspection methods rely on bus-by-bus procedures for simplification; the complexity of the simplification task depends on the number of buses. Among the induction methods, the one-measurement methods that can be realized using typical power system components are the easiest to implement because they only require one solution of the full model. Later in this dissertation (in Section 7), it will be demonstrated that simplification by inspection using a series-impedance shunt-ZIP load topology performs well for full systems.

4.0 METHOD COMPARISON

Several methods of varying complexity for simplifying distribution system segments have been introduced. In this section, circuit approximations of the demonstration circuit will be compared to the original circuit under a range of operating conditions.

4.1 BASELINE ANALYSIS OF THE DEMONSTRATION CIRCUIT

The performance of an approximated segment can be evaluated by comparing its behavior to the original segment over a range of operating conditions. To create a baseline, the demonstration circuit was simulated over two two-dimensional spaces: (1) source voltage versus the global load multiplier and (2) the internal S1 and S2 load multiplier versus the external Se load multiplier (See Figure 3).

In general, the performance of simplified segments derived by inspection depends on the validity of the simplifying assumptions; for circuits whose load closely approximates constant-current behavior, for example, the reduced equivalent constant-current segment will yield good segment approximations. The performance of simplified segments derived by induction depends on the similarity of the assumed topology to the actual topology.

The input and output voltages and currents over the source voltage vs. global load multiplier space are shown in Figure 23. The color map indicates the per-unit value of the

corresponding parameter from a load-flow at the conditions indicated by the x and y axis: values close to 1 p.u. are green, values greater than 1 p.u. are more red and values less than 1 p.u. are more blue. Decreasing the source voltage decreases the input and output voltages and has a negligible impact on the input and output currents. Decreasing the global load multiplier increases all load currents; thereby increasing the input current and output current, and decreases both the input and output voltages by increasing the voltage drop across the impedances.

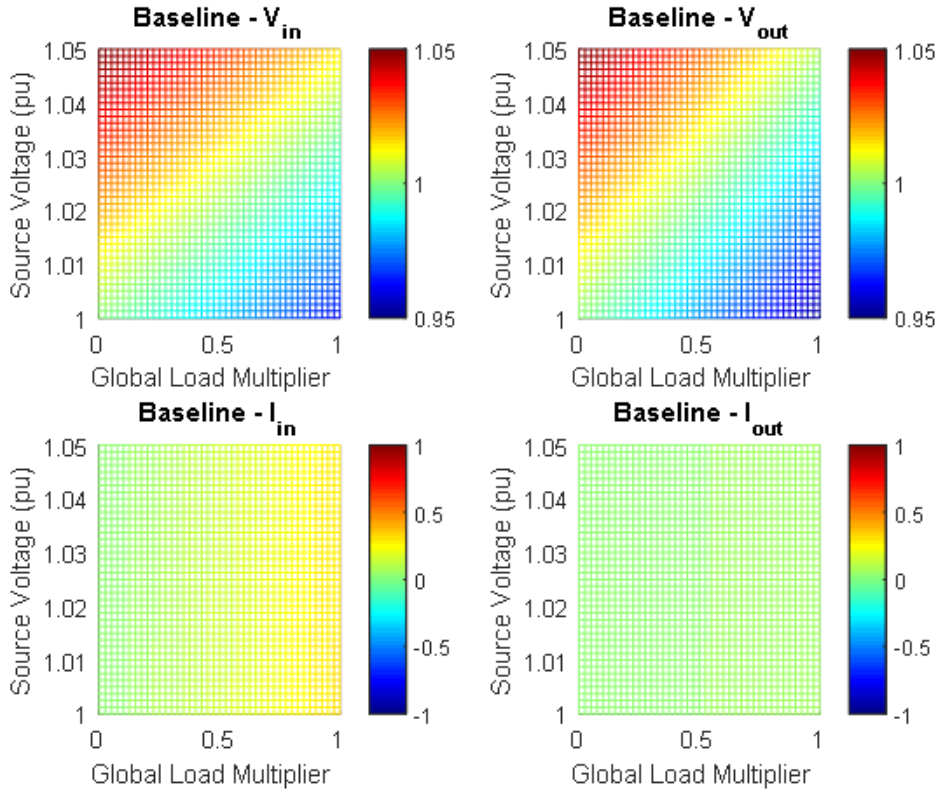

Figure 23. Load-Flow over Source Voltage vs. Global Load Multiplier Space

The input and output voltages and currents over the internal load multiplier vs. external load multiplier space are shown in Figure 24. Again, the color map indicates the per-unit value of the corresponding parameter from a load-flow at the conditions indicated by the x and y axis: values close to 1 p.u. are green, values greater than 1 p.u. are more red and values less than 1 p.u. are more blue. Increasing or decreasing either load multiplier has a roughly proportional impact on the input and output voltages as well as the input current. The output current depends only on the external load multiplier.

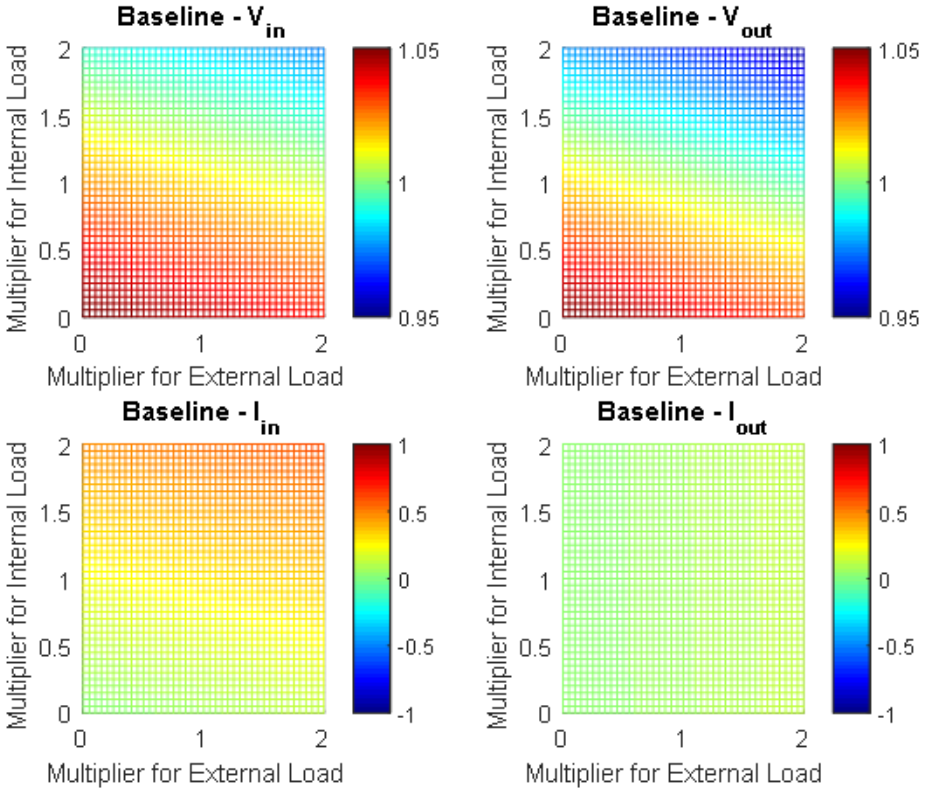

Figure 24. Load-Flow over Internal vs. External Load Multiplier Space

4.2 SEGMENT PERFORMANCE COMPARISON

The output voltage will be used to compare the performance of different methods of simplification. The magnitude of the percent absolute error of each approximation relative to the full demonstration circuit is plotted over each of the two dimensional spaces shown in the baseline analysis. The color maps in this section indicate the absolute percent error (percent of base) of a load flow solution performed using a simplified segment relative to the load flow solution performed using the full demonstration circuit (Figure 3) at the conditions indicated by the x axis and y axis. Error values close to zero are black and error values greater than 0.1 are light gray. In general, voltage error on the order of 0.1%, or 0.12 V on a 120-V base (typical wall outlet voltage). This error is expected to be acceptable for distribution system studies. The error values are specific to the topology of the system and of the original segment; they can be used to make relative comparisons between simplification methodologies.

Constant-Impedance Approximation by Inspection (Figure 5)

Figure 25 shows the percent absolute error of the output voltage relative to the baseline over the source voltage vs. global load multiplier space (left) and the internal load multiplier vs. external load multiplier space (right).

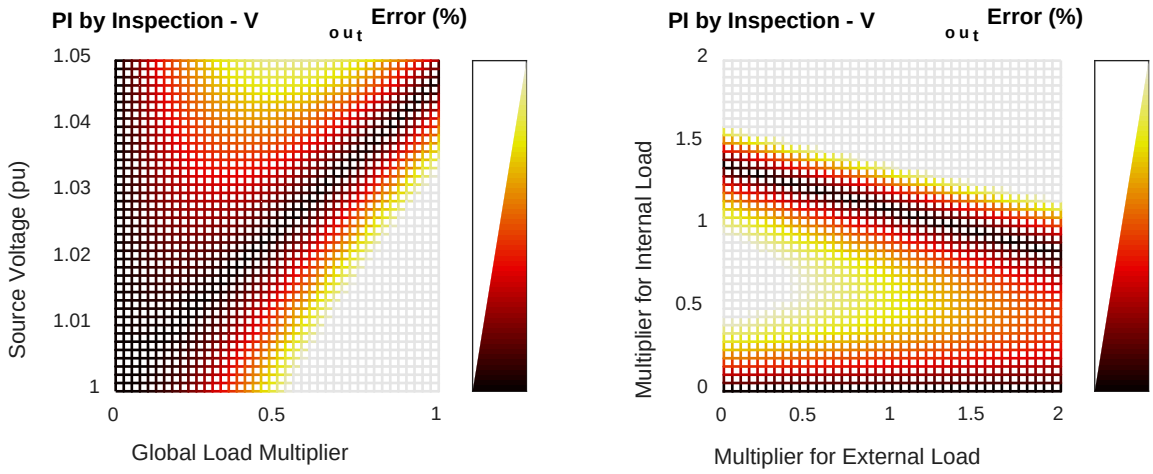

Figure 25. Performance of Segment Simplified with Constant-Z Load Approximation

Constant-impedance approximation by inspection produces a simplified segment that is reasonably accurate for low internal load conditions and under conditions where the internal load voltage matches the base voltage (used to obtain approximate the load impedance). The overall performance of the approximation is relatively poor.

Constant-Impedance Approximation by Induction (Figure 7)

Figure 26 shows the percent absolute error of the output voltage relative to the baseline over the source voltage vs. global load multiplier space (left) and the internal load multiplier vs. external load multiplier space (right).

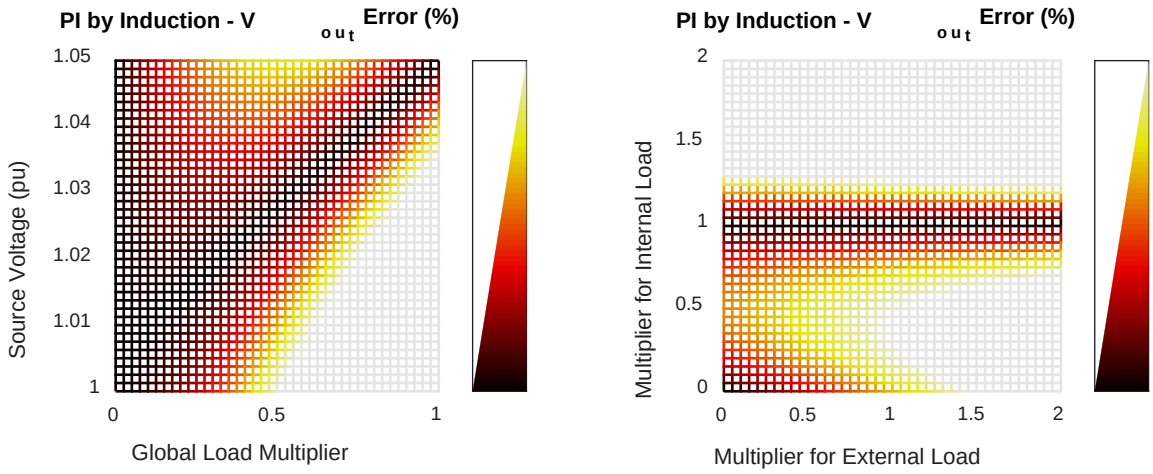

Figure 26. Performance of Segment Simplified with PI Section Topology

Constant-impedance approximation by induction produces a simplified segment that is accurate for low global load conditions and under conditions where the internal load voltage matches the load voltage in the base case. The approximation exactly matches the full segment behavior at nominal conditions. The overall performance of the approximation is similar to the constant-impedance model obtained by inspection and is relatively poor.

Constant-Current Approximation by Inspection (Figure 9)

Figure 27 shows the percent absolute error of the output voltage relative to the baseline over the source voltage vs. global load multiplier space (left) and the internal load multiplier vs. external load multiplier space (right).

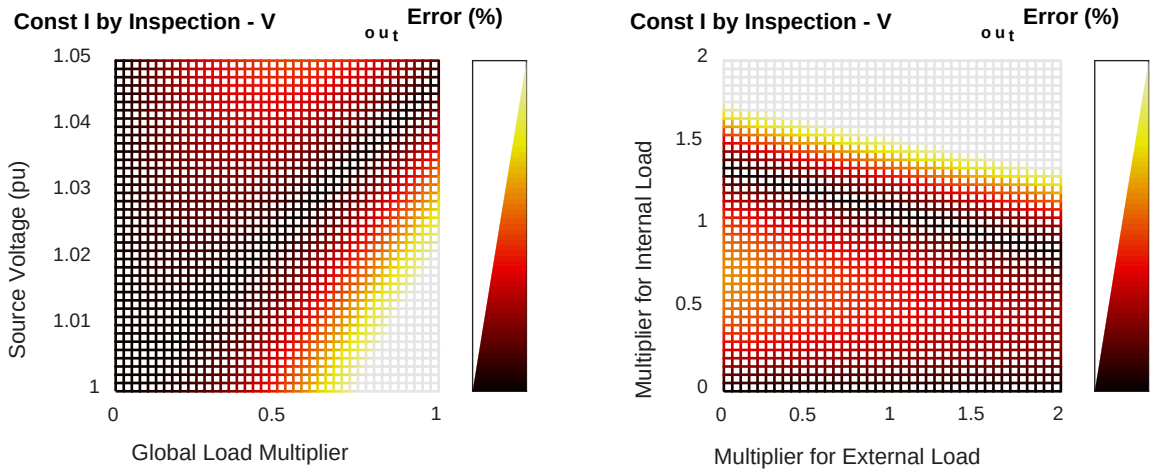

Figure 27. Performance of Segment Simplified with Constant-Current Load Approximation

Constant-current approximation by inspection produces a simplified segment that is reasonably accurate over a range of conditions, especially when the internal load voltage matches the base voltage (used to obtain approximate the load current). The performance of this approximation is significantly better than either of the constant-impedance approximations.

Constant-Current Approximation by Induction (Figure 11)

Figure 28 shows the percent absolute error of the output voltage relative to the baseline over the source voltage vs. global load multiplier space (left) and the internal load multiplier vs. external load multiplier space (right).

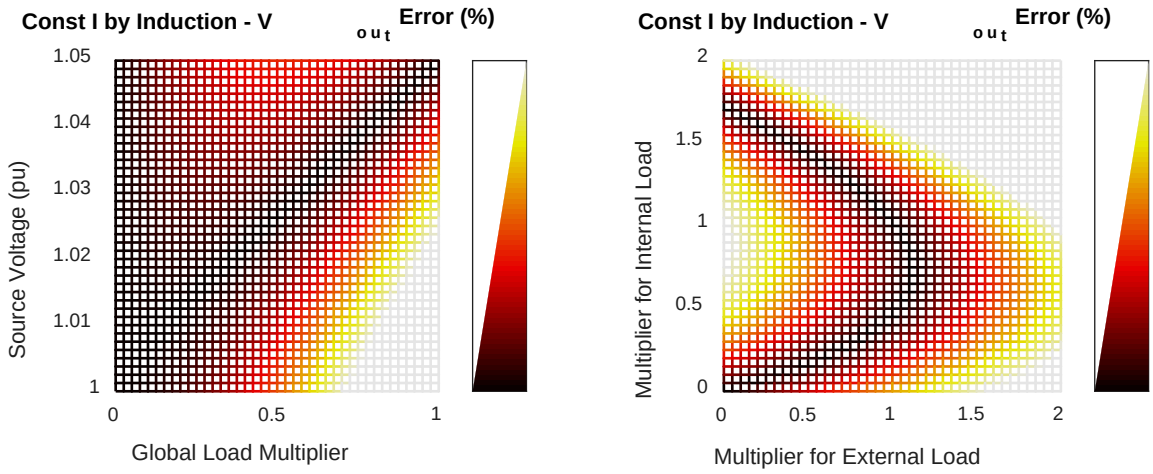

Figure 28. Performance of Segment Simplified with Constant-Current Topology

Constant-current approximation by induction exactly matches the full segment behavior at nominal conditions. The performance of this approximation is better than the approximation near nominal conditions but worse as conditions deviate from nominal; it is significantly better than either of the constant-impedance approximations.

Linear Two-Port Network Approximation (Figure 17)

Figure 29 shows the percent absolute error of the output voltage relative to the baseline over the source voltage vs. global load multiplier space (left) and the internal load multiplier vs. external load multiplier space (right).

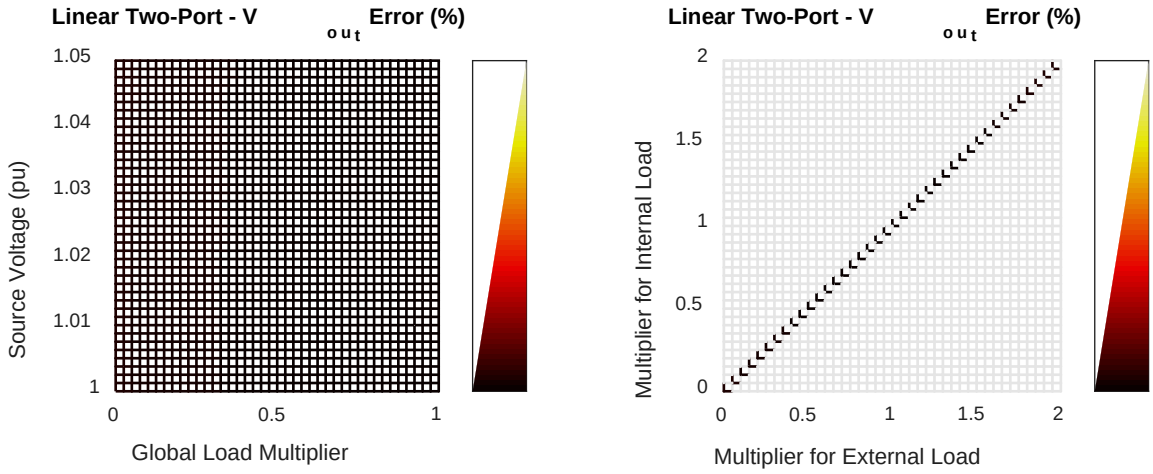

Figure 29. Performance of Segment Simplified as Linear Two-Port Network

The linear two-port network segment approximation is excellent over the range of source voltage and global load multiplier conditions but quickly deteriorates when the internal load multiplier and external load multiplier differ from each other.

Constant-Power One-Load Approximation by Induction (Figure 19)

Figure 30 shows the percent absolute error of the output voltage relative to the baseline over the source voltage vs. global load multiplier space (left) and the internal load multiplier vs. external load multiplier space (right).

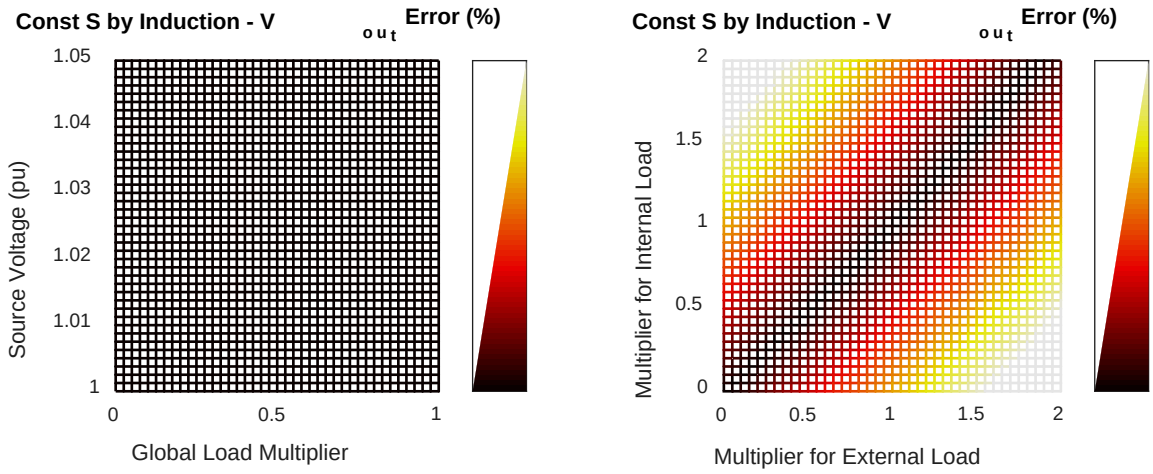

Figure 30. Performance of Segment Simplified with Constant-Power Topology

The constant-power by induction segment approximation exactly matches the full segment behavior at nominal conditions and produces an excellent approximation over the range of source voltage and global load multiplier conditions. The approximation is also relatively good for different internal and external load multipliers, except for extreme differences. Qualitatively, the constant-power one-load approximation by induction produces the best all-around approximation relative to complexity among the methods considered in this section.

Two-Measurement Distribution System Approximation by Induction (Figure 20)

Figure 31 shows the percent absolute error of the output voltage relative to the baseline over the source voltage vs. global load multiplier space (left) and the internal load multiplier vs. external load multiplier space (right).

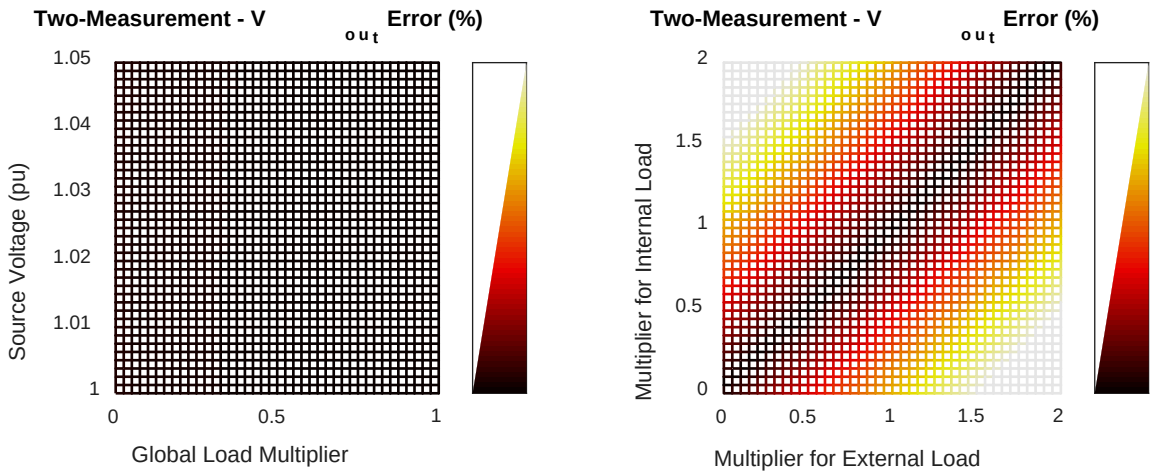

Figure 31. Performance of Segment Simplified with Z-Y-S-N Topology

The two-measurement distribution system approximation by induction produces an excellent approximation over the range of source voltage and global load multiplier conditions. The approximation is also relatively good for different internal and external load multipliers, except for extreme differences. Qualitatively, the performance of this approximation is very similar to that of the constant-power by induction approximation in spite of the increased complexity of the segment topology.

4.3 DISCUSSION

The performances of the simplified segments in this section depend on several factors including but not limited to:

- The impact of internal load current on voltage drop, which is determined by the total series impedance between the input and output nodes
- The impact of external load current on voltage drop, which depends on the total series impedance between the input node and each shunt element
- The I-V characteristics of the loads and shunt elements, which determines how much current each shunt element will draw for a given voltage across the shunt element
- The I-V characteristics of the external load, which determines how much current the external load will draw for a given output voltage

Any direct comparison of segment performance should be viewed within the context of the topology and parameters of the demonstration circuit.

4.3.1 Comparison of Induction and Inspection Methods

In contrast with inspection methods, which only work for constant-impedance or constant-current loads, induction methods can be used to produce approximations with constant-power and, in general, ZIP load behavior. In addition, the induction methods can produce an approximation that exactly matches the full system behavior at nominal conditions.

One advantage of the constant-current by inspection method is that the series impedance exactly matches that of the full circuit. This means that the component of the voltage drop across the segment that occurs in response to the external load will always be correct. The voltage drop in response to the internal load and the current drawn by the internal load have error corresponding to the I-V characteristics of the loads. In cases where the total series impedance of a segment is known, this parameter can be input into an assumed topology and used to create an enhanced approximation by induction.

4.3.2 Using Additional Measurements

For induction methods, using additional measurements allows segments to be mapped to more complex topologies. The demonstration circuit has a relatively simple topology without no-load losses and with only one node containing internal load. This simple topology obscures some of the advantages of using additional measurements; however, the ability to recover all characteristic parameters from measurements demonstrates that a segment approximation can be improved by using additional measurements.

4.3.3 Internal and External Load Multipliers

For several of the approximations analyzed in this section, the largest error occurred when the internal load multiplier and the external load multiplier were significantly different. In the demonstration circuit, roughly one quarter of the total system load is downstream of the segment of interest. Roughly 10% of the voltage drop across the segment occurs across Z3, downstream of the internal segment load and proportionate to the external load current. The demonstration

circuit may be unrealistically sensitive to the external load compared to real applications. Segments may be likely to terminate in one of the following three locations:

- A time-varying component like a regulator or switched capacitor
- An end-of-line location
- A load of interest, which may be large (i.e. a “spot load”)

In the first case, barring a large PV system (PV compensation is discussed in section 6.1.4) or a spot load with its own load shape, the load behavior is likely to be similar upstream and downstream of the component and the internal and external loads are likely to follow the same aggregate load shape. In the second case, the external segment load is likely to have a trivial impact on the voltage drop across the segment relative to the internal load. In the third case, if the load is particularly large, special attention should be given to the segment approximation to ensure that a difference in internal and external load levels will not introduce unacceptable error.

4.3.4 The Usability of the Linear Two-Port Segment

The linear two-port segment has a number of analytical advantages as discussed in Section 3. The approximation shows strong performance over a range of source voltages and global load levels; but when the local and global load multipliers deviated even slightly from each other, the error increased rapidly. The linear two-port approximation is not appropriate when the internal and external loads are modeled with different load shapes. This is consistent with the finding in section 3 that the inverse transmission parameters are inconsistent for different values of the external load relative to the global load.

5.0 CASE STUDY

In previous sections, a variety of methods were used to simplify a segment of a small demonstration circuit. The simplified segments were compared by simulating that same demonstration circuit. The demonstration circuit was constructed for this dissertation to illustrate the differences between various methods. In this section, a more realistic but still simple circuit from a common text used for distribution system analysis [4] is simplified. A QSTS simulation is performed on the full circuit and on the simplified circuit and the results are compared. The circuit under study is based on Problem 3.3 in [4]. The text specifies a three-phase circuit with 4/0 ACSR conductors and uneven load distribution.

5.1 SYSTEM MODEL DESCRIPTION

The circuit analyzed for this section is a per-phase version of the one described in Problem 3.3 of [4]; that is, the impedances and loads are balanced across the three phases and one of the phases is modeled and simulated.

System Topology

Six loads of various sizes are distributed unevenly over the length of the system. The loads are modeled as constant-power; this means that the system could not be simplified by

inspection without a constant-current (or constant-impedance) approximation. The distances and load sizes for the one-phase system are shown in Figure 32.

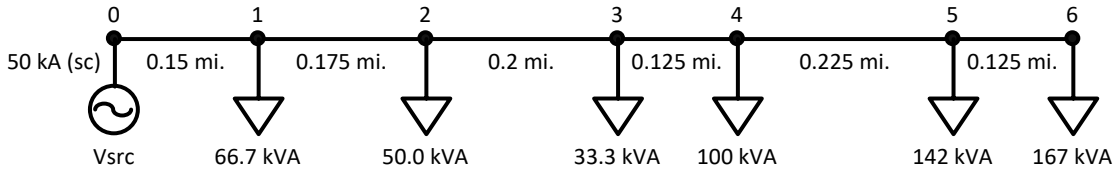

Figure 32. Circuit for Case Study: Per-Phase Version of Problem 3.3 in [4]

The short-circuit strength of the source is 50 kA; the OpenDSS default X/R ratio is used. One-phase 4/0 conductors connect all buses. All loads were assigned a power factor of 0.9.

Segmentation

For the studies performed in this section, bus 0 was considered to be the input and bus 6 was considered to be the output. This configuration represents a system with substation monitoring and a point of interest (such as a DG interconnection request or large load location). The lines and loads between the input and output buses are considered as one segment. The system is shown with a generic segment between bus 0 and bus 6 identified in Figure 33.

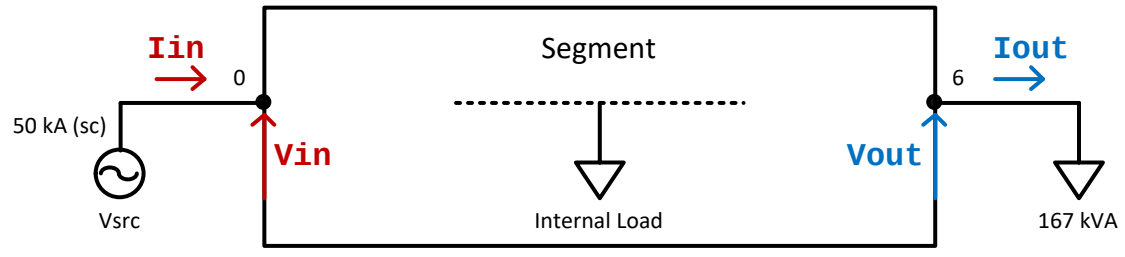

Figure 33. Circuit for Case Study with One Segment Identified for Simplification

Load Shape Files

The load shape CSV files are provided with the standard OpenDSS distribution [24] in the examples subdirectory. These load shapes contain normalized load levels for one year with one hour temporal resolution. There are 8,760 data points in each load shape; this is the number of hours in a non-leap year. The two load shape files used for this case study are shown in Figure 34.

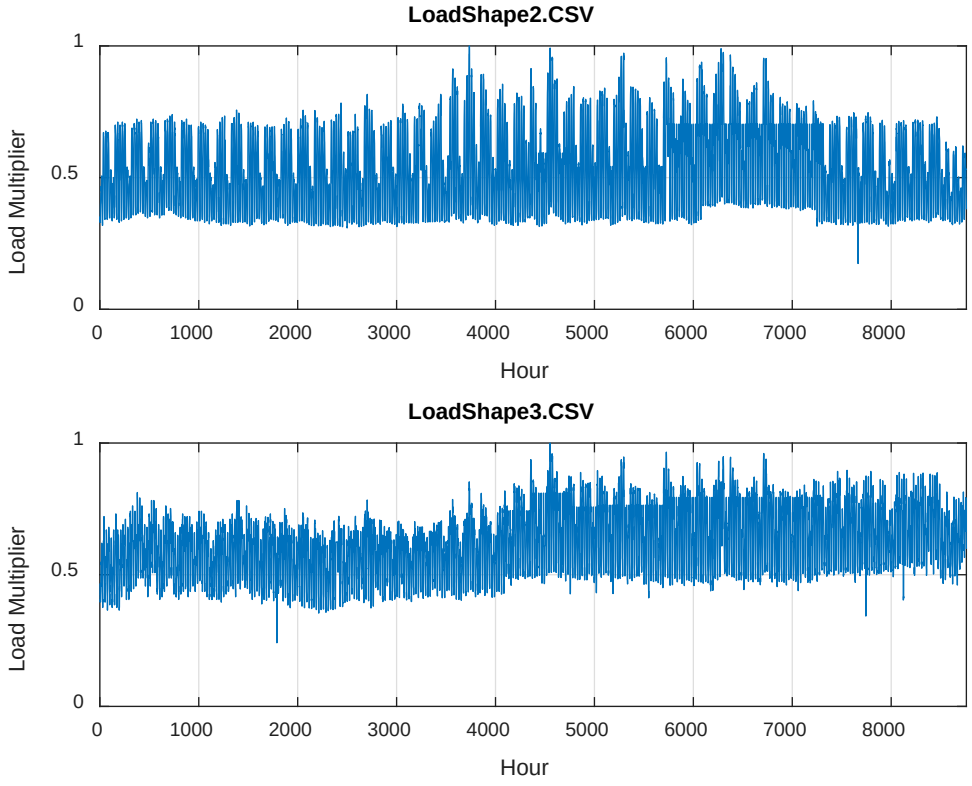

Figure 34. Load Shapes for Case Study [24]

QSTS Simulation Parameters

QSTS simulations were performed on the circuit described above. The following simulation parameters were used:

- Source voltage: 1.04 p.u.
- Global load shape (where applicable): LoadShape2.csv (Figure 34 top)
- Internal load shape (where applicable): LoadShape2.csv (Figure 34 top)
- External load shape (where applicable): LoadShape3.csv (Figure 34 bottom)

The global load shape (where applicable) is assigned to all system loads (buses 1 through 6). The internal load shape (where applicable) is assigned to loads at buses 1 through 5. The external load shape (where applicable) is assigned to the load at bus 6.

5.2 BASELINE RESULTS

The full system was simulated with one-hour time steps for one year: first with a global load shape and then with separate internal and external load shapes. Using a separate external load shape simulates the shape of a spot load or the net load shape of a load with distributed generation.

5.2.1 Global Load Shape

A QSTS simulation was performed with a global load shape applied to all loads. The input and output voltages for each hour in the year are shown in Figure 35. The output voltage and, to a lesser extent (due to the electrical proximity to the voltage source), the input voltage fluctuate with the load shape. Increased load causes the voltage to decrease.

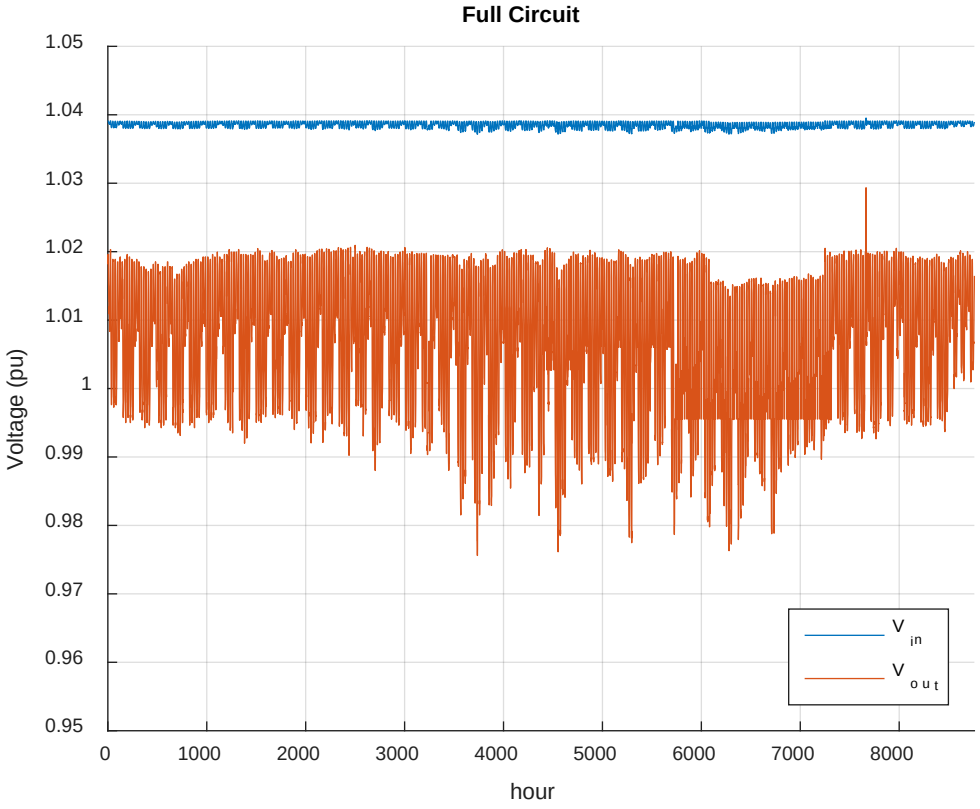

Figure 35. QSTS Results for Full Case Study Circuit with Global Load Shape

5.2.2 Separate Internal and External Load Shapes

A QSTS simulation was performed with separate load shapes for internal and external loads. The input and output voltages for each hour in the year are shown in Figure 36. The output voltage and, to a lesser extent (due to the electrical proximity to the voltage source), the input voltage fluctuate with the load shape. The voltage behavior is dominated by the internal load shape because the internal load is significantly higher than the external load.

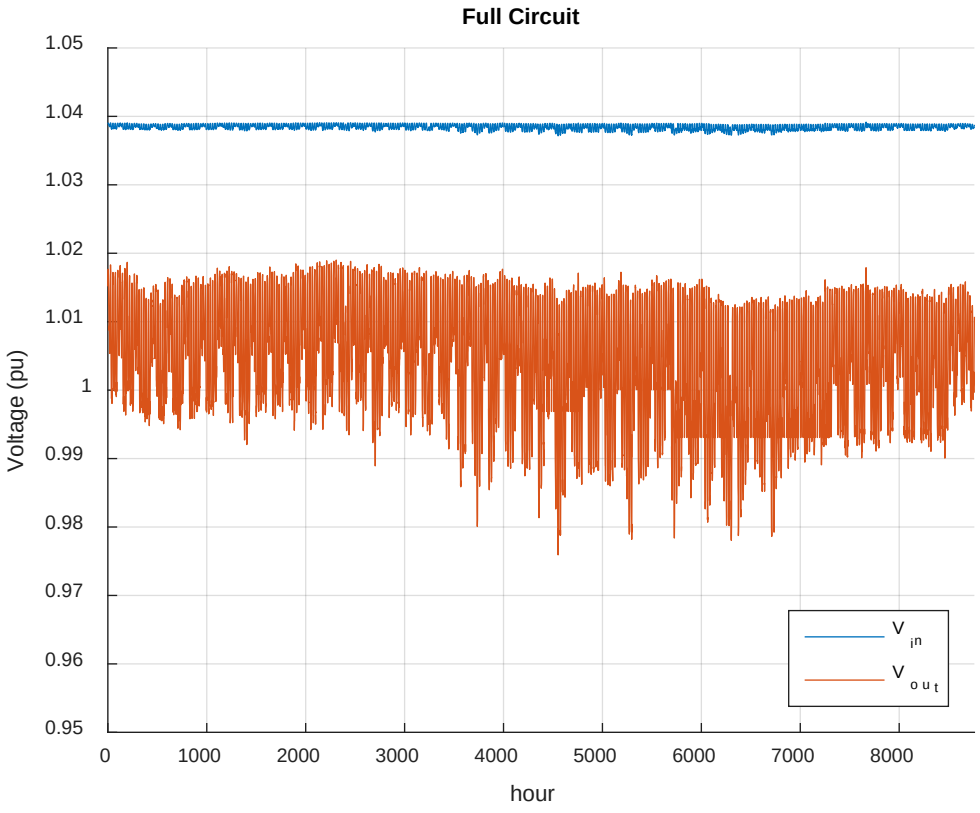

Figure 36. QSTS Results for Full Case Study Circuit with Separate Load Shapes

5.3 SIMPLIFIED MODEL ANALYSIS

The segment between the input and output buses was simplified by induction as discussed in Section 2.2.2. The constant-power one-load topology described in Section 3.4.1 was selected. For this problem, the number of buses in the model was reduced from seven to two: Buses 1 through 5 were eliminated, leaving buses 0 and 6.

Simplification

To obtain input and output measurements, the full system was simulated with the following simulation parameters:

- Source voltage: 1.04 p.u.
- Global load multiplier: 1

Under these conditions, the full system produced the measurements shown in Table 12.

Table 12. Circuit for Case Study Load-Flow Data

Measurement	Value
Vin	2489.1547 V
Vout	2341.4652 V
Iin	235.3119 A
Iout	71.3199 A

The corresponding topological parameters are shown in Table 13.

Table 13. Topological Parameters Determined by Induction from Load-Flow Data

Parameter	Value
R	0.615803525481088 ohms
X	0.167090260450550 ohms
P	345.4074898802300 W
Q	167.7365929120316 VAr

The simplified circuit is shown in Figure 37.

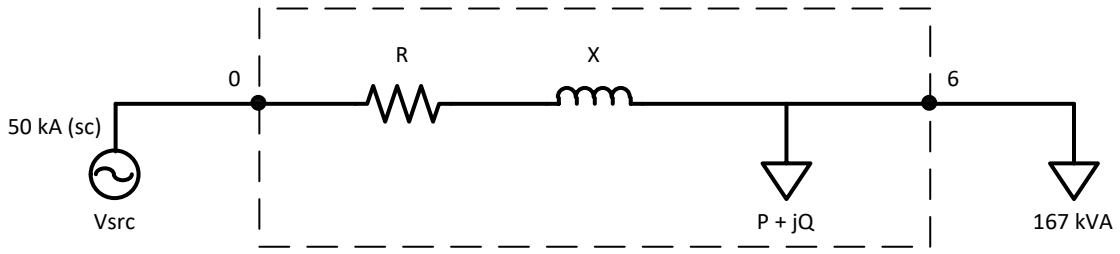

Figure 37. Circuit for Case Study with Constant-Power One Load Segment Topology

Note the complex number parameter definitions:

- Resistance R is the real component of the impedance Z.
- Reactance X is the imaginary component of the impedance Z.
- Power P is the real component of the apparent power S.
- Reactive power Q is the imaginary component of the apparent power S.

Simplification Error

To compare the simplified system to the full system, the percent error magnitude was calculated according to Equation 35.

$$\%\ Error = \frac{\left| V_{out}^{full} - V_{out}^{simplified} \right| (Volts)}{V_{base}} * 100\% \quad \textbf{(35)}$$

5.3.1 QSTS Results with Global Load Shape

The error for each hour in the year is shown in Figure 38. As expected based on the analysis in section 4, the error is very small. The error is lowest when the load multiplier is close to unity, matching the nominal conditions used to simplify the segment.

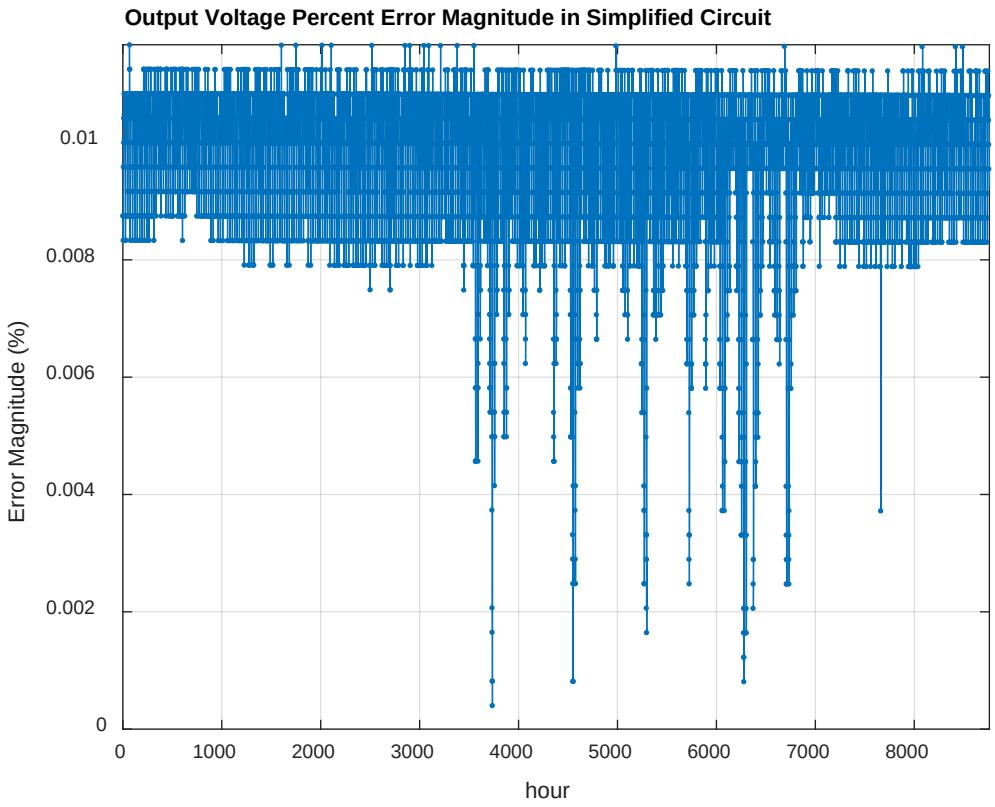

Figure 38. Error Magnitude over QSTS Simulation with Global Load Shape

Error statistics are shown in Table 14.

Table 14. Error Magnitude Statistics for QSTS Simulation with Global Load Shape

Mean	0.009734 %
Minimum	0.000417 %
Maximum	0.011667 %

When a global load multiplier was used, the simplified system produced a good approximation of the full system. The error was always less than 0.1% and was generally on the order of 0.01%. Error on the order of 0.1% is expected to be acceptable for distribution system studies. These results indicate a very good approximation.

5.3.2 QSTS Results with Separate Internal and External Load Shapes

The error for each hour in the year is shown in Figure 39. The error is generally greater than that in section 5.3.1. The error is smallest when the internal load multipliers and external load multipliers are close to each other and, to a lesser extent, when both load levels are close to unity, matching the conditions used to simplify the segment.

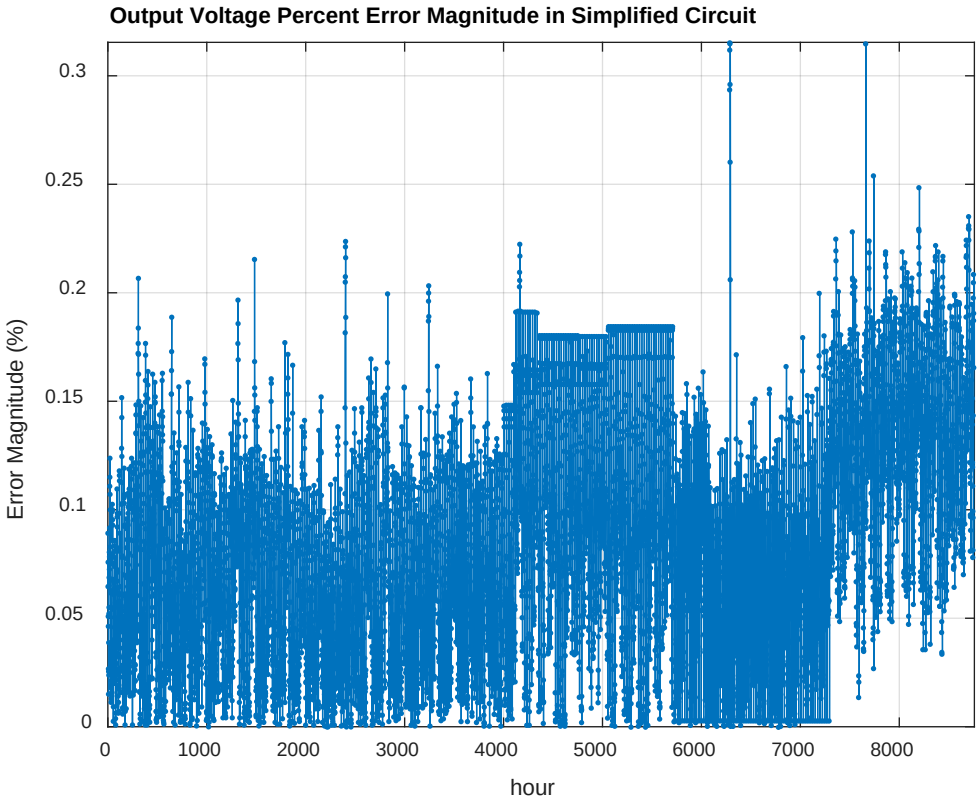

Figure 39. Error Magnitude over QSTS Simulation with Separate Load Multipliers

Error statistics are shown in Table 15.

Table 15. Error Magnitude Statistics for QSTS Simulation with Separate Load Shapes

Mean	0.082798 %
Minimum	0.000000 %
Maximum	0.315417 %

When separate internal and external load multipliers were used, the simplified system produced an approximation of the full system such that the mean error was less than 0.1% but the maximum error was greater than 0.1%. Error on the order of 0.1% is expected to be acceptable for distribution system studies. This error may still be acceptable in some cases but it is slightly higher than the target. One significant way for the internal and external load shapes to vary relative to each other is for distributed PV to reduce the net load during the day in parts of the feeder. PV compensation was developed as a method to counteract this effect as discussed in section 6.1.4.

6.0 SEGMENT SUBSTITUTION FOR FULL-SCALE MODELS

In previous sections, model simplification concepts were demonstrated using simple single-phase segment and feeder models with basic topologies and constant power loads. In this section, methods are extended to handle real mixed-phase distribution system models with ZIP loads and distributed PV. In addition, metrics are defined to characterize the impact of model simplification on simulation performance and accuracy and a stochastic characterization of segment substitution is presented.

6.1 SEGMENT SUBSTITUTION AND AUXILIARY METHODS

In this section, the one-load segment topology developed in section 3.4.1 is expanded for full-scale distribution system models. Specifically, the topology is extended for ZIP loads with any coefficients, segments from one to three phases, junctions between segments, and segments that have different internal and external effective load shapes (discussed in section 4.2).

6.1.1 ZIP Loads

The one-load topology developed in Section 3.4.1 is shown with a general ZIP load in Figure 40. This topology has two characteristic parameters: a series impedance *Z* and a shunt ZIP load with complex apparent power *S* and assumed ZIP coefficients.

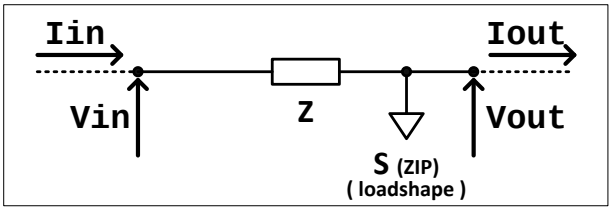

Figure 40. Series-Impedance, ZIP-Shunt Segment Topology

The ZIP load object follows the same load-shape as the loads in the original model and each phase behaves according to the ZIP coefficients model [32]:

$$P(t) = P_0\left(Z_p\left(\frac{V_{out}(t)}{V_0} + I_p \frac{V_{out}(t)}{V_0} + P_p \right) \right) \quad \textbf{(36)}$$

$$Q(t) = Q_0\left(Z_q\left(\frac{V_{out}(t)}{V_0} + I_q \frac{V_{out}(t)}{V_0} + P_q \right) \right) \quad \textbf{(37)}$$

Where Z_p, I_p, P_p, Z_q, I_q, and P_q are the ZIP coefficients. The seventh, ZIP coefficient, cutoff voltage, V_{cut}, below which, *P* and *Q* are equal to zero, was not relevant to this analysis. The coefficients for aggregate load classes in Equation 36 range from -2.5 to 2.0, and the coefficients in Equation 37 range from -17 to 10, depending on the type of load [32]. ZIP coefficients are assumed as part of the topology, usually corresponding to the predominant load type in the model. The segment characteristic parameter *S* is related to *P* and *Q* by equation 38.

$$S^{\phi} = P_0^{\phi} + jQ_0^{\phi} \quad \textbf{(38)}$$

Equation (38) is per-phase. *S* is the complex apparent power of the ZIP load with assumed ZIP coefficients.

6.1.2 Multi-Phase Segments

The characteristic equations for the segment shown in figure 40 are obtained using KCL at the output bus and KVL across the segment.

$$I_{out}^{\phi} = I_{in}^{\phi} - \left(\frac{S^{\phi}}{V_{out}^{\phi}}\right)^{*} \quad \textbf{(39)}$$

$$V_{out} = V_{in} - I_{in}Z \quad \textbf{(40)}$$

6.1.2.1 Three-Phase Segments

Equation 39 is per-phase; it is duplicated and rearranged to solve for *S* and shown for a three-phase system in equation 41.

$$\begin{bmatrix} S^a \\ S^b \\ S^c \end{bmatrix} = \begin{bmatrix} V_{out}^a * (I_{in}^a - I_{out}^a)^* \\ V_{out}^b * (I_{in}^b - I_{out}^b)^* \\ V_{out}^c * (I_{in}^c - I_{out}^c)^* \end{bmatrix} \quad \textbf{(41)}$$

In Equation 40, for a three-phase segment, V_{out}, I_{out}, V_{in}, I_{in}, and S are 3-by-1 vectors and Z is an 3-by-3 matrix. For a three-phase system, equation 42 is used to solve for Z, which is under-constrained. The pseudo-inverse of the matrix in equation 42 can be used to solve for the minimum-norm solution of Z, constrained to be a symmetric matrix.

$$\begin{bmatrix} V_{in}^{a} - V_{out}^{a} \\ V_{in}^{b} - V_{out}^{b} \\ V_{in}^{c} - V_{out}^{c} \end{bmatrix} = \begin{bmatrix} I_{in}^{a} & I_{in}^{b} & I_{in}^{c} & 0 & 0 & 0 \\ 0 & I_{in}^{a} & 0 & I_{in}^{b} & I_{in}^{c} & 0 \\ 0 & 0 & I_{in}^{a} & 0 & I_{in}^{b} & I_{in}^{c} \end{bmatrix} \begin{bmatrix} z_1 \\ z_2 \\ z_3 \\ z_4 \\ z_5 \\ z_6 \end{bmatrix} \quad \textbf{(42)}$$

Where Z is composed of elements z_1 through z_6 as shown in equation 43.

$$Z = \begin{bmatrix} z_1 & z_2 & z_3 \\ z_2 & z_4 & z_5 \\ z_3 & z_5 & z_6 \end{bmatrix} \quad \textbf{(43)}$$

6.1.2.2 Two-Phase Segments

Equation 39 is per-phase; it is duplicated and rearranged to solve for S and shown for a two-phase system consisting of phases x and y in equation 44.

$$\begin{bmatrix} S^{x} \\ S^{y} \end{bmatrix} = \begin{bmatrix} V_{out}^{x} * \left(I_{in}^{x} - I_{out}^{x}\right)^{*} \\ V_{out}^{y} * \left(I_{in}^{y} - I_{out}^{y}\right)^{*} \end{bmatrix} \quad \textbf{(44)}$$

In 40, for a two-phase segment, V_{out}, I_{out}, V_{in}, I_{in}, and S are 2-by-1 vectors and Z is an 2-by-2 matrix. For a two-phase system consisting of phases x and y, equation 45 is used to solve

for *Z*, which is under-constrained. The pseudo-inverse of the matrix in equation 45 can be used to solve for the minimum-norm solution of *Z*, constrained to be a symmetric matrix.

$$\begin{bmatrix} V_{in}^{x} - V_{out}^{x} \\ V_{in}^{y} - V_{out}^{y} \end{bmatrix} = \begin{bmatrix} I_{in}^{x} & I_{in}^{y} & 0 \\ 0 & I_{in}^{x} & I_{in}^{y} \end{bmatrix} \begin{bmatrix} z_1 \\ z_2 \\ z_3 \end{bmatrix} \quad \textbf{(45)}$$

Where *Z* is composed of elements z_1 through z_6 as shown in equation 46.

$$Z = \begin{bmatrix} z_1 & z_2 \\ z_2 & z_3 \end{bmatrix} \quad \textbf{(46)}$$

6.1.2.3 One-Phase Segments

Equation 39 is per-phase; it is rearranged to solve for *S* and shown for a one-phase system in equation 47.

$$S^{\phi} = V_{out}^{\phi} * \left(I_{in}^{\phi} - I_{out}^{\phi}\right)^{*} \quad \textbf{(47)}$$

Equation 40 is used to solve for *Z*, which is fully-constrained for a one-phase system, shown in equation 48.

$$V_{in}^{\phi} - V_{out}^{\phi} = I_{in}^{\phi} Z \quad \textbf{(48)}$$

6.1.3 Junction Aggregation

Junctions are formed at the intersection of two or more segments. Components may be connected to a junction without being a part of any segment. In this case, in order to eliminate all unnecessary buses, all components connected to a junction can be approximated by an aggregate load. The following process, similar to the segment substitution process, may be used:

1. Assume an aggregate load behavior.
2. Use the total shunt currents at the junction bus and the bus voltages as necessary to determine the magnitude of the aggregate load.

A simplified junction with aggregated constant power load is shown in Fig. 3.

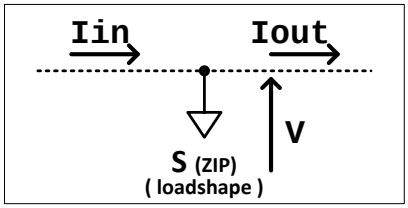

Figure 41. Junction Parameters Used for Aggregation

The apparent power of a ZIP load can be computed:

$$S = (V)^T (I_{in} - I_{out})^* \quad \textbf{(49)}$$

For an n-phase junction bus, V, I_{in}, I_{out}, and S are n-by-1 vectors.

6.1.4 PV Compensation

PV systems inject power into the system, changing the net load shape such that the segment can effectively have separate internal and external load shapes (as discussed in section 4.2). This has two effects on the simplified segment: (1) any PV systems inside the segment decrease the current shunted by the segment, and (2) any PV systems inside of or downstream of the segment decrease the voltage drop across the segment; because the characteristic Z matrix of the segment does not necessarily equal the Thevenin impedance of the full segment, this change in voltage drop can affect the full and simplified segments differently. PV compensation is introduced to the segment to counteract both of these effects. Two constant-power generators that follow the time-shape (similar to a load shape, representing the generator output over time) of the PV systems in the model are added to the segment as shown in figure 42.

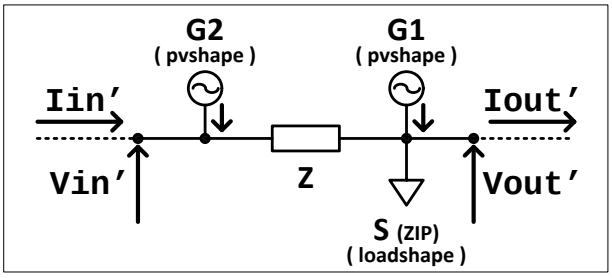

Figure 42. Series Impedance, ZIP Shunt Topology with PV Compensation

The size of the generators *G1* and *G2* can be determined using the following procedure:

1. Obtain the characteristic parameters *Z* and *S* using equations 39 and 40 with input and output voltage and current data obtained when the PV systems are not producing power.

2. Using the same system load level as the previous step, obtain input and output voltage and current data with the PV systems at full power (V'_{in}, V'_{out}, I'_{in}, and I'_{out}).
3. Solve equations 50 and 51 for complex constant-power magnitudes of the generators *G1* and *G2*.

$$G2^{\phi} = V_{in}^{\prime\phi}\left(I_{G2}^{\phi}\right)^{*} \quad \textbf{(50)}$$

$$G1^{\phi} = V_{out}^{\prime\phi}\left(I_{G1}^{\phi}\right)^{*} \quad \textbf{(51)}$$

Equations 50 and 51 are per-phase, where vectors I_{G2} and I_{G1} are defined in equations 52 and 53, respectively.

$$I_{G2} = \boldsymbol{Z}^{-1}\left(\left(V'_{in} - V'_{out}\right) - \boldsymbol{Z}I'_{in}\right) \quad \textbf{(52)}$$

$$I_{G1} = \left(I_{in} - I_{out}\right) - \left(I'_{in} - I'_{out}\right) - I_{G2} \quad \textbf{(53)}$$

If PV systems are within or downstream of a segment, *G1* is expected to be positive and *G2* negative for that segment.

6.2 SIMPLIFICATION METRICS

In this section, metrics that can be used to quantify the performance of a simplified model relative to the full model are described. Examples in previous sections used relatively simple

models with no more than one segment. The intent of this section is to provide a quantifiable framework to discuss full-scale distribution model simplification using the nonlinear segment substitution method.

6.2.1 Topological Reduction Factor

The topological reduction factor, *TRF*, as defined in this dissertation, compares the number of buses in the full and simplified models.

$$TRF = \frac{[B_{FULL} - B_{SIMP}]}{[B_{FULL}]} \quad \textbf{(54)}$$

B_{FULL} is the number of buses in the full model and B_{SIMP} is the number of buses in the simplified model.

6.2.2 Computational Savings Factor

The computational savings factor, *CSF*, as defined in this dissertation, quantifies the computational time savings afforded by simplification for a benchmark simulation.

$$CSF = \frac{[T_{FULL} - T_{SIMP}]}{[T_{FULL}]} \quad \textbf{(55)}$$

T_{FULL} is the computational time required to perform a benchmark simulation with the full system model and T_{SIMP} is the computational time required to perform the benchmark simulation with a simplified system model. The *CSF* does not consider any computational requirement for

performing the simplification procedure; this time is fixed, mo matter how long the QSTS simulation will be and is at least an order of magnitude less than the QSTS simulation time. The *CSF* accounts for the number of iterations in a solution so it is affected by approximation error.

6.2.3 System State Error

Segment substitution attempts to simplify a distribution system model without affecting the system state at preserved buses. The segment endpoint voltages can be examined using a benchmark QSTS simulation. The absolute difference between the voltage magnitudes at the preserved buses of interest for the full model and the simplified model can be computed for each time step. This QSTS simulation should be performed with voltage regulator and switched capacitor controls disabled to avoid small voltage errors causing a controlled device actuation that results in a substantial voltage error in other segments.

The voltage error is a random variable (the distribution is not necessarily normal). The average and maximum absolute voltage magnitude error are computed as shown in equations 56 and 57, respectively.

$$V_{err}^{avg} = \sum_{i=1}^{n}\sum_{k=1}^{r}\frac{1}{n*r}\left(\sum_{j=1}^{m_k}\frac{1}{m_k}\left(\left\|V_{i,j,k}^{full}\right\| - \left\|V_{i,j,k}^{simp}\right\|\right)\right) \quad \textbf{(56)}$$

$$V_{err}^{max} = \max_{i,j,t}\left\{\left\|V_{i,j,k}^{full}\right\| - \left\|V_{i,j,k}^{simp}\right\|\right\} \quad \textbf{(57)}$$

Where n is the number of samples in the benchmark QSTS simulation, r is the number of segments, m_k is the number of phases at the output terminal of segment k, $V_{i,j,k}$ is the phase j

voltage at the output terminal of segment *k* at time step *i* for the full or simplified model according to the superscript. This formulation weights the error of each segment equally, regardless of the number of phases.

6.2.4 Voltage Regulator Tap Operation Impact

The effect of model simplification on voltage regulator tap change operation frequency can be examined using a benchmark PV impact study: QSTS simulations are performed with and without PV and the number of tap changes recorded by each voltage regulator is compared. The QSTS simulations should be performed with any switched capacitor controls disabled.

The regulator tap change operation error, *RTE*, quantifies the error introduced by model simplification as shown in equation 58. The voltage regulator tap change operation impact, *RTI*, compares the tap change increase caused by PV in the simplified model to the full model as shown in equation 59.

$$RTE = \frac{\sum_i N_i' - \sum_i N_i}{\sum_i N_i} \quad \textbf{(58)}$$

$$RTI = \frac{\sum_i (M_i' - N_i') - \sum_i (M_i - N_i)}{\sum_i (M_i - N_i)} \quad \textbf{(59)}$$

Where N_i is the number of tap changes without PV for voltage regulator *i* in the full model, N_i' is the number of tap changes without PV for voltage regulator *i* in the simplified model, M_i is the number of tap changes with PV for voltage regulator *i* in the full model, and M_i'

is the number of tap changes with PV for voltage regulator *i* in the simplified model throughout the benchmark QSTS simulation.

Because the tap position of voltage regulators is extremely sensitive to bus voltages as well as the tap positions of other regulators throughout the system, in addition to the *RTE* and *RTI*, the operations of each individual regulator will be tabulated in this dissertation.

6.3 STOCHASTIC ERROR CHARACTERIZATION

The error introduced by nonlinear simplification methods, including segment substitution, depends on the physical topology of the original segment relative to the simplified segment. In this section, a Monte Carlo method is described to characterize this simplification error. A random radial feeder is constructed, one segment of the feeder is simplified, and then both the full and simplified models are simulated under a variety of conditions.

The stochastically generated feeders can represent a range of feeders that are described by the inputs:

1. Topology
2. Substation Voltage
3. Substation Current
4. Branch Impedances
5. Line Resistance

The inputs are intended to correspond to decisions made at the system planning level. They may vary between regions, and utilities. The values selected in this section attempt to

represent feeders United States feeders similar to the EPRI J1 circuit [47], which is simplified and analyzed in detail later in this document.

6.3.1 Stochastic Feeder Topology

Topologies are assumed to be radial, beginning at the substation. Topological depth of a bus refers to the number of branches between the substation and the bus. The topologies of the Pacific Northwest National Lab (PNNL) radial distribution feeder taxonomy [48], were analyzed to obtain a depth-dependent PMF of buses downstream of a bus at known depth. Stochastic feeder topologies can be constructed dynamically by, for each bus, sampling the depth-dependent PMF to determine the number of downstream buses. Examples of topologies constructed in this way are shown in figure 43. In order to control the number of buses, topologies are scrapped and recreated until the number of buses is within the desired range.

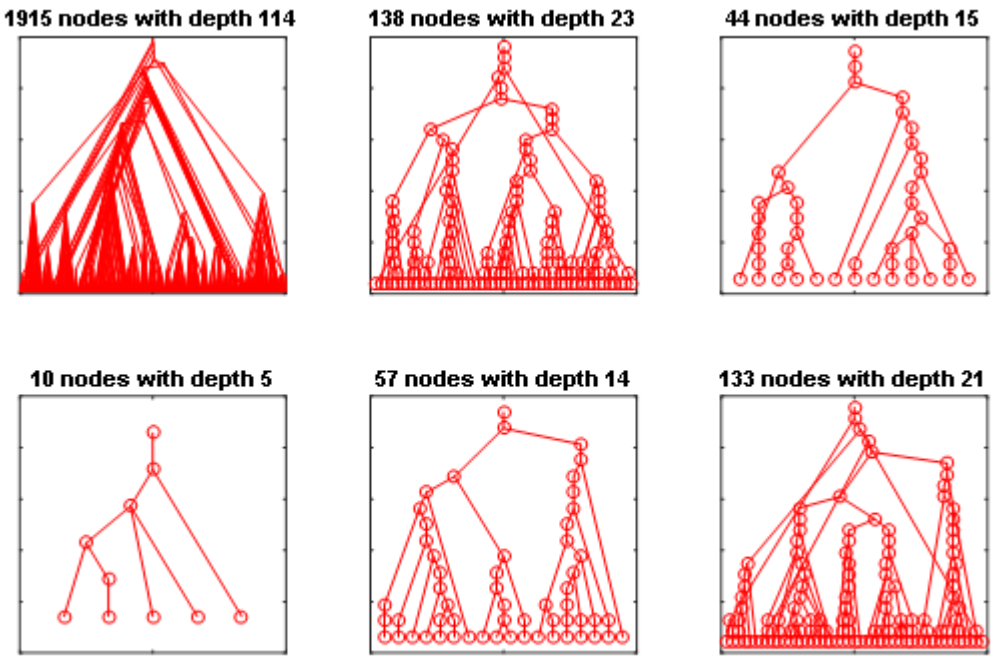

Figure 43. Example Stochastic Feeder Topologies

A series of 10,000 stochastic feeder topologies with between 500 and 5,000 nodes (or single-phase buses) was created. The distribution of the number of buses is shown in figure 44.

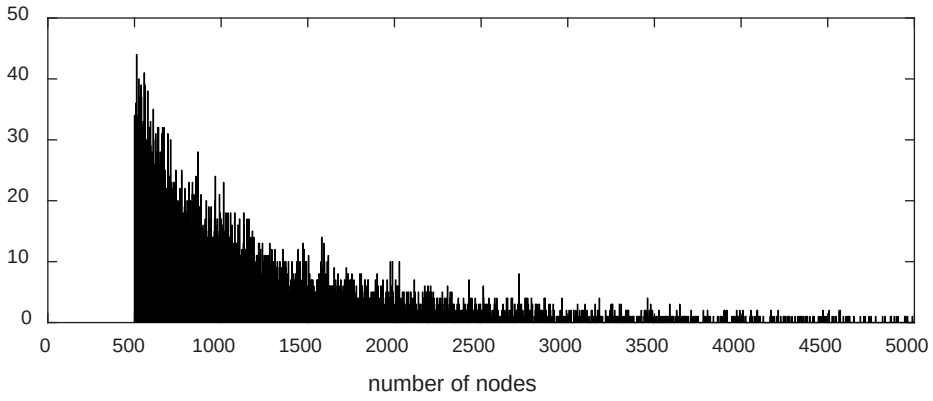

Figure 44. Buses of 10,000 Stochastically Generated Feeders

The distribution of the maximum depth of the feeders is shown I figure 45.

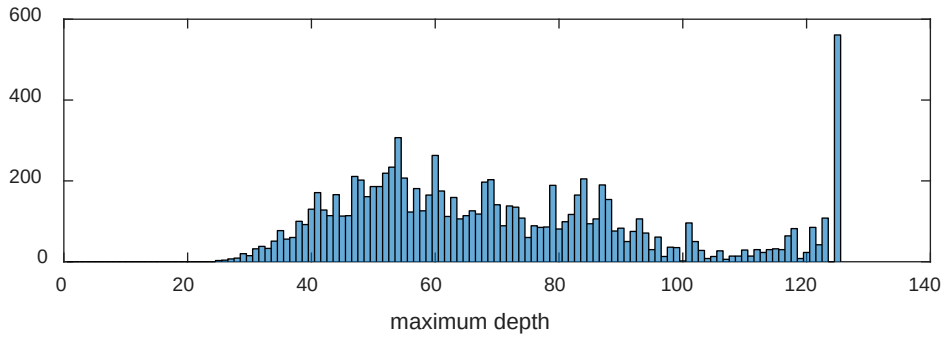

Figure 45. Histogram of Maximum Depth for 10,000 Stochastically Generated Feeders

Note that the maximum depth present in the PNNL feeder taxonomy is 125, which corresponds to the maximum possible depth for a stochastic feeder generated using this algorithm.

6.3.2 Input Random Variables

For each stochastic feeder topology, the following input random variables were sampled from normal distributions.

6.3.2.1 Substation Voltage

The substation per-unit voltage, V_{sub}, is assumed to be held constant by a substation voltage regulator or line tap changer (LTC). V_{sub}, therefore, corresponds to the set point of the LTC. A mean value of 1.03 pu and a three-sigma value of 0.02 pu were used for the Monte Carlo simulations.

$$V_{sub} \sim N\left(1.03, \left(\frac{0.02}{3}\right)^2\right) \quad \textbf{(60)}$$

6.3.2.2 Substation Current

The substation current, I_{sub}, is specified such that 1 pu of this current would cause a last house voltage (the voltage at the point of farthest electrical distance or highest impedance from the substation) of 0.95 pu at nominal substation voltage and nominal line impedance with no voltage regulators. The substation current is allowed to exceed 1 pu to represent the total voltage drop of systems with distributed voltage regulators. A mean value of 1.5 pu and a three-sigma value of 0.5 pu were used for the Monte Carlo simulations.

$$I_{sub} \sim N\left(1.5, \left(\frac{0.5}{3}\right)^2\right) \quad \textbf{(61)}$$

With no distributed generation on the feeder, the substation current is equal to the sum of the load currents. Constant-power customer load with unity power factor is allocated to each bus with normal distribution such that the desired substation current distribution would be achieved at nominal values of other parameters.

6.3.2.3 Line Resistance

Total line resistance for the trunk and each lateral is specified such that the voltage at the end of each lateral would be 0.95 pu at 1-pu load with load current evenly distributed among all buses and nominal voltage. The three standard deviation span corresponds to +/- 0.02 pu voltage drop.

6.3.2.4 Load Shape

A yearly load shape with 5-minute resolution was sampled uniformly to obtain a realistic set of load multipliers for stochastic simulation, a histogram of the load shape is shown in figure 46.

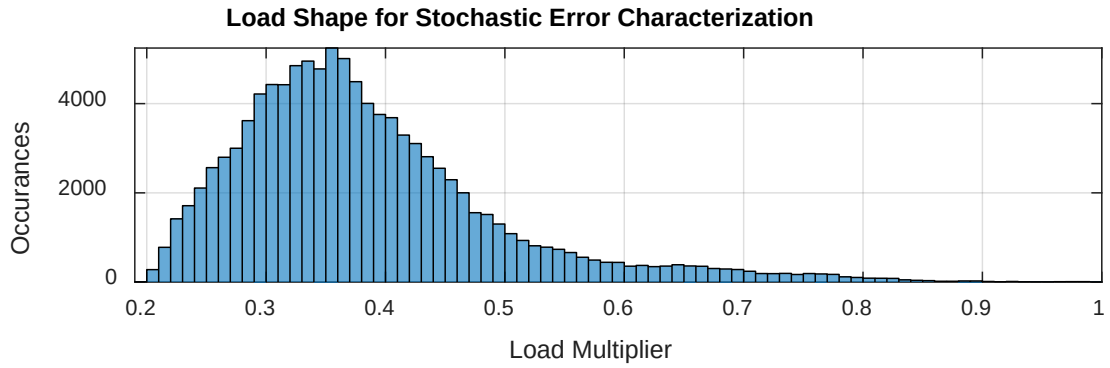

Figure 46. Load Shape Histogram for Monte Carlo Simulation

6.3.3 Monte Carlo Simulation Results

Using the input random variables described, 10,000 single-phase feeders were constructed with between 500 and 5000 buses, inclusive. A segment spanning half of the topological depth was selected randomly for simplification. A simplified version of each feeder was obtained using segment substitution. The full and simplified feeders were each simulated 1000 times each using load levels sampled from the load shape distribution shown in Figure 46. The voltage at the output of the segment was analyzed. Results are summarized in Table 16 and Table 17.

Table 16. Stochastic Error Characterization - Average Absolute Voltage Magnitude Error

Feeders	Simulations	Mean V^{avg}_{err}	Min V^{avg}_{err}	Max V^{avg}_{err}
1,000	100	0.000969	0.000001	0.005718
10,000	1,000	0.001002	0.000001	0.006439

Table 17. Stochastic Error Characterization - Maximum Absolute Voltage Magnitude Error

Feeders	Simulations	Mean V^{max}_{err}	Min V^{max}_{err}	Max V^{max}_{err}
1,000	100	0.001789	0.000004	0.008469
10,000	1,000	0.001948	0.000009	0.009502

A histogram of all voltage errors across feeders and simulations is shown in figure 47. The maximum error was 0.001 pu, but the mean and median errors were much lower due to skew.

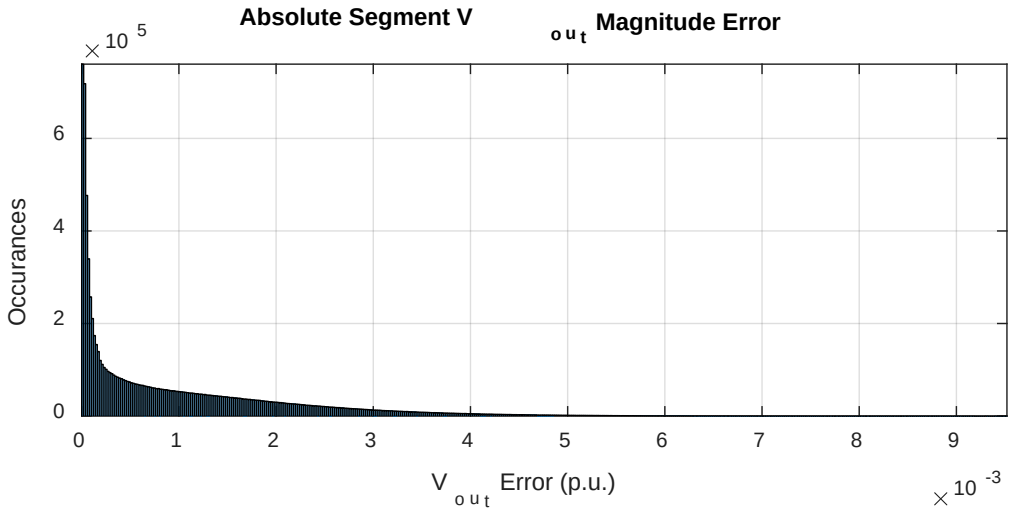

Figure 47. Histogram of Segment Absolute Output Voltage Error Magnitude

The results of the stochastic error characterization show that the error for stochastically generated feeders was usually higher than the simulation performed in section 5 with a global load shape. This is expected because the segments being simplified have significantly more complex topologies and the substation current is generally higher than it was in Section 5. However, the errors are within the range that is expected to be acceptable as discussed in Section 5 (on the order of 0.1% or 0.001 pu). The case of separate load multipliers was not included in this analysis; compensation, discussed in Section 6.1.4, reduces error associated with PV or other independent load sources to a level that is comparable with the global load shape case. This is demonstrated in Section 7.2.

7.0 FULL MODEL STUDIES

In this section, simplification using segment substitution will be demonstrated on two full distribution system models. Each model consists of over 2,000 buses. The first feeder, EPRI ckt5 [24], is a passive model with no distributed voltage regulators and no PV. The second feeder, EPRI J1 [47], is an active model that includes both distributed voltage regulators and distributed PV.

7.1 EPRI CKT 5

In this section, the process of distribution system model simplification using segment substitution will be demonstrated using a full electric power distribution system model. The model is EPRI Feeder ckt5, which is provided with a standard OpenDSS installation. The performance of the simplified model is examined using the metrics discussed in section 6.2. The model is simplified using series-impedance constant-power shunt segments. The model does not contain any distributed regulators or PV.

7.1.1 Feeder Description

The following changes were made to the original J1 feeder model described in section 2:

- The model type for all loads was changed to constant-power (ZIP parameters for shown in Table 21).
- A global load shape was applied for QSTS simulations.
- A load multiplier equal to 0.383392207, the average value of the load shape, was used for snapshot simulations and as an initial condition when controls were locked for QSTS simulations.

Table 18. ZIP Coefficients for Constant-Power

	Z_p	I_p	P_p	Z_q	I_q	P_q
Constant-Power	0	0	1	0	0	1

A three-phase voltage profile of the full system, showing primary and secondary voltage as a function of distance from the substation, is shown in figure 48.

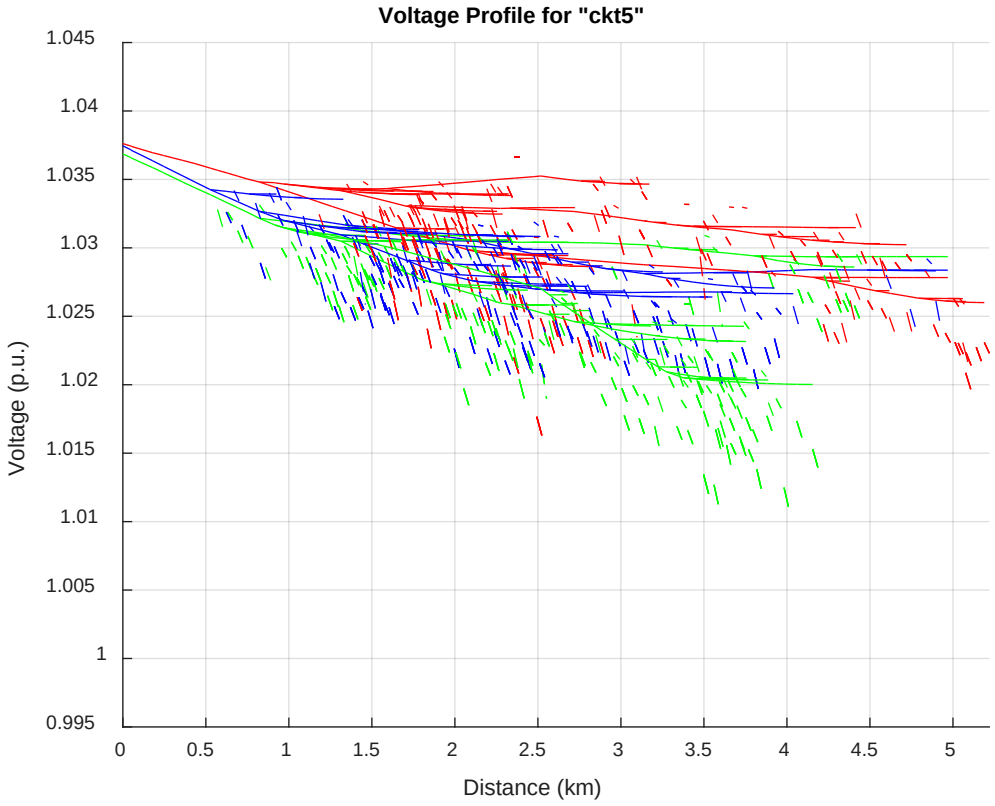

Figure 48. Three-Phase Voltage Profile for EPRI J1 Feeder

In Figure 48, distance is in km. Primary voltages are indicated by solid lines, and secondaries are indicated by lighter dashed lines located below the corresponding primary.

An overhead view of the feeder is shown in figure 49. The four capacitors are static (i.e. not switch on or off under local autonomous control).

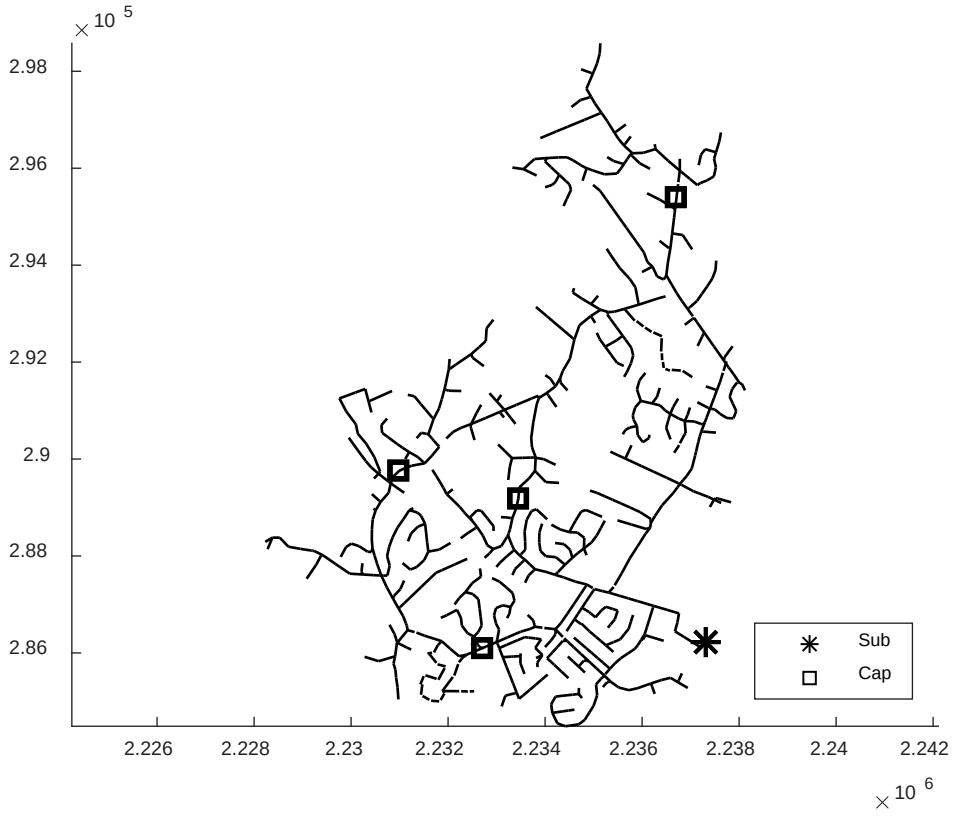

Figure 49. Overhead View of the EPRI ckt5 Feeder

The model was partitioned into 11 segments. Buses connected to capacitors, relevant junctions, and relevant laterals were preserved. The segment definitions are included in table 22 alongside the number of buses reduced by each segment.

Table 19. Segment Definitions for ckt5

Segment #	First Bus	Last Bus	Internal Buses[a]	Junction Buses[b]
1	Substation	Junction	97	2
2	Seg-1	Cap-1	568	0
3	Seg-2	End-of-Line-1	233	0
4	Seg-1	Junction	141	0
5	Seg-2	Cap-2	345	0
6	Seg-5	Laterals	62	97
7	Seg-5	Cap-3	430	0
8	Seg-7	Cap-4	552	0
9	Seg-8	End-of-Line-2	38	2
10	Seg-6	End-of-Line-3	271	0
11	Seg-6	End-of-Line-4	65	88

Segments are identified between key power system and topological features.
[a]Internal buses exist as part of a segment in the full model and are eliminated by segment substitution.
[b]Junction buses exist between the last bus of a segment and any downstream segments; they are not part of any segment and are eliminated by junction aggregation as described in Section 6.1.3.

The overhead view of the simplified model is shown in figure 50.

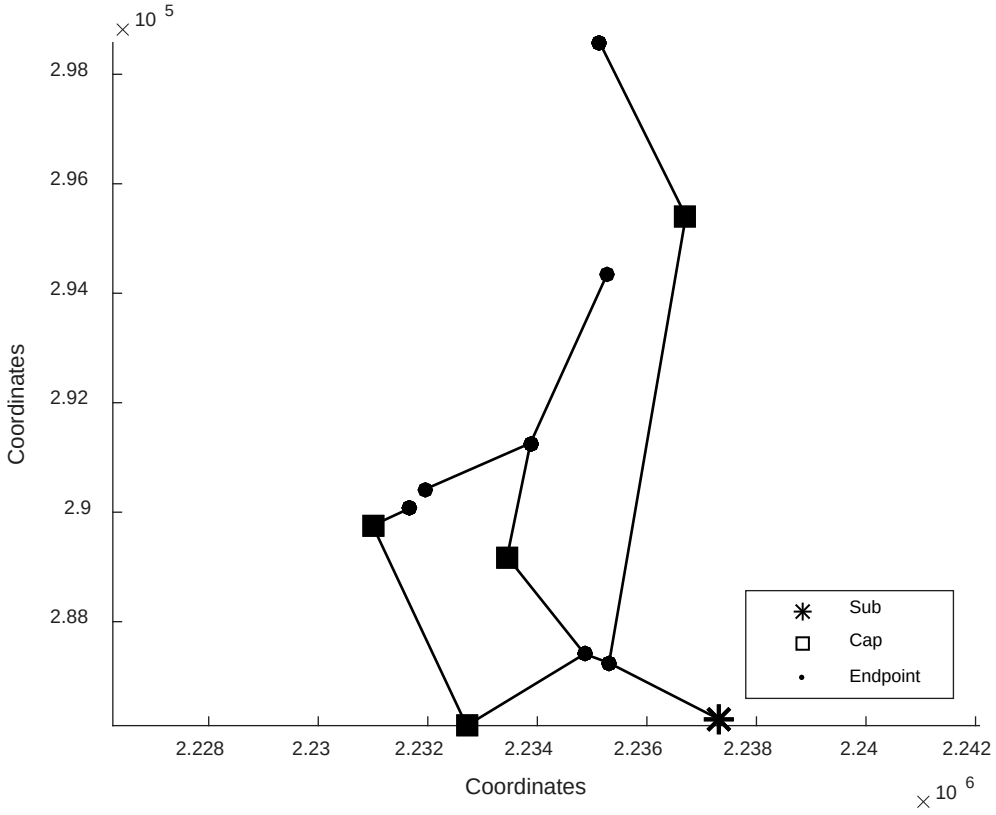

Figure 50. Overhead View of Simplified EPRI ckt5 Feeder

The overhead view of the simplified model shows that the buses of interest have been preserved while the other buses have been eliminated.

7.1.2 QSTS Benchmark for Segment Substitution

The model was simplified using segment substitution with the constant-power one-load segment. A QSTS simulation was performed for both the full and simplified models at 5-minute resolution for a duration of one year.

7.1.2.1 Benchmark Results for ckt5

A summary of the QSTS simulation performed on the full and simplified models is shown in Table 23.

Table 20. Benchmark Summary for ckt5

Performance Metrics	
B_{FULL}: 2998 B_{SIMP}: 15	T_{FULL}: 432.9098 T_{SIMP}: 8.4269
TRF: 0.995	*CSF*: 0.981
State Error Metrics	
V^{avg}_{err}: 0.000169	V^{max}_{err}: 0.001294

The simplification reduced the QSTS simulation time by 98.1% (*CSF* = 0.981) and introduced a state error of less than 0.13% (V^{max}_{err} = 0.001294).

The voltage at the output bus of segment 9, which is located at the end of the three-phase trunk line shown as the uppermost segment in Figure 50, throughout the simulation is shown in figure 51. This segment voltage plot provides a visual representation of a component of the state error metrics. Usually, the results from both models are nearly identical.

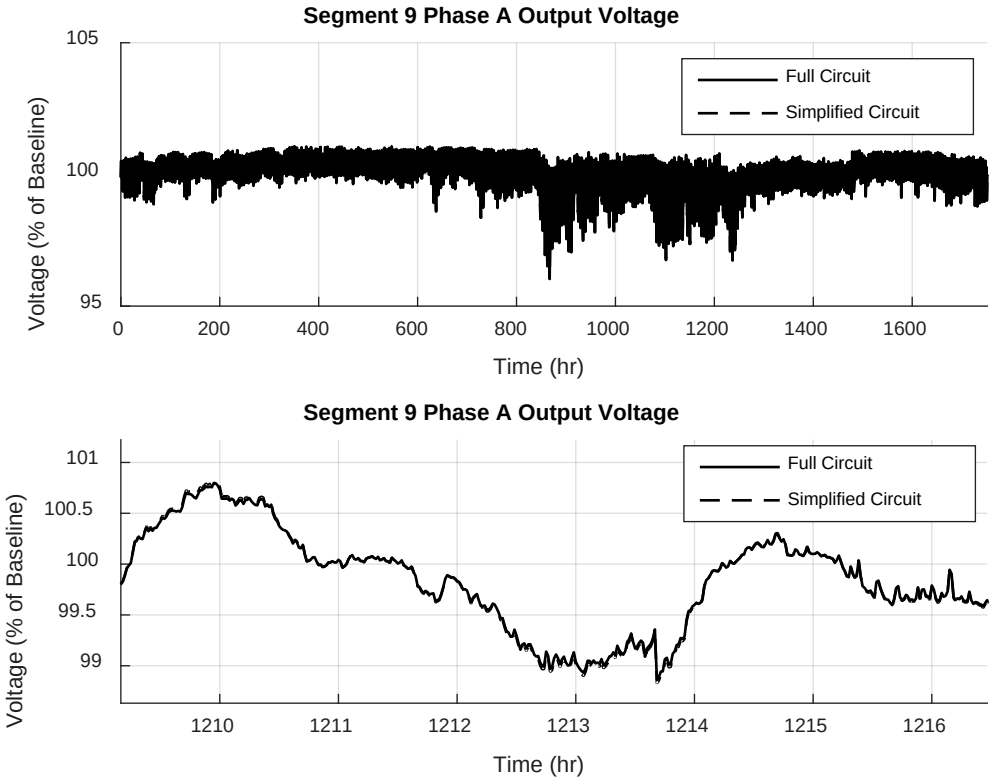

Figure 51. Segment 9 Output Voltage for Full and Simplified Models

7.1.3 Comparison to Constant-Current Load Assumption

To provide a point of comparison for error, the model was simplified by changing all loads to constant-current. This simplifying assumption is a pre-requisite for eliminating buses using linear

combination techniques as in [31]. No buses were eliminated in this section and performance metrics are not included in the summary. A QSTS simulation was performed at 5-minute resolution for a duration of one year. The results show that segment substitution introduced less error than the constant-current load approximation, even without considering any simplification error that might be introduced after using a constant-current load approximation.

7.1.3.1 Results for ckt5 with Constant-Current Loads

A summary of the QSTS simulations performed on the original model and the model modified with constant-current loads is shown in Table 24.

Table 21. Constant-Current Load Summary for ckt5

State Error Metrics	
V^{avg}_{err}: 0.000420	V^{max}_{err}: 0.002644

Because no buses were eliminated, performance metrics were not analyzed. The constant-current load assumption introduced a state error of less than 0.3% (V^{max}_{err} = 0.002644). This shows more error than was introduced by segment substitution (bottom row of Table 20).

The voltage at the output bus of segment 9, which is located at the end of the three-phase trunk line, throughout the simulation is shown in figure 52.

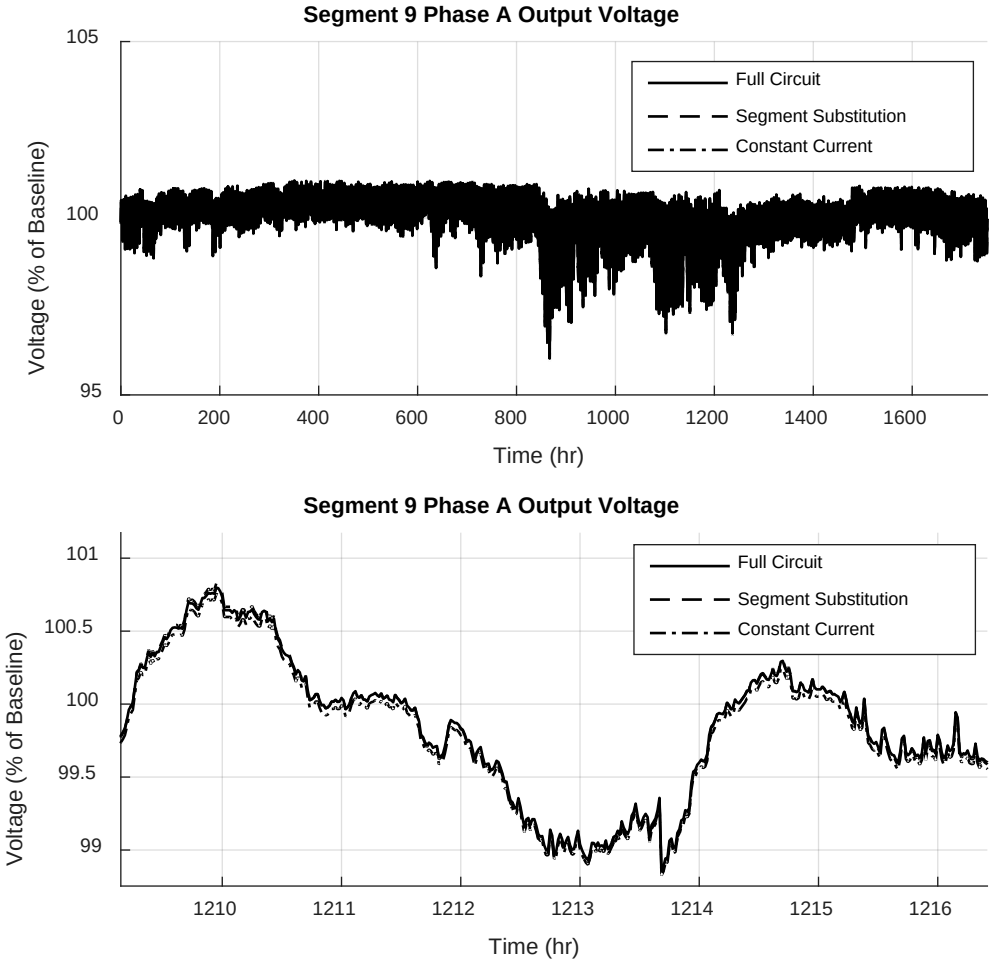

Figure 52. Segment Substitution and Constant-Current Comparison

The model simplified using segment substitution tracks the full circuit model better than the full circuit modified to have constant-current loads. The constant-current results are noticeably different than the full circuit and segment substitution results.

7.2 EPRI FEEDER J1

In this section, the process of distribution system model simplification using segment substitution will be demonstrated using a full electric power distribution system model with multiple distributed voltage regulators and distributed PV. The model is EPRI Feeder J1, provided to the public on the Distributed PV (DPV) website [47]. The performance of the simplified model is examined using the metrics discussed in section 6.2. The model is simplified using series-impedance ZIP-load shunt segments with PV compensation.

7.2.1 Feeder Description

The following changes were made to the original J1 feeder model described in section 2:

- The model type for all loads was changed to ZIP coefficients with parameters for residential sub-class D defined in [32] and shown in Table 25.
- A global load shape and global PV generation shape were applied for QSTS simulations.
- A load multiplier equal to 0.543414847, the average value of the load shape, was used for snapshot simulations and as an initial condition when controls were locked for QSTS simulations.

Table 22. ZIP Coefficients for residential sub-class D [32]

	Z_p	I_p	P_p	Z_q	I_q	P_q
Residential Sub-Class D	1.31	-1.94	1.63	9.2	-15.27	7.07

Note that the real coefficients (Z_p, I_p, P_p,) and the reactive coefficients (Z_q, I_q, P_q,) each sum to 1.

A three-phase voltage profile of the full system, showing primary and secondary voltage as a function of distance from the substation, is shown in figure 53.

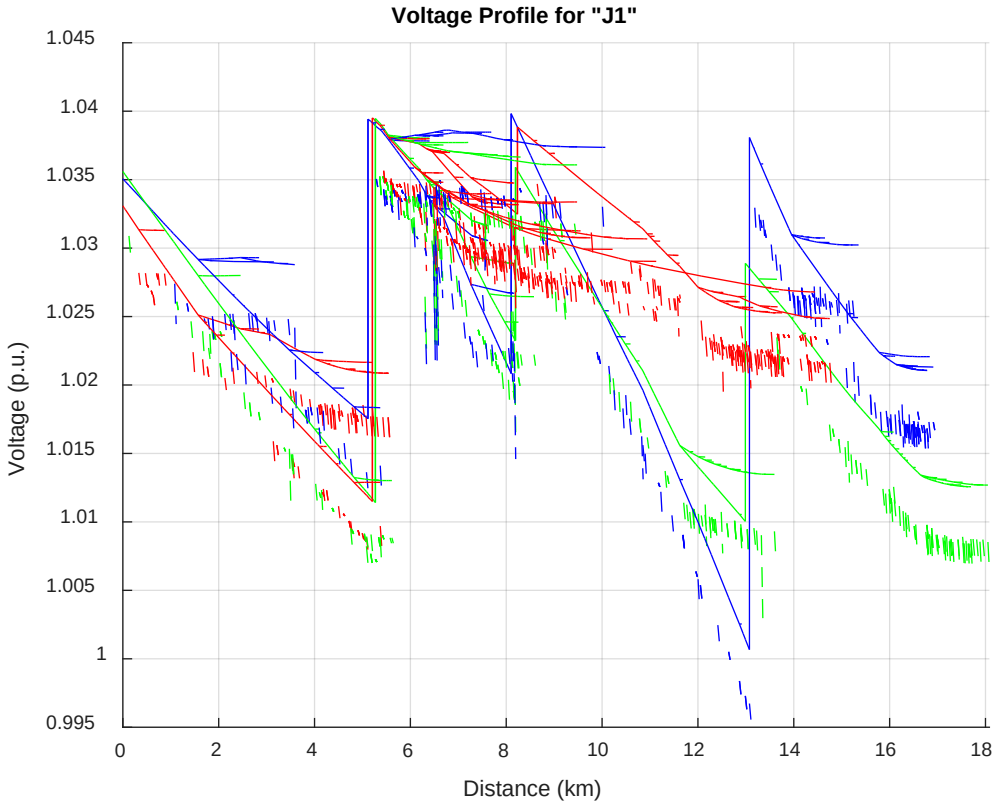

Figure 53. Three-Phase Voltage Profile for EPRI J1 Feeder

In Figure 53, distance is in km. Primary voltages are indicated by solid lines, and secondaries are indicated by lighter dashed lines located below the corresponding primary. Distributed voltage regulators cause discontinuities in the voltage profile. The large PV cluster is located between the 6-km and 8-km grid lines.

An overhead view of the feeder is shown in figure 54. The four large PV systems are clustered near the middle of the figure. The eight voltage regulators are in three groups: (1) along the trunk upstream of the large PV cluster, (2) along the trunk downstream of the large PV cluster, and (3) near the beginning of a two-phase lateral towards the end of the feeder. There are five capacitors located along the trunk line.

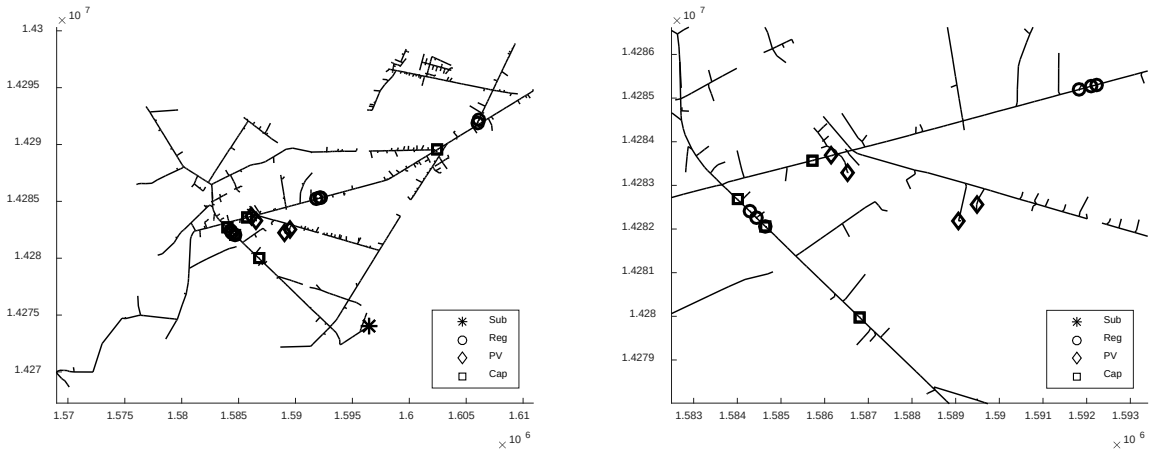

Figure 54. Overhead View of the EPRI J1 Feeder (Left) with Central Detail (Right)

The model was partitioned into 23 segments. Buses connected to capacitors, regulators, distribution transformers with large PV systems on the secondary, relevant junctions, and relevant laterals were preserved. The segment definitions are included in table 26 alongside the number of buses reduced by each segment.

Table 23. Segment Definitions for J1

Segment #	First Bus	Last Bus	Internal Buses[a]	Junction Buses[b]
1	Substation	Cap-1	448	0
2	Seg-1	Reg-1A and Cap-2	112	0
3	Seg-2	Reg-1C	5	5
4	Seg-3	Reg-1B	1	12
5	Seg-4	Cap-3	15	0
6	Seg-5	Junction	29	1133
7	Seg-6	Cap-4	80	0
8	Seg-7	LargePV-2	0	6
9	Seg-8	Junction	0	34
10	Seg-9	LargePV-1	3	1
11	Seg-9	Junction	12	11
12	Seg-11	Junction	15	0
13	Seg-12	LargePV-3	1	1
14	Seg-12	LargePV-4	50	1
15	Seg-11	Reg-2A	194	6
16	Seg-15	Reg-2B	0	0
17	Seg-16	Reg-2C	0	0
18	Seg-17	Cap-5	307	4
19	Seg-18	Lateral	200	120
20	Seg-19	Reg-3B	1	3
21	Seg-20	Reg-3A	0	2
22	Seg-21	Lateral	445	85
23	Seg-22	Last Bus	44	2

Segments are identified between key power system and topological features.
[a]Internal buses exist as part of a segment in the full model and are eliminated by segment substitution.
[b]Junction buses exist between the last bus of a segment and any downstream segments; they are not part of any segment and are eliminated by junction aggregation as described in Section 6.3.1.

The overhead view of the simplified model is shown in figure 55.

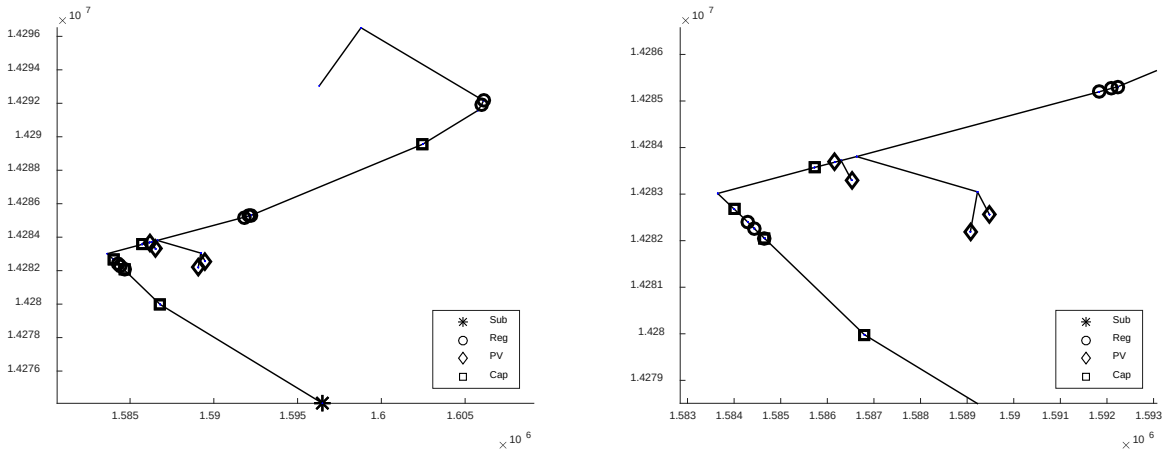

Figure 55. Overhead View of Simplified EPRI J1 Feeder (Left) with Central Detail (Right)

The overhead view of the simplified model shows that the buses of interest have been preserved while the other buses have been eliminated.

7.2.2 QSTS Benchmark for Segment Substitution

The model was simplified using segment substitution with the Z-ZIP segment with residential sub-class D coefficients and PV compensation around a base case at mean load. Two QSTS simulations were performed for both the full and simplified models at 1-minute resolution for a duration of one day: one without PV and one with PV. Where applicable, regulator and capacitor controls are locked with PV off at mean daily load to avoid a small voltage error causing an element to change state, introducing a much larger voltage error.

7.2.2.1 Benchmark Results for J1 with No PV

A summary of the QSTS simulations performed on the full and simplified models without PV is shown in Table 27.

Table 24. Benchmark Summary for J1 with No PV

<table>
<tr><td colspan="9">Performance Metrics – No controls locked</td></tr>
<tr><td colspan="4">B_{FULL}: 3434 B_{SIMP}: 46</td><td colspan="5">T_{FULL}: 10.1723 T_{SIMP}: 0.5147</td></tr>
<tr><td colspan="4">TRF: 0.987</td><td colspan="5">CSF: 0.949</td></tr>
<tr><td colspan="9">State Error Metrics – Regulator and Capacitor Controls Locked</td></tr>
<tr><td colspan="4">V^{avg}_{err}: 0.000236</td><td colspan="5">V^{max}_{err}: 0.001169</td></tr>
<tr><td colspan="9">Voltage Regulator Tap Changes Operations[a] – Capacitor Controls Locked</td></tr>
<tr><td colspan="3">Group 1[b]</td><td colspan="3">Group 2[b]</td><td colspan="2">Group 3[c]</td><td>Sub[d]</td></tr>
<tr><td>6</td><td>10</td><td>8</td><td>7</td><td>9</td><td>7</td><td>10</td><td>11</td><td>3</td></tr>
<tr><td>6</td><td>8</td><td>8</td><td>6</td><td>11</td><td>7</td><td>10</td><td>11</td><td>3</td></tr>
<tr><td colspan="9">RTE: -0.014</td></tr>
</table>

[a]First row: full model; second row: simplified model.
[b]Phases A, B, and C.
[c]Phases A and B.
[d]Ganged three-phase.

The simplification reduced the QSTS simulation time by 94.9% (CSF = 0.949) and introduced a state error of less than 0.12% (V^{max}_{err} = 0.001169).

The voltage at the output bus of segment 12, which is located near the PV systems, throughout the simulation is shown in figure 56.

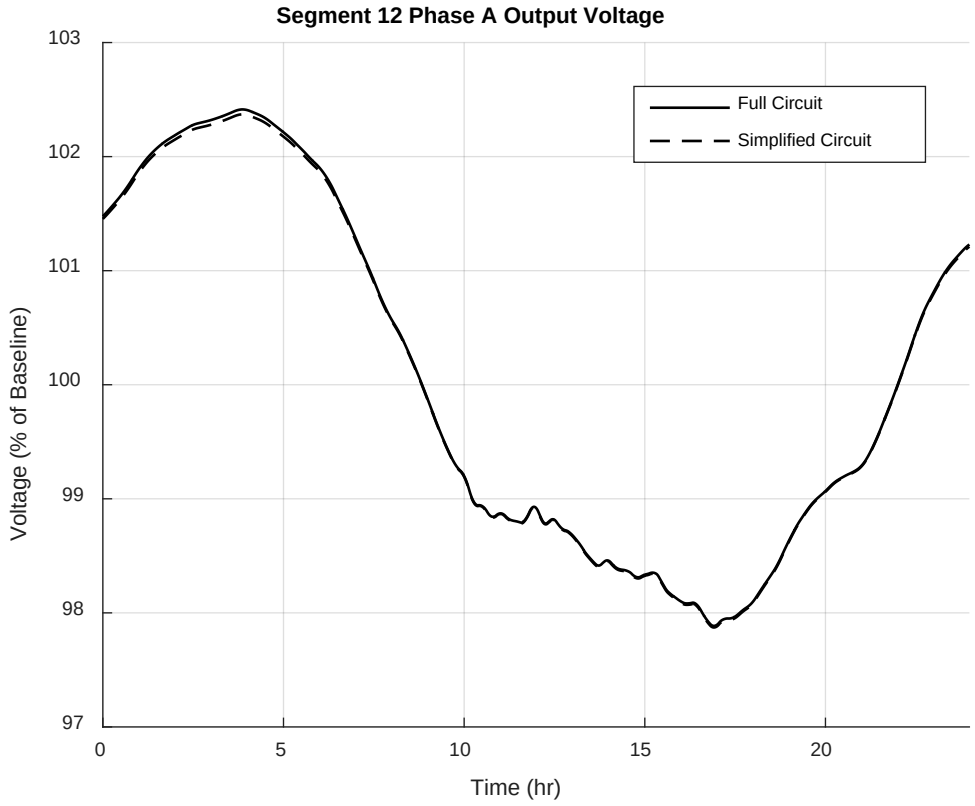

Figure 56. Segment 12 Output Voltage for Full and Simplified Models

This segment voltage plot provides a visual representation of a component of the state error metrics. Visually, the full and simplified models are nearly identical.

7.2.2.2 Benchmark Results for J1 with PV

A summary of the QSTS simulations performed on the full and simplified models with PV is shown in Table 28.

Table 25. Benchmark Summary for J1 with PV

<table>
<tr><td colspan="9">Performance Metrics – No Controls Locked</td></tr>
<tr><td colspan="4">B_{FULL}: 3434 B_{SIMP}: 46</td><td colspan="5">T_{FULL}: 10.1431 T_{SIMP}: 0.7465</td></tr>
<tr><td colspan="4">TRF: 0.987</td><td colspan="5">CSF: 0.926</td></tr>
<tr><td colspan="9">State Error Metrics – Regulator and Capacitor Controls Locked</td></tr>
<tr><td colspan="4">V^{avg}_{err}: 0.000229</td><td colspan="5">V^{max}_{err}: 0.001697</td></tr>
<tr><td colspan="9">Voltage Regulator Tap Changes Operations[a] – Capacitor Controls Locked</td></tr>
<tr><td colspan="3">Group 1[b]</td><td colspan="3">Group 2[b]</td><td colspan="2">Group 3[c]</td><td>Sub[d]</td></tr>
<tr><td>6</td><td>10</td><td>8</td><td>11</td><td>17</td><td>11</td><td>12</td><td>25</td><td>3</td></tr>
<tr><td>8</td><td>17</td><td>13</td><td>13</td><td>27</td><td>21</td><td>17</td><td>33</td><td>4</td></tr>
<tr><td colspan="9">RTE: 0.485</td></tr>
</table>

[a]First row: full model; second row: simplified model.
[b]Phases A, B, and C.
[c]Phases A and B.
[d]Ganged three-phase.

The simplification reduced the QSTS simulation time by 92.6% (CSF = 0.926) and introduced a state error of less than 0.17% (V^{max}_{err} = 0.001397). The introduction of PV to the model did not have a significant impact on the state error metrics. The increase in CSF relative to the no-PV case is believed to be caused by additional hunting by voltage regulators (RTE = 0.485

compared to -0.013 in Table 24). The voltage at the output bus of segment 12, which is located near the PV systems, throughout the simulation is shown in figure 57.

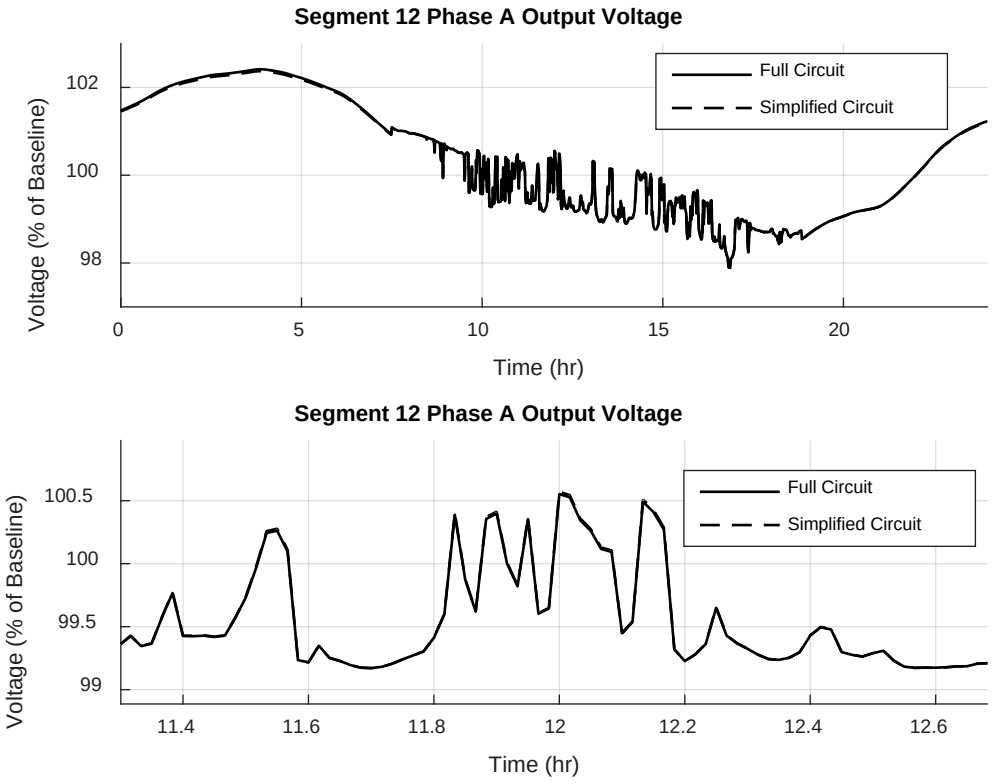

Figure 57. Segment 12 Output Voltage with PV (Detail, Bottom)

This segment voltage plot provides a visual representation of a component of the state error metrics. Visually, the full and simplified model results are nearly identical. This is a more severe test due to the rapid fluctuations of PV output on a cloudy day, which can be observed by comparing Figure 57 to Figure 56.

7.2.2.3 Regulator Tap Change Operation Impact for J1

The regulator tap change operation impact, *RTI*, quantifies the impact of simplification on a PV impact study. It depends on the results from the QSTS simulations both without and with PV and is summarized in table 29.

Table 26. *RTI* for J1 Simplified by Segment Substitution

PV Impact on Tap Changes
RTI: 1.594

The introduction of PV (without mitigating the voltage impact of the PV) is expected to increase the number of tap changes in the benchmark simulation. Simplification using segment substitution with PV compensation caused the number of tap changes throughout the system to increase even more. Over-representing the number of tap changes caused by PV is conservative relative to underrepresenting the number. This can occur when a relatively small voltage error causes a voltage regulator to change taps, which can cause downstream voltage regulators to change taps in turn.

The impact of simplification, using segment substitution or the constant current load assumption, on voltage regulator tap change operations, in spite of the low error in bus voltages (which is monitored to determine the need for a tap change), underscores the sensitivity of voltage regulators in distribution system models. However, the full and simplified models both indicate a substantial increase in the number of tap change operations when PV is present and would likely lead to similar conclusions for a PV impact analysis.

7.2.3 Comparison to Constant-Current Load Assumption

To provide a point of comparison, the model was simplified by changing all loads to constant-current. This simplifying assumption is a pre-requisite for eliminating buses using linear combination techniques as in [31]. No buses were eliminated in this section and performance metrics are not included in the summary. A QSTS simulation was performed at 1-minute resolution for a duration of one day. The results show that segment substitution has less error than the constant-current load approximation, even without considering any simplification error that might be introduced after using a constant-current load approximation [31].

7.2.3.1 Results for J1 with Constant-Current Loads and No PV

A summary of the QSTS simulations performed on the original model and the model modified with constant-current loads without PV is shown in Table 30.

Table 27. Constant-Current Load Summary for J1 with No PV

State Error Metrics – Regulator and Capacitor Controls Locked								
V^{avg}_{err}: 0.002168						V^{max}_{err}: 0.006843		
Voltage Regulator Tap Changes Operations[a] – Capacitor Controls Locked								
Group 1[b]			Group 2[b]			Group 3[c]		Sub[d]
6	10	8	7	9	7	10	11	3
8	12	10	11	6	5	10	12	3
RTE: 0.085								

[a]First row: ZIP load model; second row: constant-current load model.
[b]Phases A, B, and C.
[c]Phases A and B.
[d]Ganged three-phase.

Because no buses were eliminated, performance metrics were not analyzed. The constant-current load assumption introduced a state error of less than 0.70% (V^{max}_{err} = 0.006843) compared to 0.12% when simplified by segment substitution as shown in Table 24.

The voltage at the output bus of segment 12, which is located near the PV systems, throughout the simulation is shown in figure 58.

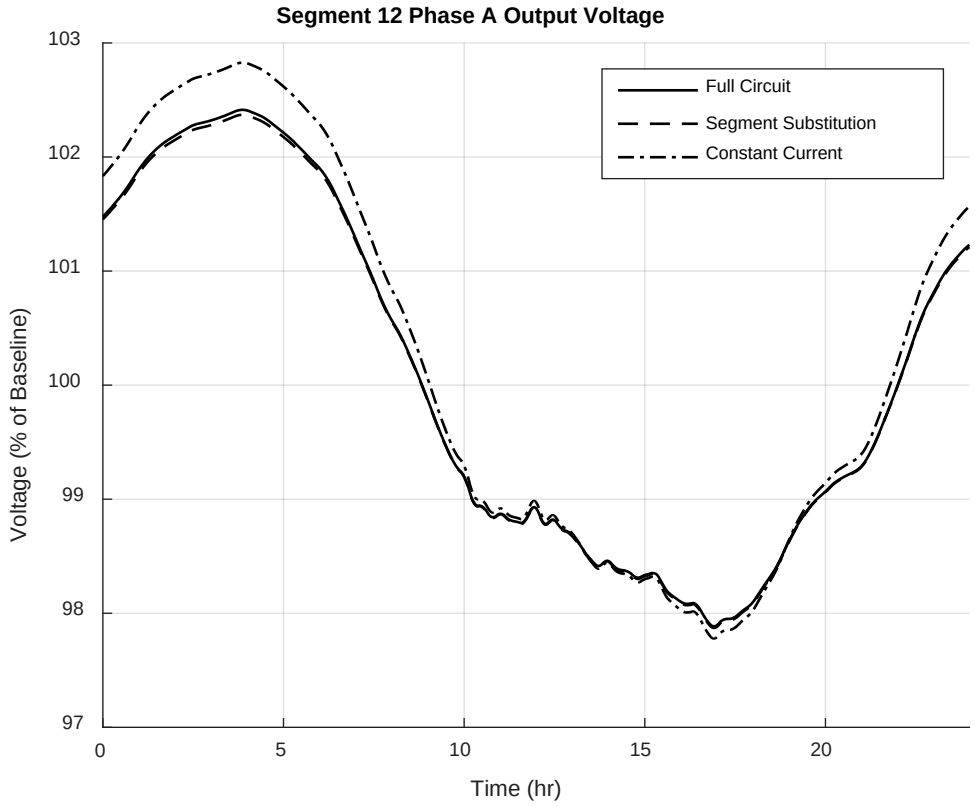

Figure 58. Segment Substitution and Constant-Current Comparison with no PV

The model simplified using segment substitution tracks the full circuit model better than the full circuit modified to have constant-current loads. The constant-current load model

performs best when the local voltage is close to the system base (in this case, about 98.5% of baseline).

7.2.3.2 Results for J1 with Constant-Current Loads and PV

A summary of the QSTS simulations performed on the original model and the model modified with constant-current loads with PV is shown in Table 31.

Table 28. Constant-Current Load Summary for J1 with PV

State Error Metrics – Regulator and Capacitor Controls Locked								
V^{avg}_{err}: 0.002251			V^{max}_{err}: 0.006843					
Voltage Regulator Tap Change Operations[a] – Capacitor Controls Locked								
Group 1[b]			Group 2[b]			Group 3[c]		Sub[d]
6	10	8	11	17	11	12	25	3
6	16	10	11	29	20	14	42	3
RTE: 0.466								

[a]First row: ZIP load model; second row: constant-current load model.
[b]Phases A, B, and C.
[c]Phases A and B.
[d]Ganged three-phase.

Because no buses were eliminated, performance metrics were not analyzed. The constant-current load assumption introduced a state error of less than 0.7% (V^{max}_{err} = 0.006843) compared to 0.17% when simplified by segment substitution as shown in Table 25. The impact on voltage regulator taps was slightly less than for the model simplified by segment substitution (*RTE* = 0.466 compared to 0.485). This is believed to be a coincidence because the impact on phase B regulators was significantly larger with the constant-current load assumption, while the phase A

and C errors were lower for the constant-current load assumption. In both cases, the number of regulator tap changes was overestimated by the simplified (by segment substitution or by constant-current load approximation) model. The voltage at the output bus of segment 12, which is located near the PV systems, throughout the simulation is shown in figure 39.

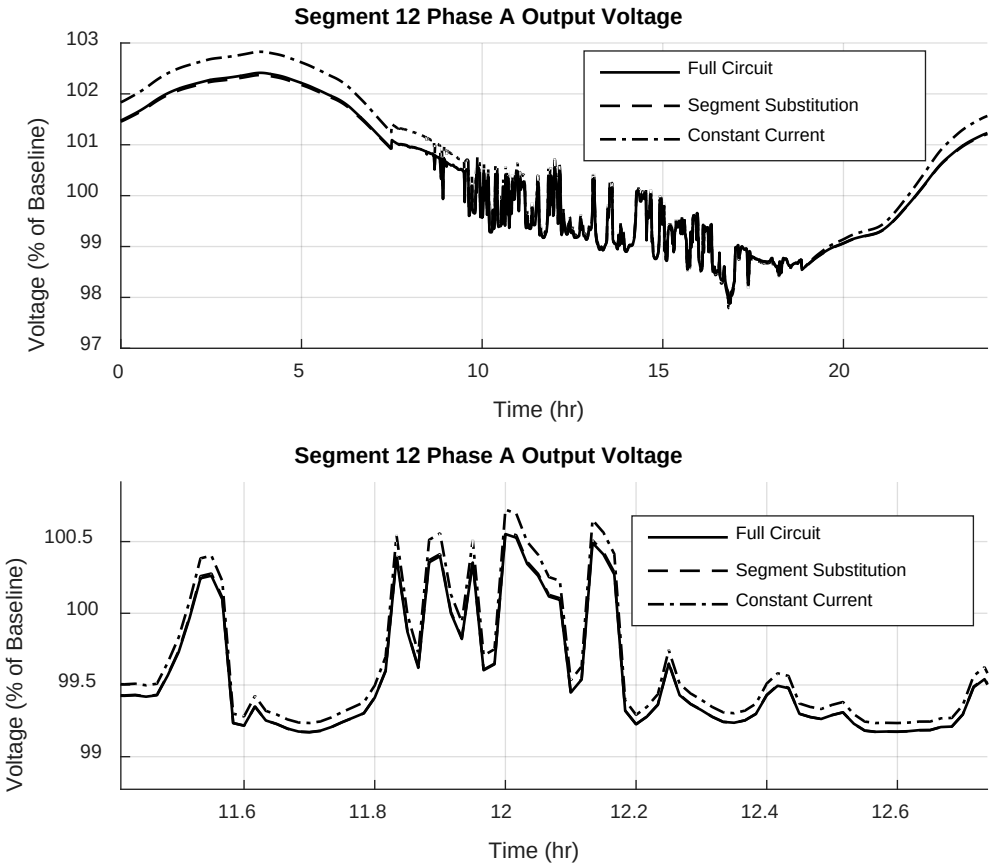

Figure 59. Segment Substitution and Constant-Current Comparison with PV

Again, the model simplified using segment substitution tracks the full circuit model better than the full circuit modified to have constant-current loads.

7.2.3.3 Regulator Tap Change Operation Impact for J1 with Constant-Current Loads

The regulator tap change operation impact, *RTI*, quantifies the impact of simplification on a PV impact study. It depends on the results from the QSTS simulations both without and with PV, is summarized in table 32.

Table 29. *RTI* for J1 with Constant-Current Loads

PV Impact on Tap Changes
RTI: 1.313

The constant-current assumption had an impact on the number of tap changes that exceeds the state error introduced by the assumption. Again, this highlights the sensitivity of voltage regulators to voltage errors. However, in all cases, the introduction of PV caused a noticeable increase in the number of tap change operations compared to the corresponding no-PV cases.

8.0 RESEARCH SUMMARY

This dissertation investigated electric power distribution system model simplification. In the literature, no methods were found that could simplify distribution system models with realistic constant-power or ZIP loads. In order to address this gap, the segment substitution method was developed. The segment substitution method treats topological segments as non-linear two-port networks with an assumed simplified topology. Segment substitution was demonstrated to be capable of reducing the number of buses in a full mixed-phase distribution system model with ZIP loads by over 98% while introducing a state error of less than 0.2% (0.002 per-unit voltage) and to introduce less error than the constant-current load assumption, which is a pre-requisite for simplification using the leading method found in the literature.

8.1 CONTRIBUTIONS

This dissertation describes the following contributions.

Distribution System Model Simplification Using Segment Substitution

Segment substitution, using the series-impedance, shunt-ZIP topology has been demonstrated to reduce the number of buses on full mixed-phase distribution system models by over 98%, while introducing a state error of less than 0.2% (0.002 per-unit voltage).

Photovoltaic Compensation with Segment Substitution

In distribution models with PV, the effective or net load shape at buses with and upstream of PV is different than the load shape without PV. PV compensation alongside the series-impedance, shunt-ZIP topology was demonstrated to simplify a full mixed-phase distribution system model with multiple distributed PV systems without having a significant impact on the state error of the simplified model relative to the full model. The compensation framework used for PV compensation is applicable to other components that affect net load shapes such as distributed capacitors and large loads with an independent load shape.

Metrics for Quantification of Distribution System Model Simplification

The following metrics have been introduced to quantify distribution model simplification:

- *Topological Reduction Factor (TRF)*: Quantifies the number of buses eliminated by simplification.

- *Computational Savings Factor (CSF)*: Quantifies the computational savings of simplification for a benchmark QSTS simulation.
- *Average and Maximum Absolute Voltage Magnitude Error*: Quantifies the contribution of simplification to state error in the model; calculated with voltage regulators locked.
- *Regulator Tap Change Operation Error (RTE)*: Quantifies the impact of simplification on the number of regulator tap change operations in a QSTS benchmark.
- *Regulator Tap Change Operation Impact (RTI)*: Quantifies the impact of simplification on regulator tap changes for a PV impact study.

Stochastic Distribution Feeder Generation

A method was developed to generate radial distribution system feeder models stochastically. The method treats topological characteristics of a radial feeder as random variables, characterized by a representative set of real feeder models. In addition, topological parameters (e.g. line impedance and customer load) are treated as random variables, characterized by a planning strategy. This stochastic feeder generation method was used to characterize the simplification error associated with segment substitution and to correctly predict (within a range) the simplification error observed in a set of two full realistic distribution system models simplified using segment substitution.

8.2 OPPORTUNITIES FOR FURTHER RESEARCH

The following items are identified as opportunities for further research.

Segment Substitution for Models with Behavioral Loads

Segment substitution has been developed for distribution system models with ZIP loads and PV systems that follow a time-shape of multipliers. An alternative way to model loads for static or quasi-static distribution system simulation is an agent-based framework [25]. Agent based load modeling allows customer and appliance behavior in response to stimuli such as market signals and weather. An effort is underway at the University of Pittsburgh to extend segment substitution to distribution system models with behavioral agent-based loads.

State Estimation Using Simplified Models

Similar to QSTS simulations, state estimation requires repetitive static simulation of power system models. Simplified models could be used to enable distribution system state estimation for available real-time data. An interpolation can be used to estimate voltage values between segment endpoints that have measurements.

Improved Parameter Estimation Using Segment Substitution Topologies

In the literature, parameter estimation [36, 37] is concerned with determining physical parameters to populate a distribution system model using measurement data. An opportunity exists to use measurement data to estimate simplified segment topologies (such as the series-impedance, shunt-ZIP topology) that have been demonstrated to provide a good approximation of distribution system models without attempting to estimate physical parameters.

8.3 PUBLICATIONS

Published

- Reiman, McDermott, “Guidelines for high penetration of single-phase PV on power distribution systems,” *2015 PES General Meeting*

In Review

- Reiman, McDermott, Akcakaya, Reed, “Electric Power Distribution System Model Simplification Using Segment Substitution,” *submitted to IEEE Transactions on Power Systems*

In Preparation

- Reiman, Abate, McDermott, Reed, Croushore, Price, “Automation of Distributed PV Impact Analysis,” *for 2018 IEEE PES T&D Conference*

REFERENCES

[1] F. C. Schweppe and J. Wildes, "Power System Static-State Estimation, Part I: Exact Model," *IEEE Transactions on Power Apparatus and Systems,* vol. PAS-89, pp. 120-125, 1970.

[2] R. Fujiwara, T. Sakaguchi, Y. Kohno, and H. Suzuki, "An Intelligent Load Flow Engine for Power System Planning," *IEEE Transactions on Power Systems,* vol. 1, pp. 302-307, 1986.

[3] C. Mo-Shing and W. E. Dillon, "Power system modeling," *Proceedings of the IEEE,* vol. 62, pp. 901-915, 1974.

[4] W. H. Kersting, *Distribution System Modeling and Analysis*, Third ed., 2012.

[5] T. H. Chen, M. S. Chen, K. J. Hwang, P. Kotas, and E. A. Chebli, "Distribution system power flow analysis-a rigid approach," *IEEE Transactions on Power Delivery,* vol. 6, pp. 1146-1152, 1991.

[6] M. F. AlHajri and M. E. El-Hawary, "Exploiting the Radial Distribution Structure in Developing a Fast and Flexible Radial Power Flow for Unbalanced Three-Phase Networks," *IEEE Transactions on Power Delivery*, vol. 25, pp. 378-389, 2010.

[7] D. Shirmohammadi, H. W. Hong, A. Semlyen, and G. X. Luo, "A compensation-based power flow method for weakly meshed distribution and transmission networks," *IEEE Transactions on Power Systems*, vol. 3, pp. 753-762, 1988.

[8] R. D. Zimmerman and C. Hsiao-Dong, "Fast decoupled power flow for unbalanced radial distribution systems," *IEEE Transactions on Power Systems,* vol. 10, pp. 2045-2052, 1995.

[9] G. W. Chang, S. Y. Chu, and H. L. Wang, "An Improved Backward/Forward Sweep Load Flow Algorithm for Radial Distribution Systems," *IEEE Transactions on Power Systems*, vol. 22, pp. 882-884, 2007.

[10] V. H. M. Quezada, J. R. Abbad, and T. G. S. Roman, "Assessment of energy distribution losses for increasing penetration of distributed generation," *IEEE Transactions on Power Systems*, vol. 21, pp. 533-540, 2006.

[11] A. Woyte, V. V. Thong, R. Belmans, and J. Nijs, "Voltage fluctuations on distribution level introduced by photovoltaic systems," *IEEE Transactions on Energy Conversion,* vol. 21, pp. 202-209, 2006.

[12] A. P. Reiman, T. E. McDermott, G. F. Reed, and B. Enayati, "Guidelines for high penetration of single-phase PV on power distribution systems," in *2015 IEEE Power & Energy Society General Meeting*, 2015, pp. 1-5.

[13] K. Clement-Nyns, E. Haesen, and J. Driesen, "The Impact of Charging Plug-In Hybrid Electric Vehicles on a Residential Distribution Grid," *IEEE Transactions on Power Systems*, vol. 25, pp. 371-380, 2010.

[14] M. Nick, R. Cherkaoui, and M. Paolone, "Optimal Allocation of Dispersed Energy Storage Systems in Active Distribution Networks for Energy Balance and Grid Support," *IEEE Transactions on Power Systems,* vol. 29, pp. 2300-2310, 2014.

[15] Y. F. Huang, S. Werner, J. Huang, N. Kashyap, and V. Gupta, "State Estimation in Electric Power Grids: Meeting New Challenges Presented by the Requirements of the Future Grid," *IEEE Signal Processing Magazine,* vol. 29, pp. 33-43, 2012.

[16] M. E. Baran and A. W. Kelley, "A branch-current-based state estimation method for distribution systems," *IEEE Transactions on Power Systems,* vol. 10, pp. 483-491, 1995.

[17] C. N. Lu, J. H. Teng, and W. H. E. Liu, "Distribution system state estimation," *IEEE Transactions on Power Systems,* vol. 10, pp. 229-240, 1995.

[18] I. Roytelman and S. M. Shahidehpour, "State estimation for electric power distribution systems in quasi real-time conditions," *IEEE Transactions on Power Delivery,* vol. 8, pp. 2009-2015, 1993.

[19] J. B. Leite and J. R. S. Mantovani, "Distribution System State Estimation Using the Hamiltonian Cycle Theory," *IEEE Transactions on Smart Grid*, vol. 7, pp. 366-375, 2016.

[20] R. Seguin, J. Woyak, D. Costyk, J. Hambrick, and B. Mather, "High-Penetration PV Integration Handbook for Distribution Engineers," NREL2016.

[21] B. A. Mather, "Quasi-static time-series test feeder for PV integration analysis on distribution systems," in *2012 IEEE Power and Energy Society General Meeting*, 2012, pp. 1-8.

[22] J. E. Quiroz, M. J. Reno, and R. J. Broderick, "Time series simulation of voltage regulation device control modes," in *2013 IEEE 39th Photovoltaic Specialists Conference (PVSC)*, 2013, pp. 1700-1705.

[23] R. C. Dugan and T. E. McDermott, "An open source platform for collaborating on smart grid research," in *2011 IEEE Power and Energy Society General Meeting*, 2011, pp. 1-7.

[24] *OpenDSS* [Online]. Available: https://sourceforge.net/projects/electricdss/

[25] D. P. Chassin, J. C. Fuller, and N. Djilali, "GridLAB-D: An agent-based simulation framework for smart grids," *Journal of Applied Mathematics*, vol. 2014, pp. 1-12, 2014.

[26] *GridLAB-D* [Online]. Available: http://www.gridlabd.org/

[27] *CYMDIST* [Online]. Available: http://www.cyme.com/

[28] *Synergi Electric* [Online]. Available: https://www.dnvgl.com/

[29] *WindMil* [Online]. Available: http://www.milsoft.com/

[30] J. B. Ward, "Equivalent circuits for power-flow studies," *Electrical Engineering*, vol. 68, pp. 794-794, 1949.

[31] M. J. Reno, K. Coogan, R. Broderick, and S. Grijalva, "Reduction of distribution feeders for simplified PV impact studies," in *2013 IEEE 39th Photovoltaic Specialists Conference (PVSC)*, 2013, pp. 2337-2342.

[32] A. Bokhari, A. Alkan, R. Dogan, M. Diaz-Aguilo, F. d. Leon, D. Czarkowski, *et al.*, "Experimental Determination of the ZIP Coefficients for Modern Residential, Commercial, and Industrial Loads," *IEEE Transactions on Power Delivery*, vol. 29, pp. 1372-1381, 2014.

[33] M. Diaz-Aguilo, J. Sandraz, R. Macwan, F. d. Leon, D. Czarkowski, C. Comack, *et al.*, "Field-Validated Load Model for the Analysis of CVR in Distribution Secondary Networks: Energy Conservation," *IEEE Transactions on Power Delivery*, vol. 28, pp. 2428-2436, 2013.

[34] I. T. F. o. L. R. f. D. Performance, "Load representation for dynamic performance analysis [of power systems]," *IEEE Transactions on Power Systems*, vol. 8, pp. 472-482, 1993.

[35] I. T. F. o. L. R. f. D. Performance, "Standard load models for power flow and dynamic performance simulation," *IEEE Transactions on Power Systems*, vol. 10, pp. 1302-1313, 1995.

[36] J. Peppanen, M. J. Reno, R. J. Broderick, and S. Grijalva, "Distribution System Model Calibration With Big Data From AMI and PV Inverters," *IEEE Transactions on Smart Grid*, vol. 7, pp. 2497-2506, 2016.

[37] F. Mahmood, H. Hooshyar, J. Lavenius, A. Bidadfar, P. Lund, and L. Vanfretti, "Real-Time Reduced Steady-State Model Synthesis of Active Distribution Networks Using PMU Measurements," *IEEE Transactions on Power Delivery*, vol. 32, pp. 546-555, 2017.

[38] N. Balabanian and T. Bickart, *Linear Network Theory: Analysis, Properties, Design and Synthesis*, 1981.

[39] C.-T. Chen, *Linear System Theory and Design*, 2013.

[40] C. K. Alexander and M. N. O. Sadiku, *Fundamentals of Electric Circuits*, Third ed., 2007.

[41] E. Muljadi, S. Pasupulati, A. Ellis, and D. Kosterov, "Method of equivalencing for a large wind power plant with multiple turbine representation," in *Power and Energy Society General Meeting - Conversion and Delivery of Electrical Energy in the 21st Century, 2008 IEEE*, 2008, pp. 1-9.

[42] J. D. Glover, M. S. Sarma, and T. J. Overbye, *Power System Analysis and Design*, Fifth ed., 2012.

[43] J. J. Grainger and W. D. Stevenson, *Power System Analysis*, 1994.

[44] J. A. Martinez, R. Walling, B. A. Mork, J. Martin-Arnedo, and D. Durbak, "Parameter determination for modeling system transients-Part III: Transformers," *IEEE Transactions on Power Delivery*, vol. 20, pp. 2051-2062, 2005.

[45] J. A. Martinez and D. W. Durbak, "Parameter determination for modeling systems transients-Part V: Surge arresters," *IEEE Transactions on Power Delivery*, vol. 20, pp. 2073-2078, 2005.

[46] P. A. N. Garcia, J. L. R. Pereira, S. Carneiro, V. M. d. Costa, and N. Martins, "Three-phase power flow calculations using the current injection method," *IEEE Transactions on Power Systems*, vol. 15, pp. 508-514, 2000.

[47] (2013). *EPRI Feeder J1, Distributed PV (DPV) Monitoring and Feeder Analysis*. Available: dpv.epri.com

[48] K. P. Schneider, Y. Chen, D. Engle, and D. Chassin, "A Taxonomy of North American radial distribution feeders," in *2009 IEEE Power & Energy Society General Meeting*, 2009, pp. 1-6.